8-9-2014

Probing Heteroatom-Containing Substrate Oxidation in P450-Cam for Non-Ferryl Reactive Intermediates and Heme Iron Coordination Structural Analysis Using Magnetic Circular Dichroism Spectroscopy

Anuja Ratnakar Modi
University of South Carolina - Columbia

PROBING HETEROATOM-CONTAINING SUBSTRATE OXIDATION IN P450-CAM FOR NON-FERRYL REACTIVE INTERMEDIATES AND HEME IRON COORDINATION STRUCTURAL ANALYSIS USING MAGNETIC CIRCULAR DICHROISM SPECTROSCOPY.

by

Anuja Ratnakar Modi

Bachelor of Science
University of Mumbai, 2007

Master of Science
Virginia Commonwealth University, 2009

Submitted in Partial Fulfillment of the Requirements

For the Degree of Doctor of Philosophy in

Chemistry

College of Arts and Sciences

University of South Carolina

2014

Accepted by:

John H. Dawson, Major Professor

Caryn E. Outten, Committee Member

Stephen L. Morgan, Committee Member

Michael Wyatt, Committee Member

Lacy Ford, Vice Provost and Dean of Graduate Studies

DEDICATION

This dissertation is dedicated in the memory of my loving dad, late Mr. Ratnakar M. Modi, you are missed a lot!

ACKNOWLEDGEMENTS

An undertaking of this nature is never possible by one person alone and I would like to thank everyone who has helped me in my Ph.D. journey. My first and utmost gratitude is to my adviser Dr. John Dawson, his unconditional support and encouragement have made it possible for me to make it this far in my academic career. Thanks to his attention, thoughtful feedback, and patience I have grown a lot as a researcher. He also has been a great advisor out of the academic area, always sharing interesting anecdotes and lessons. I would like to extend thanks to the rest of my committee, Dr. Caryn Outten, Dr. Stephen Morgan and Dr. Michael Wyatt for their time, support and helpful critique.

I am indebted to Dr. Masanori Sono for his time, patience and insight in helping me learn MCD spectroscopy and good data analysis techniques. His excellent work ethic and demand for excellence have helped me to build up my own, and I will always look up to him. I am also very thankful to the Dawson lab members, Dr. Indika Bandara, Dr. Jing Du, Dr. Dan Collins, Emily Johnson and Shengfang Sun for their guidance, humor and optimism. I have been fortunate to work on many collaborative projects and would like to thank my collaborators Dr. Nicole Dinkel-Frankenberg, Dr. Eleanor Wurtzel, Dr. Lionel Cheruzel and Dr. Angela Wilks for making me a part of their exciting projects.

I am thankful to all the wonderful people, here in the department of Chemistry and Biochemistry, particularly Dr. Mike Walla, Dr. Sheryl Wiskur, Dr. Thomas Makris and Dr. George Handy with whom I had the privilege to work and have valuable discussions. I would like to specially mention the staff in the Chemistry department office and stockroom for all their help. I would also like to mention all my friends here in Chemistry, Ravish, Anand, Purbasha, Diana, Andrea, Nikki, Timothy (Max), Avneesh, Atri, Sandipan, Kinkini, Rabindra and Tanya, thanks to you all it was great fun working here.

I would also like to specially mention my friends and roommates in Columbia for being my family away from home. Their presence, emotional support and humor at all times made for a smooth sailing journey. Thank you for giving me unforgettable memories of Columbia, Amit, Dhaval, Debopam, Pulkit, Prasanth, Chaitali, Krishna, Aditi, Gehana, Rupa, Swati, Rahul, Anshika, Kumud, and Rahul Tomar. I would also like to acknowledge my friends and relatives back home in India for their encouragement and good wishes.

Above everything I would like to thank my dear husband Ganesh for being a pillar of strength. Had it not been for his unconditional love, support and perseverance, it would have been impossible for me to accomplish this PhD through our long distance marriage! Many thanks to my dear mom and brother, Amit for their love, sacrifices, and prayers, words cannot express the gratitude I feel for them. On this occasion, I truly miss my Dad’s presence; his desire for me to be a PhD scholar was a major driving force in my work.

And last but not the least I would like to thank the Department of Chemistry and Biochemistry, the Graduate School and the International Student Services for giving me this wonderful opportunity and support to study at the University of South Carolina.

ABSTRACT

Cytochrome P450 (P450 or CYP) catalysis involves the oxygenation of organic compounds via a series of catalytic intermediates, namely, the ferric-peroxo, ferric-hydroperoxo, Compound I (Cpd I), and Fe^{III}–(H_2O_2) intermediates. The general consensus is that the Cpd I intermediate is the most reactive species in the reaction cycle, especially when the reaction involves hydrocarbon hydroxylation. Other than Cpd I, there is a multitude of evidence, both experimental as well as theoretical, supporting the involvement of other intermediates in various types of oxidation reactions. In part I of this work, the multiple oxidant hypothesis of P450 catalysis has been probed using P450-CAM from *Pseudomonas putida*, a prototypical P450 enzyme. P450-CAM is a versatile catalyst that has been shown to catalyze many typical P450 reactions in camphor analog substrates. The active site threonine-252 to alanine (T252A) mutant of P450-CAM on reaction with camphor yields H_2O_2 and minimal oxidized camphor, presumably because it makes very little Compound I while still generating the ferric-peroxo and ferric-hydroperoxo species. This makes T252A P450-CAM an ideal catalyst to probe the multiple oxidant hypothesis. Using heteroatom-containing substrates, including camphor analog substrates modified at the fifth position, we have compared the quantitative product formation between WT and T252A P450-CAM to gain an insight in the multiple oxidant hypothesis.

Magnetic circular dichroism (MCD) spectroscopy also known as the Faraday effect, is an excellent fingerprinting tool of various heme systems.

It can be used for assigning axial ligand identity, coordination numbers as well as spin state determination of the heme iron, which can lead to important information about their structures and functions. In part two of this work, we present results from the application of MCD spectroscopy in the axial ligand(s) identification analysis of three novel heme proteins, sGAF2, Z-ISO and Phu_R, and in the characterization of the dioxygen complex of an engineered P450BM3 protein.

TABLE OF CONTENTS

LIST OF TABLES

LIST OF FIGURES

LIST OF SCHEMES

LIST OF ABBREVIATIONS

CAM ....camphor

Cpd I or Cpd II .... compound I or II of a heme enzyme an Fe^{IV}=O radical cation species CPO, chloroperoxidase

CYP or P450 .... cytochrome P450

CYP119A1 .... orphan P450 from *Sulfolobus acidocaldarius*

CYP2B4 . phenobarbital-inducible rabbit liver microsomal P450 enzyme (P450LM2)

CYP2E1 .... alcohol-inducible rabbit liver microsomal P450 enzyme (P450LM3)

CYP51A1 .... lanosterol 14α-demethylase

Cyt b_5 .... cytochrome b_5

ENDOR ....electron-nuclear double resonance

ES ....enzyme-substrate complex

FAD ....flavin adenine dinucleotide

FMN .... flavin mononucleotide

heme iron protoporphyrin IX (heme-b)

H93G ....Myoglobin cavity mutant

HRP ....horseradish peroxidase

Im ....imidazole

KIE .... kinetic isotope effect

LA ....lauric acid

Mb .... myoglobin

MCD ....magnetic circular dichroism spectroscopy

NOS .... nitric oxide synthase enzyme

NPG .... N-palmitoylglycine

P450BM3 .... fatty acid hydroxylating P450 enzyme from *Bacillus megaterium*

P450BM3-Ru .... Ruthenium diimine photosensitizer bound P450BM3

P450CAM .... camphor-hydroxylating P450 enzyme from *Pseudomonas putida*

PA .... palmitic acid

phenol Lb A .... phenol bound legehemoglobin A

Phu_R ....heme containing outer membrane receptor from *Pseudomonas aeruginosa*

RH .... hydrocarbon substrate

ROH .... oxidized substrate

sGAF2 .... heme domain containing variant of MA4561 protein

ShuT .... periplasmic heme-binding protein from *Shigella dysenteriae*.

T252A .... Threonine 252 to Alanine mutant of P450CAM

THT .... tetrahydrothiphene

WT .... wild type

CHAPTER 1

Oxidizing Intermediates in P450 Catalysis:

A Case for Multiple Oxidants[1]

[1] Anuja R. Modi and John H. Dawson, accepted for publication in *Monooxygenase, Peroxidase and Peroxygenase Properties of Cytochrome P450 Enzymes and their Mechanisms of Action*. 5/23/2014.

Abstract:

Cytochrome P450 (P450 or CYP) catalysis involves the oxygenation of organic compounds via a series of catalytic intermediates, namely, the ferric-peroxo, ferric-hydroperoxo, Compound I (Cpd I) and Fe^{III}–(H_2O_2) intermediates. Now that the structures of P450 enzymes have been well established, a major focus of current research in the P450 area has been unraveling the intimate details and activities of these reactive intermediates. The general consensus is that the Cpd I intermediate is the most reactive species in the reaction cycle, especially when the reaction involves hydrocarbon hydroxylation. Cpd I has recently been characterized experimentally. Other than Cpd I, there is a multitude of evidence, both experimental as well as theoretical, supporting the involvement of other intermediates in various types of oxidation reactions. The involvement of these multiple oxidants has been experimentally demonstrated using P450 active-site mutants in epoxidation, heteroatom oxidation and dealkylation reactions. In this chapter, we will review the P450 reaction cycle and each of the reactive intermediates to discuss their role in oxidation reactions.

1.1 Introduction

Cytochrome P450 enzymes are heme-thiolate ligated monooxygenases that are ubiquitous in the biological kingdom and catalyze a variety of oxidation reactions covering a wide range of substrates.[1, 2] Hemeproteins are classified as P450s when their Fe^{II}–CO complex has a maximum Soret absorbance at 450 nm.[3] P450s were discovered five decades ago because of their important role in xenobiotic clearance from the human body, but the interesting nature of their chemistry has attracted attention from chemists, biochemists, biophysicists, structural biologists and now even biotechnologists. Oxygen activation is central to life as spin forbiddance makes ground-state triplet molecular oxygen by itself inert toward organic molecules.[4] Living beings therefore use enzyme systems for oxygen activation to perform biologically important reduction-oxidation (redox) reactions. P450s are one of the metal-containing oxygenases that utilize molecular oxygen to stereo- and regioselectively oxygenate substrates under physiological conditions. While P450s are capable of diverse reactions, they are in fact mostly known for their ability to catalyze the oxidation of inert substrate C–H bonds under physiological conditions. To put into perspective, the bond strength of a typical secondary C–H bond is about 101 kcal mol.[1 5] Present understanding of the P450 catalytic mechanism has been developed over the course of the last four decades by advances in genomics, molecular biology and spectroscopy.[6] Comparison with analogous heme oxygen activation systems has also greatly contributed to our current understanding of its mechanism. Knowledge of the P450 intermediates is now being used for development of efficient inorganic catalysts for laboratory and commercial use.[7] Alternatively, in biotechnological setups, P450s are being modified to catalyze stereoselective oxidation reactions.[8]

Oxidation of substrates by P450 can be summarized by the following equation:

$$\mathrm{R-H + NAD(P)H + O_2 + H^+ \rightarrow R-OH + NAD(P)^+ + H_2O}$$

The catalytic mechanism of P450s occurs in a cyclic fashion involving systematic generation of intermediates, some of which are transient.[9] Electrons for this oxidation reaction are provided by NAD(P)H and are shuttled to the P450 active site with the aid of reductase enzymes. Protons are donated by water molecules in the active site. Based on associated redox systems, P450s can be classified as type I or type II as shown in

Scheme. 1.1.[10] Type I P450s are mainly the mammalian mitochondrial and bacterial P450s, which utilize a flavoprotein to transfer electrons to P450s via an intervening iron-sulfur cluster protein (Fe_2S_2). Type II P450s are the mammalian xenobiotic-metabolizing enzymes that receive electrons via FAD- and FMN-containing reductases. There are certain exceptions such as P450BM3 in which the heme and FMN/FAD-containing reductase domains are part of a single polypeptide that functions as a self-sufficient unit.[11, 12]

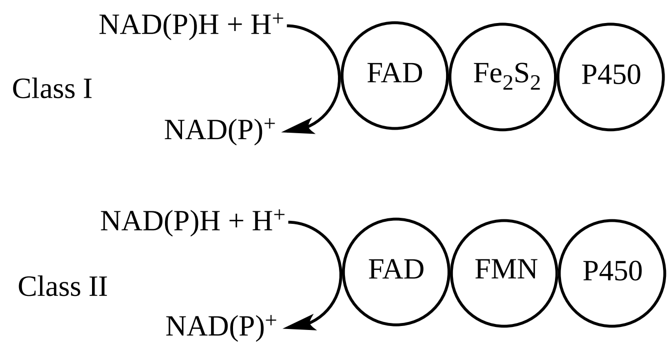

Scheme 1.1 Electron transfer chains in class I and class II of P450 enzymes, see Ref. 10.

1.2 The P450 Catalytic Cycle

P450-CAM (CYP101) is a bacterial P450 enzyme from *Pseudomonas putida* that converts 1R-(+)-camphor to 5-*exo*-hydroxycamphor. This enzyme is soluble and therefore easy to purify and was the first P450 whose crystal structure was solved.[13] Since then, its structure has been extensively studied and it has served as a prototype for structure-function studies of the entire P450 family. The reaction cycle for P450-CAM also holds true for the entire P450 family. The putative catalytic mechanism of P450s in which the substrate RH is oxidized to R-OH in a series of steps is shown in Scheme. 1.2. The catalytic cycle begins with the reversible substrate binding to the water-coordinated low-spin (S=1/2) resting state of the ferric enzyme (Scheme. 1.2, **1**). Substrate binding causes displacement of water as the sixth ligand to the heme with formation of the high-spin (S=5/2) pentacoordinate enzyme-substrate adduct (Scheme. 1.2, **2**). This causes the midpoint redox potential of the heme to shift to a more positive value (from −330 mV to −173 mV).[14] The sharp shift in the reduction potential resulting from substrate binding enables electrons to flow from NAD(P)H to the P450 enzyme via an associated reductase. The first electron generates the reduced ferrous-substrate adduct (Scheme. 1.2, **3**). Subsequent binding of dioxygen generates the oxyferrous complex or a resonance-stabilized ferric superoxide complex Fe^{+3}-$OO^{\bullet -}$, a η^1 superoxide radical anion coordinated to the ferric heme center with an unpaired electron on the terminal oxygen atom (Scheme. 1.2, **4**).[15] The second electron from NAD(P)H then reduces the oxyferrous complex resulting in the Fe^{+3}-OO^- (Scheme. 1.2, **5**) ferric-peroxo intermediate. This is also the rate-limiting step. Protonation of this intermediate leads to the Fe^{+3}-OOH (Scheme. 1.2, **6**) ferric-hydroperoxo intermediate, also known as Compound 0 (Cpd 0). A second protonation of this intermediate leads to O–O bond heterolysis forming the highly transient and reactive porphyrin π radical cation ferryl complex (Scheme. 1.2, **7**) known as Cpd I. Cpd I derives its name from the analogous high-valent Cpd I species of heme peroxidases.[16, 17] According to the now well-accepted mechanism for hydrocarbon hydroxylation, Cpd I abstracts a H atom from the substrate resulting in a ferryl hydroxyl intermediate (Scheme. 1.2, **8**) known as protonated Compound II (Cpd II) and a substrate radical. In what is known as the oxygen rebound, the hydroxyl moiety on the iron combines with the substrate radical to give the hydroxylated product, while the enzyme returns to its resting ferric state.

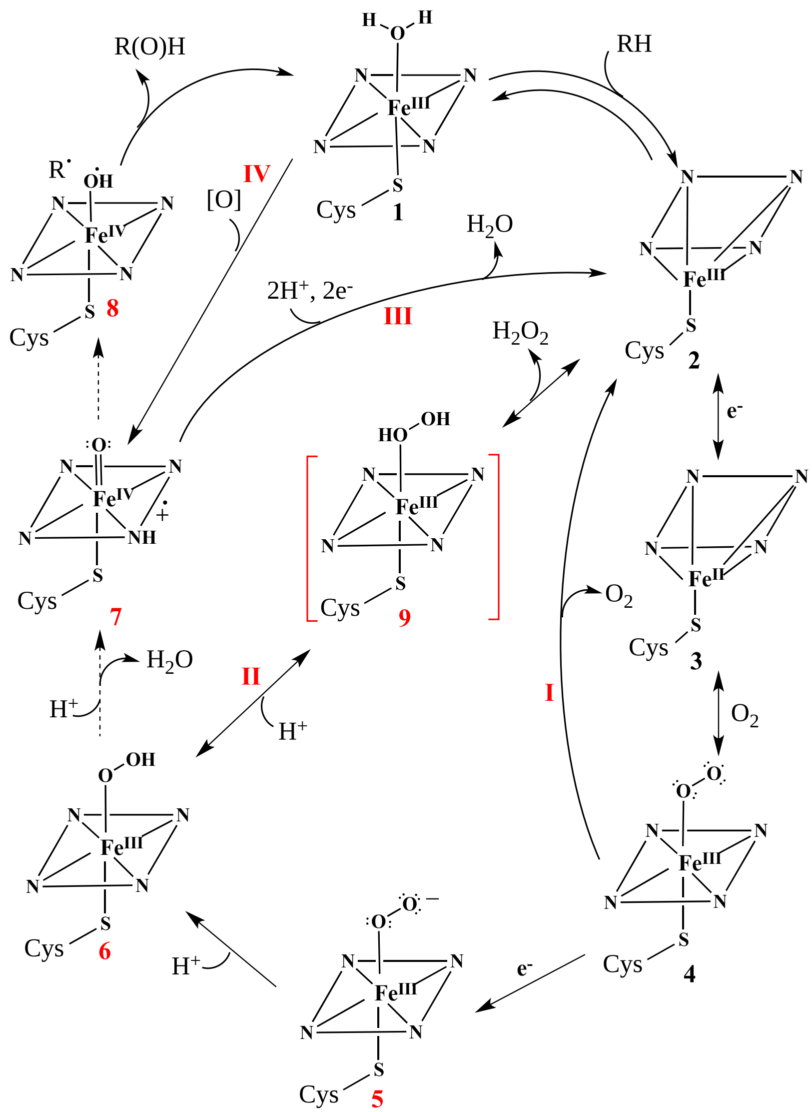

Scheme 1.2 Reactive intermediates and shunt pathways in the catalytic cycle of P450 enzymes.

In addition to the normal catalytic pathway, there are three uncoupling reactions within the cycle that lead back to the enzyme-substrate adduct without any product formation. The first is the auto-oxidation of the oxyferrous enzyme with simultaneous generation of a superoxide anion (Scheme. 1.2, **I**). In the second shunt pathway, the hydroperoxo anion dissociates from the ferric-hydroperoxo intermediate (Scheme. 1.2, **II**). Heterolytic cleavage of the O–O bond is critical for Cpd I formation. Incorrect protonation at the distal oxygen generates the Fe^{+3}-H_2O_2 intermediate (Scheme. 1.2, **9**) followed by dissociation of hydrogen peroxide without substrate turnover. This pathway is often seen in the active-site alcohol-alanine mutant.[18] In the oxidase shunt (Scheme. 1.2, **III**), the ferryl intermediate is reduced to water in lieu of substrate oxidation. In an alternative pathway to the normal reaction cycle, the enzyme can be turned over without the nucleotide-reducing equivalents via the peroxide shunt (Scheme. 1.2, **IV**). Cpd I can be generated from this pathway using oxygen atom donors such as peracids, peroxides and iodosobenzene.[19-21]

1.3 Nature of the P450 Active Site

There are over 20,000 known CYP genes (http://drnelson.uthsc.edu/CytochromeP450.html). P450s share their catalytic capabilities with other heme-containing enzymes, catalases, peroxidases and oxygenases, but they are all very different structurally. The architecture of the active site in P450s plays an important role in the sequential generation of intermediates in the catalytic cycle. For a complete understanding of P450 monooxygenation chemistry, the majority of research has focused on the factors influencing electron delivery and dioxygen binding to the heme iron, proton addition to the bound dioxygen in the distal pocket of the heme and cleavage of the O–O bond. Residues most important for oxygen activation are the heme proximal cysteine ligand (Cys357 in P450CAM) and the acid-alcohol pair in the distal pocket of the heme (Thr252-Asp251 in P450CAM). These amino acids are conserved in the active site of almost all P450s. Since the active site is hydrophobic, a chain of water molecules provides access to bulk solvent outside and is held in place by H-bonding to each other and to the alcohol residue in the active site (Thr252 in P450CAM).[22] The active site of camphor-bound oxy-P450-CAM is shown in Figure. 1.1.

In this landmark work, Schlichting and coworkers structurally characterized the oxyferrous complex of P450CAM using cryocrystallography. [9] Important residues involved in oxygen activation were Cys357, Asp251, Thr252 as well as the bound camphor substrate and are shown in Fig. 3. The hydroxyl group of Tyr96 H-bonds to the keto group of camphor to orient the site of oxygenation above the heme. The water molecules Wat901 and Wat902 seen in the active site are implicated as the source of protons required for formation of the active Fe^{IV}=O species. Accordingly, the Thr252 H-bonds to Wat901, which serves as the H-bond donor to the distal oxygen atom of the heme-bound dioxygen in P450CAM.

1.3.1 Role of Cys as Proximal Heme Ligand

The heme in P450 enzymes is of the heme-b type, where the iron protoporphyrin-IX is covalently linked to the protein backbone via a Fe-S bond to cysteine. In the case of P450CAM, Cys357 serves as the cysteine residue as seen in Figure. 1.1. The proximal cysteine thiolate ligand is indispensible for P450 catalytic activity and mutation of the cysteine residue leads to loss of activity.[23] In the P450 catalytic cycle, one electron reduction of the oxyferrous state followed by protonation of the distal oxygen leads to the ferric-hydroperoxo intermediate. A second protonation of the ferric-hydroperoxo intermediate followed by heterolytic cleavage of the O–O bond leads to formation of Cpd I, which is the primary oxidant in the cycle. Maintaining the cysteine as a thiolate anion on the proximal side of the heme at the same time as the iron in the ferrous state is crucial for Cpd I generation.[24]

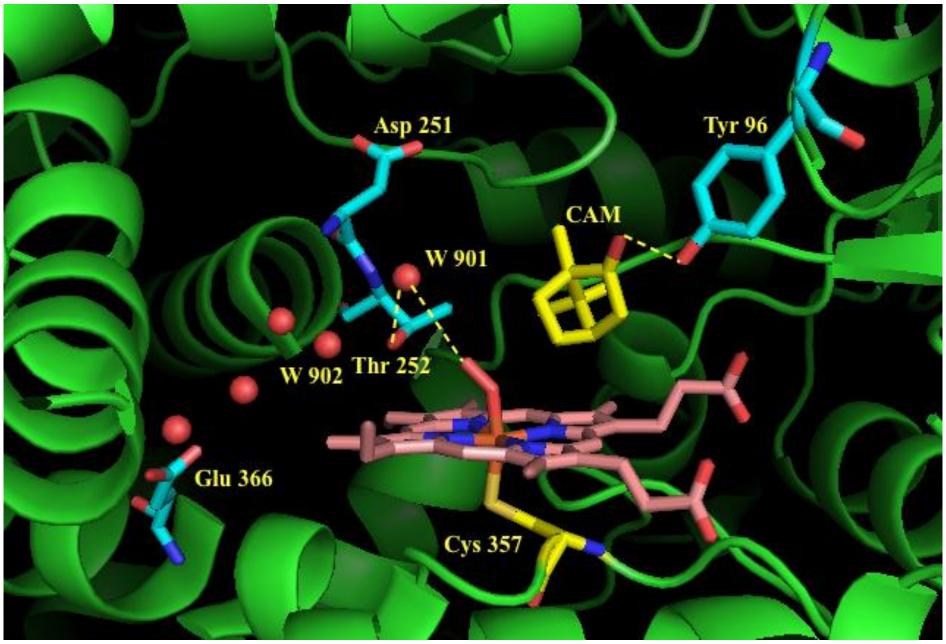

Figure 1.1 Active site of camphor-bound oxy-P450-CAM constructed using PDB file 1DZ8.[9]

The thiolate anion is stabilized by H bonds from the protons of the adjacent residues, Leu 358 (3.5 Å), Gly 359 (3.3 Å), Gln 360 (3.3 Å). Mutation of these residues led to distortion in H-bonding and an increase in the uncoupling of the ferric-hydroperoxo intermediate.[25, 26]

Dawson and coworkers suggested that the polarizable nature of the cysteine thiolate anion ligand provides a strong ‘push’ of electron density via the heme onto the O–O bond of the ferric-hydroperoxo intermediate, thus promoting heterolytic O–O bond cleavage.[27, 28] Furthermore, the electron-donating nature of the thiolate ligand also helps to stabilize the resulting Cpd I intermediate. This result is similar to the effect seen in cytochrome *c* peroxidase that contains a partially deprotonated proximal histidine ligand, wherein the imidazolate ‘push’ in concert with a ‘pull’ from the conserved distal His-Arg amino acids lead to heterolytic cleavage of the O–O bond to generate Cpd I.

1.3.2 Role of the Acid-Alcohol Pair in Oxygen Activation

An acid-alcohol pair that is highly conserved in almost all P450 enzymes aids oxygen activation in the distal heme pocket. The alcohol in most cases is threonine or serine and the acid can be aspartate or glutamate. In the case of P450CAM, these residues are Asp251-Thr252. Given their highly conserved nature and proximity to the heme-dioxygen binding site, the role of this acid-alcohol pair in catalysis has been examined in several mutagenesis studies. Specifically, the role of Thr was investigated by changing the residue to Ala. In P450CAM, the Thr252Ala mutant was almost completely uncoupled, leading to normal NADH and O_2 consumption but essentially no product formation.[18, 29] Based on this result in P450CAM and other P450s as well,[30, 31] the alcohol residue is thought to stabilize water molecules in the active site by H-bonding during substrate oxygenation.[18, 29, 32] Ishimura and coworkers demonstrated that the uncoupling reaction is promoted when the Thr in P450CAM is mutated to a Ser or Asn, thereby ascertaining the role of Thr in stabilizing the H-bonding network in the distal pocket and controlling proton delivery to the distal oxygen of bound dioxygen.[22] The Thr252Ser and Thr252Asn mutant enzymes retained more than half of the hydroxylating capability of the enzyme. The Thr252 residue also participated in H-bonding with the distal oxygen of the oxyferrous-P450 complex in P450CAM.[33] The high-resolution crystal structure of the P450CAM Thr252Ala mutant showed a clearly perturbed H-bonding network and excess water molecules in the active site.[32] It is thought that this perturbation leads to uncoupling due to incorrect delivery of the second proton to the proximal oxygen.[34] Just as in P450CAM, the Thr268 in P450BM3 has been shown to play an important role in sustaining the proton pathway from the bulk solvent to the dioxy-bound heme. Mutation of Thr268 to Ala also leads to uncoupling followed by reduced substrate oxidation.[30, 35]

Unlike the alcohol residue, the acid residue has an important role in electron transfer following oxyferrous intermediate formation. In P450CAM, the mutagenesis of Asp251 to Asn leads to decreased turnover in the mutant enzyme rather than uncoupling.[36, 37] The Asp251Asn mutant displays an increased kinetic solvent isotope effect compared to the wild-type enzyme and a directly linear correlation to NADH consumption on bulk proton concentration, indicating that the proton delivery pathway has been modified in the Asp251Asn mutant.[36] Structural analysis of the Asp251Asn mutant reveals significant changes in the active site. The Asn251 and Lys178 side chains rotate away from the active site and the Asn251 H-bonds to Asp182, causing open access to the heme.[36] The flexibility of the Asp251 side chain stabilized by electrostatic bonding plays an important role in dioxygen scission in P450CAM and suggests a similar role for the conserved acid functionality in other P450 enzymes.

1.4 Multiple Oxidants in P450 Catalysis

Although the P450s are a single family of enzymes, the wide variety of substrates oxidized by P450 is quite astounding. The catalytic cycle of P450s has been well established based on P450CAM as the prototype. The key catalytic intermediates have been detected and well characterized. Even the ferryl Cpd I intermediate, initially thought to be too short lived to detect has now been well characterized.[38] Despite the fact that this intermediate has not been detected in the normal P450 catalytic cycle, it has been observed in the peroxide shunt pathway and there is little doubt about its involvement in substrate oxidation. While the ferryl Cpd I intermediate is thought to be the oxidant of choice in most oxidation reactions, the nature of certain catalytic intermediates and comparison with analogous reactions catalyzed in other enzyme systems make it difficult to deny the existence of multiple oxidizing species in the catalytic cycle. As seen in Scheme 1.3, several reaction intermediates other than Cpd I are thought to be capable of catalyzing some oxidation reactions depending on the type of substrate.

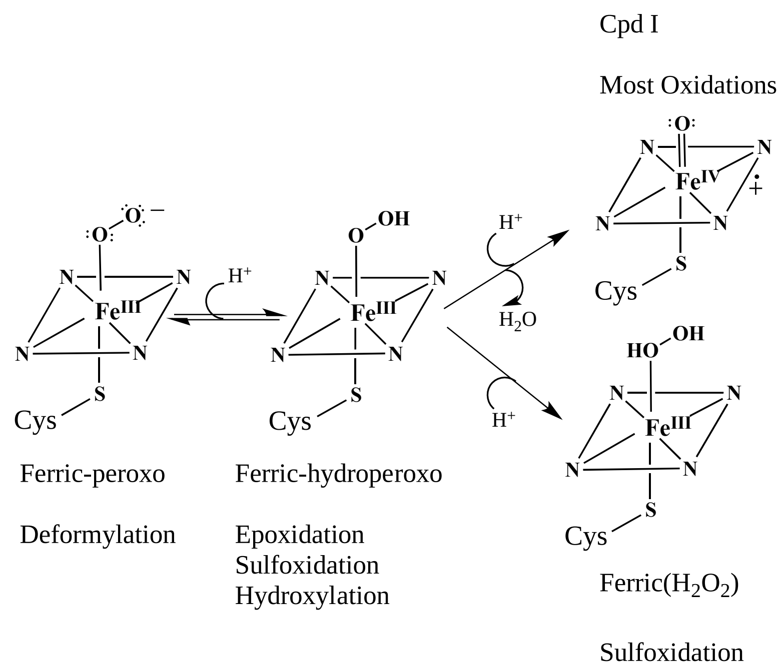

Scheme 1.3 Multiple P450 oxidants and types of reactions catalyzed.

1.4.1 The P450 Dioxygen Complex

In P450 enzymes, binding of dioxygen to the ferrous heme traps O_2 for substrate oxidation. This generates the ferrous-dioxygen complex (Fe^{+2}-OO), which is in resonance with the ferric superoxide complex (Fe^{+3}-OO^{-}) (Fig. 2, **4**). The binding constant of dioxygen to P450CAM is 1.7×10^6 M^{-1} s^{-1} at 4^o C.[39] The oxyferrous complex of P450s is not as stable as that of oxygen carrier proteins. In P450CAM, it is moderately stable in the presence of camphor and auto-oxidizes back to the ferric state at the rate of 0.01 s^{-1} at room temperature.[39, 40] The oxyferrous-P450 complex is similar to that of many of the analogous hemeproteins such as myoglobin, hemoglobin, CPO, NOS, etc.[41-44] The oxyferrous stretching band of oxyferrous P450CAM as determined by resonance Raman spectroscopy is 1141 cm^{-1}, which is typical for superoxide complexes.[45] Using cryocrystallization, the oxyferrous complex of P450CAM was determined at atomic resolution. A representative figure is shown in Scheme 1.4.[9]

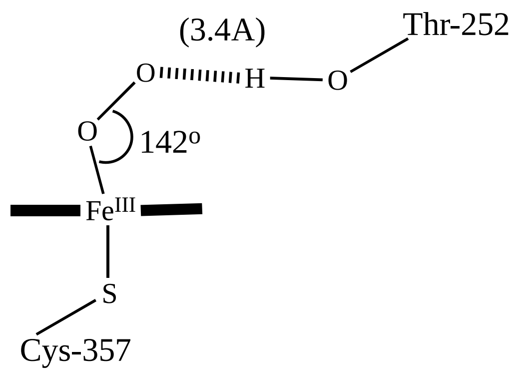

Scheme 1.4 Oxyferrous complex of P450-CAM determined using PDB file 1DZ8.[9]

The oxygen is coordinated to the heme iron in a slightly bent fashion with the Fe-O–O angle being 142°. The oxyferrous complex is stabilized with the aid of a H-bond between the distal oxygen and hydroxyl of the nearby Thr252 residue. While the oxyferrous complex by itself is not known to catalyze any oxidation reaction, its formation is necessary to generate the subsequent catalytic intermediates in the reaction cycle.

1.4.2 Ferric-peroxo Intermediate as a Nucleophilic Oxidant

Akhtar and coworkers first proposed a role for the ferric-peroxo intermediate in the final step of oxidative deformylation catalyzed by lanosterol 14 α-demethylase.[46, 47] The enzyme catalyzes the oxidative deformylation of lanosterol, concomitantly forming olefin in three oxidative steps, and each step utilizing a single equivalent of NADPH and O_2 as seen in Scheme 1.5. The final step results in cleavage of the C14–C32 bond with stereoselective removal of 15α-H, resulting in the formation of a 14,15 double bond and release of formic acid. The proposed mechanism involves homolytic cleavage of the O–O bond in a peroxy-aldehyde adduct to give an alkoxy free radical that decays to the olefin as a result of H abstraction by the simultaneously-created ferryl species.

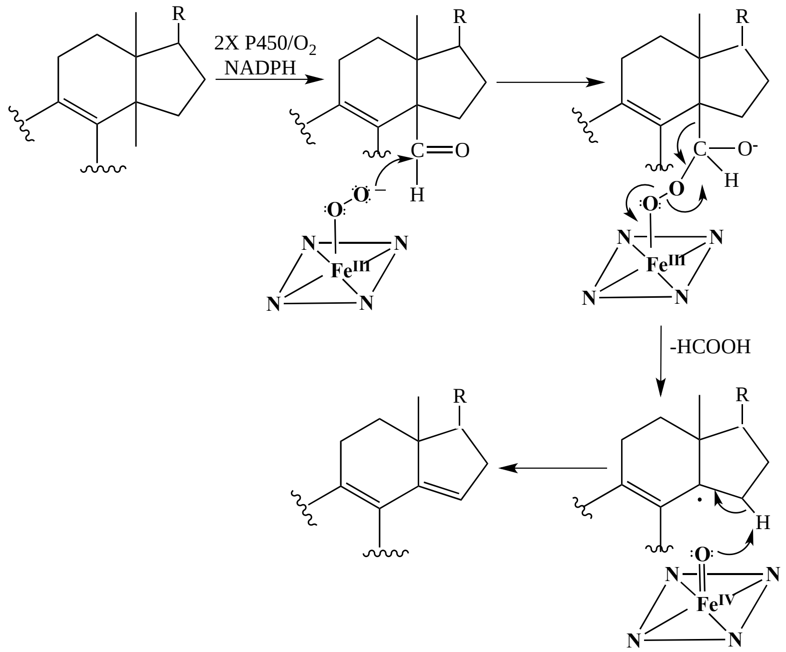

Scheme 1.5 Mechanism of oxidative deformylation catalyzed by lanosterol 14α-demethylase, see Ref. 47.

Similar mechanisms have also been proposed for demethylation in estrogen formation by aromatase (CYP19A1) and in the CYP17A1-catalyzed C–C bond scission of 17α-hydroxyprogesterone.[47, 48] The formic acid formed in these P450-catalyzed oxidative deformylations has been shown to retain the original carbonyl oxygen and hydrogen as well as an atom from molecular oxygen, clearly pointing to the involvement of the ferric-peroxo intermediate in the mechanism. In the CYP17A1 (17α-hydroxylase-17,20-lyase)–catalyzed reaction, oxygen labeling experiments also point to homolytic scission of the O–O bond in the peroxo-substrate adduct.[49] Vaz and coworkers analyzed the elimination reaction of the aliphatic aldehyde in the rabbit drug-metabolizing CYP2B4 enzyme. These reactions also seem to corroborate the involvement of peroxy anion-supported homolytic scission, followed by fragmentation of the adduct into a carbon radical and a formyl species that yields olefin products.[50] Further evidence supporting this mechanism is found when the carbon radical formed during the reaction inactivates the heme in P450.[51, 52]

The electrophilic nature of aldehydes makes them easily susceptible to attack from the nucleophilic peroxy anion. Such an example of nucleophilic attack is also seen in nitric acid synthase (NOS) (Scheme 1.6). NOS is a heme-containing enzyme that catalyzes the conversion of arginine to *N*-hydroxyarginine and then to citrulline and nitric oxide. The second step of this reaction has been proposed to involve nucleophilic addition of the ferric-peroxo species to the –C=NOH bond of the substrate.[53] Inorganic metalloporphyrins mimicking the ferric-peroxo intermediate have also been shown to catalyze the deformylation, as well as epoxidation, of α,β-unsaturated carbonyl groups.[54, 55]

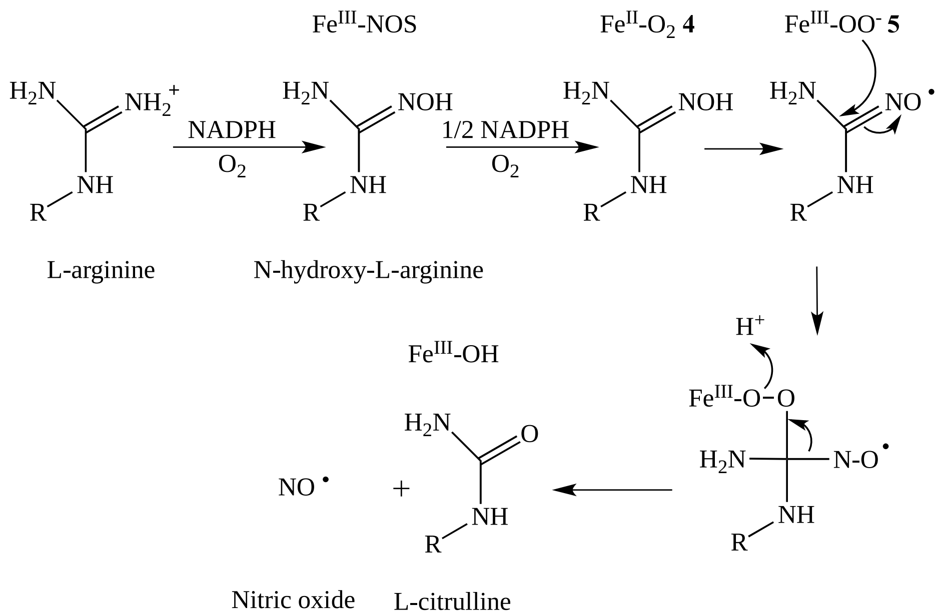

Scheme 1.6 Mechanism of oxidative deformylation catalyzed by NOS, see Ref. 53.

1.4.3 The Ferric-hydroperoxo Intermediate as an Electrophilic Oxidant

The ferric-hydroperoxo intermediate has been proposed as an oxidant in catalysis involving nucleophilic substrates. However, unlike in the case of the ferric-peroxo intermediate, the hypothetical involvement of the ferric-hydroperoxo species in oxidative catalysis is not supported by solid evidence. Given the electrophilic nature of most substrates oxidized by P450s, Cpd I is the clear favorite oxidant in these cases due to its high reactivity. The most compelling evidence for involvement of the ferric-hydroperoxo intermediate was demonstrated via substrate oxidation by active-site mutants in P450s. In P450CAM, the Thr252 alcohol side chain was mutated to Ala and the resulting Thr252Ala mutant was unable to catalyze the hydroxylation of camphor. Instead, the mutant was highly capable of accepting electrons from the nucleotide cofactor to convert dioxygen to hydrogen peroxide (Scheme 1.2, **II**).[18, 29] Improper protonation to the proximal oxygen of the ferric-peroxo intermediate thus leads to uncoupling. This mutant is, therefore, unable to form Cpd I but generates both the ferric-peroxo and ferric-hydroperoxo intermediates. ENDOR spectroscopic analysis of the cryoreduced Thr252Ala mutant shows a buildup of the ferric-hydroperoxo intermediate at 77 K. Annealing at high temperatures yields the ferric enzyme but no hydroxylated product.[56, 57] As such, the Thr mutant of several P450s has been used in the study of a number of electrophilic oxidation reactions.

Vaz, Coon and coworkers were the first to study the effects of the active-site Thr to Ala mutation in rabbit drug-metabolizing CYP2B4 and CYP2E1 enzymes using various alkene substrates (Scheme 1.7).[58] The researchers observed a decrease in allylic oxidation of the alkenes. In contrast, the Thr303Ala mutation in CYP2E1 significantly increased the rates of epoxidation compared to the wild-type enzyme.

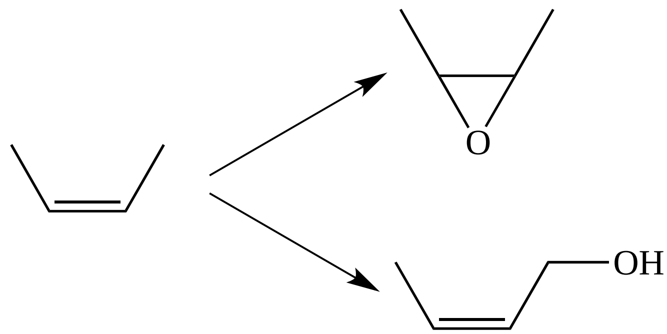

Scheme 1.7 Possible epoxidation reaction products in P450 enzymes.

On the other hand, the corresponding Thr302Ala mutant of CYP2B4 demonstrated reduced rates of both allylic hydroxylation and epoxidation. Increased epoxidation *versus* allylic hydroxylation was observed in the CYP2E1 Thr303Ala mutant and was construed as evidence that epoxidation could be catalyzed by the ferric-hydroperoxo intermediate, while decreased Cpd I formation led to decreased hydroxylation. However, failure to observe similar results with CYP2B4 along with high quantities of hydroxylated product made the data somewhat less reliable, apparently because Cpd I was still being generated to a significant extent.

Dawson and coworkers, in collaboration with the Sligar laboratory, studied the reactivity of the ferric-hydroperoxo intermediate in the Thr252Ala mutant of P450CAM using the alkene epoxidation reaction. Unlike the CYP2B4 and CYP2E1 enzymes, the Thr252Ala P450CAM mutant catalyzed the formation of less than 1% of the hydroxylated product, thus providing a more robust system to analyze the presence of a second oxidant, in this case the ferric-hydroperoxo intermediate. Both substrates were easily oxidized to epoxides (Scheme 1.8) at a rate of ~15–20% compared to that of wild-type P450CAM.[59] These results substantiated the work of Vaz and coworkers regarding the involvement of a second electrophilic oxidant. Shaik and coworkers examined alkene epoxidation in the context of the two-state reactivity theory involving Cpd I[60, 61] and proposed that the ferric-hydroperoxo species is a sluggish oxidant compared to the highly reactive Cpd I species. The researchers concluded that the ferric-hydroperoxo species has a large energy barrier to overcome, whereas ferric-hydroperoxo conversion to Cpd I is barrierless.[62] P450 reactivity also appears to be influenced by H-bonding to the proximal thiolate ligand and polarity changes in the vicinity.[62-64]

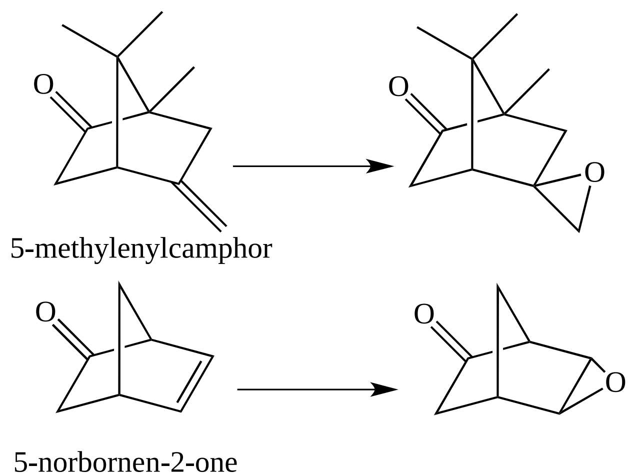

Scheme 1.8 Olefin epoxidation by P450 CAM, see Ref. 59.

P450 reactivity is also proposed to be influenced by changes in the relative amounts of high-spin and low- spin Cpd I, rather than amounts of the ferric-hydroperoxo and Cpd I species.[62]. However, the ‘two-state’ reactivity theory cannot clearly explain why the Thr252Ala mutant does not hydroxylate camphor. If the Cpd I oxidizing species only displays variation in the amounts of high-spin and low-spin states, the mutant enzyme should have displayed significant hydroxylation activity.

The ferric-hydroperoxo intermediate has also been investigated as a potential oxidant in heteroatom oxidations. Jones and coworkers have looked particularly at sulfoxidation and *N*-dealkylation reactions utilizing P450BM3. Using clever substrate design and the Thr268Ala mutant, the researchers sought to test whether the two products originated from the same oxidant species (Scheme 1.9).[65] Thus, substrate **10a** showed four times increased sulfoxidation activity compared to *N*-dealkylation activity. Next, the investigators used an isotopically-sensitive *N*-dealkylation substrate, **10b**, to test the premise that due to a large kinetic isotope effect (KIE), sulfoxidation activity would be higher than *N*-dealkylation activity if both products arose from a single oxidant.

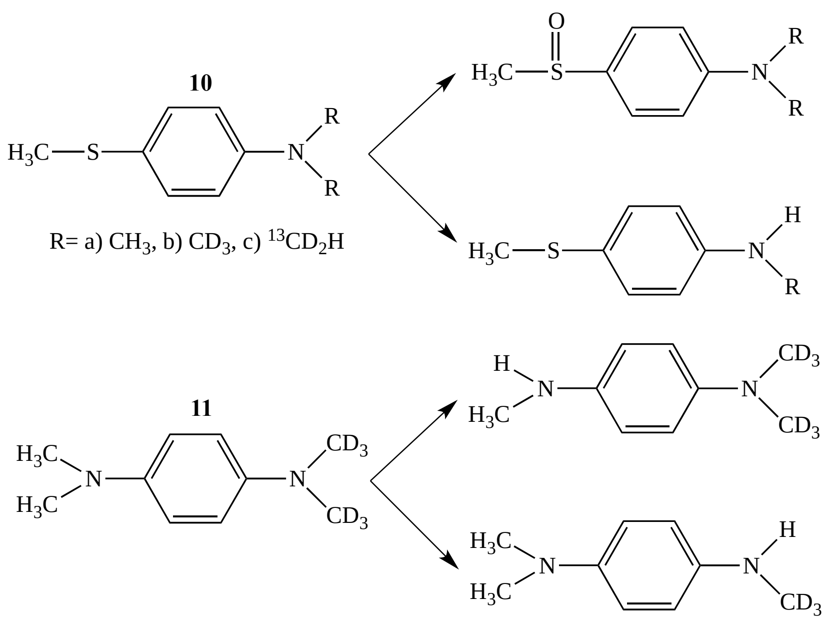

Scheme 1.9 Heteroatom oxidation by P450 BM3, see Ref. 65.

However, a negligible KIE was observed leading to several possible conclusions: (1) both products arose from different oxidants, (2) binding of substrate to the P450BM3 enzyme caused an interchange in the position of substituents, thereby changing their position in the catalytic site, and (3) the inherent KIE of *N*-dealkylation was very small. Using substrate **11**, the researchers were able to demonstrate the rapid interchange of substituents at the end of the molecule. This result combined with an intramolecular KIE for substrate **10c** eliminated the last two possibilities, leading to the proposal that both the *N*-dealkylation and sulfoxidation products arose from two different oxidants. The authors suggested that *N*-dealkylation was a product of Cpd I-mediated oxidation while sulfoxidation likely involved the ferric-hydroperoxo intermediate, without eliminating the possibility that the data could result from different forms of the same active oxygen species i.e Cpd I. In accordance with the ‘two-state’ state theory, where the low spin and high spin states form different enzyme-substrate (ES) complexes, the N-dealkylation and sulfoxidation reactions products can result from two non-interchangeable ES complexes.[63, 65] Watanabe has also proposed that the altered reactivity in the active site threonine to alanine mutants may be a result of the altered water molecule network in the active site, which affects the hydrogen bonding of the Cpd I-ES complex.[66] This alteration can skew the ratios of the low spin and high spin state of Cpd I, thereby affecting the mutant reactivity.

The ferric-hydroperoxo species has also been implicated as an oxidant in hydrocarbon hydroxylation reactions. Catalysis by the ferric-hydroperoxo species was proposed to involve a cationic protonated alcohol intermediate[67] (Scheme 1.10) as opposed to a radical intermediate formed in the radical rebound pathway (Scheme 1.2).

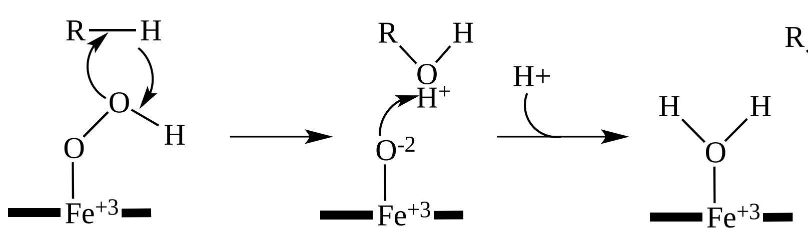

Scheme 1.10 Proposed hydrocarbon hydroxylation mechanism by the ferric-hydroperoxo species, see Ref. [67,68].

Newcomb and coworkers used ‘radical clock’ experiments to provide evidence for involvement of a cationic intermediate.[67-71] In the first of such studies, the oxidation of trans-1-methyl-2-(4-trifluoromethyl)-phenylcyclopropane was examined. The substrate could be oxygenated either on the methyl group yielding methyl alcohol as an unrearranged product or on the phenyl ring giving a ring-opened alcohol as a rearranged product. Using CYP2B1 as a biocatalyst, the substrate **12b** was shown to generate a ring-opened product, characteristic of a cationic rearrangement pathway (Scheme 1.11).[72]

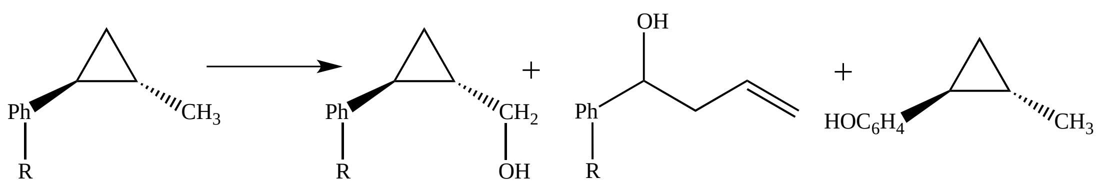

12a) R = H
12b) R= CF_3

Scheme 1.11 Radical clock probes for mechanistic elucidation in CYP2B4, see Ref. 72.

Reaction of substrate **12a** with the CYP2B4 Thr302Ala mutant enzyme showed a mixture of products, both unrearranged and rearranged methyl oxidation as well as phenyl ring oxidation products. There was little difference in the ratio of rearranged to unrearranged product between the wild-type and mutant enzyme. However, a higher ratio of phenyl oxidation was seen in the mutant enzyme. The authors suggested that this result clearly indicated an alternative oxidant at play in the mutant enzyme that preferred the easier phenyl ring oxidation. To suppress phenyl ring oxidation in substrate **12b**, the phenyl ring was replaced with an electron withdrawing $-CF_3$ group, which produced an altered ratio between the ring-opened and ring-closed products. This intimated a change in the oxidant in the hydroxylation reaction for that substrate. While these results satisfyingly conveyed involvement of the ferric-hydroperoxo species in the hydroxylation of certain substrates, the species is indeed a sluggish oxidant whereas Cpd I appears to be the oxidant of choice in hydrocarbon hydroxylations.[61] While the ferric-hydroperoxo species appears in almost all heme-based oxygen activation enzymes, there are a few examples where it plays a primary role in substrate oxidation. For example, heme oxygenase catalyzes the oxidation of heme to biliverdin[73] and the first step of this oxidation involves an α-*meso*-hydroxylation of the heme group that is thought to be catalyzed by an electrophilic oxidant, most likely, the ferric-hydroperoxo intermediate.[74-76]

1.4.4 Cpd I as the Most Powerful Oxidant

The mechanism of oxidation in P450s has been established by comparison with other heme-based oxygen activating enzymes as well as spectroscopic characterization of the reaction intermediates. P450s are similar to other metalloenzymes such as NOS and chloroperoxidase (CPO) in that they all have heme coordinated to a cysteine thiolate ligand. P450s and NOS are oxidoreductases that activate molecular oxygen.[77, 78] The P450s have long been presumed to oxidize substrates via a reactive porphyrin radical cation ferryl species known as Cpd I. Additional evidence for reactive intermediates was also collected by direct observation through a combination of various spectroscopic techniques.[79] Based on the observed activation of P450s by hydrogen peroxide, alkyl hydroperoxides, periodate and iodosobenzene, oxygen activation was assumed to occur by a two-electron reduction of dioxygen to the level of H_2O_2 followed by formation of the ferryl intermediate as seen in heme-containing peroxidases.[80] Synthetic metalloporphyrins could form a porphyrin radical cation (ferryl) species at low temperature in polar medium on reaction with peroxy acids and this intermediate had the reactivity to insert an oxygen atom into hydrocarbon substrates (Scheme 1.12).[81]

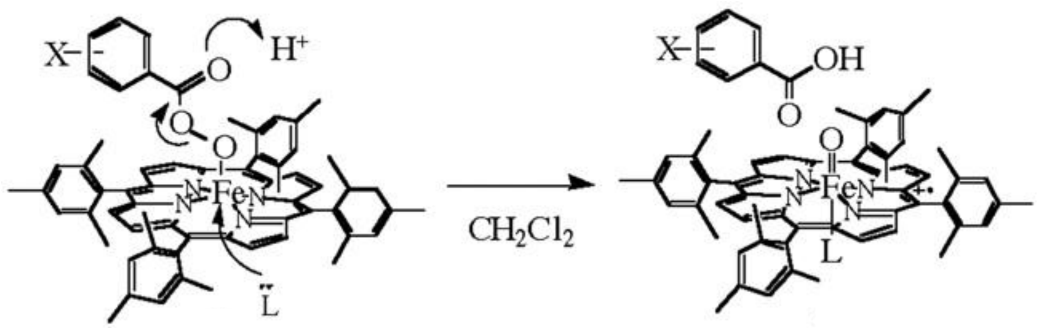

Scheme 1.12 Cpd I formation in synthetic metalloporphyrins by peroxy acids, reproduced with permission from Groves, J. T. (2003) The bioinorganic chemistry of iron in oxygenases and supramolecular assemblies, *Proc. Natl. Acad. Sci. U. S. A. 100*, 3569-3574, Copyright 2003 National Academy of Sciences, U.S.A.

When the transfer of an oxygen atom from the peroxy acid to produce the ferryl intermediate occurs, then the substrate is referred to as an 'oxygen-rebound' substrate.[82] Cpd I has been well characterized in CPO[83] and was thought to be elusive in P450s. However, recently, Green and coworkers were successfully able to directly observe Cpd I in CYP119A1 for the first time.[38] Cpd I was formed in about 75% yield by the reaction of ferric CYP119A1 with *m*-chloroperbenzoic acid. The resulting Cpd I species could then hydroxylate C–H bonds in lauric acid with an apparent rate constant of $k_{app} = 1.1 \times 10^7$. The Mossbauer spectrum of this Cpd I species was similar to that seen using Cpd I of CPO. The mechanism of oxygen transfer from Cpd I to form the hydroxylated product has been a hotly debated topic. The initially proposed concerted mechanism of oxygen insertion[84] fell aside in favor of the two-step H atom abstraction/oxygen rebound mechanism[82]. As explained in subsection 4.3, the ferric-hydroperoxo intermediate has also been implicated as an oxidant in a few hydrocarbon hydroxylations. ENDOR spectroscopic studies with cryoreduced wild-type P450CAM and its active-site mutants provided compelling evidence in favor of H atom abstraction/hydroxyl rebound.[57] Active oxidant species of P450CAM were prepared by cryoreduction at 77 K of the oxyferrous intermediate in the P450CAM-camphor complex. The ferric-peroxo and ferric-hydroperoxo intermediates were observed upon slowly warming to 119 K and were subsequently characterized by EPR and ENDOR spectroscopy. Around 200 K, the ferric-hydroperoxo species was quantitatively converted to 5-*exo*-hydroxycamphor, the natural product of camphor hydroxylation. While the ferryl intermediate was not observed directly, this oxidation was assumed to proceed through the hydroxyl intermediate because of the following observations in the experiment. After formation of the ferric-hydroperoxo species upon slowly warming of the sample, the first species observed had the hydroxyl group bound to the heme iron, as was expected for the H atom abstraction in the ferryl-involved mechanism. Had the ferric-hydroperoxo species been involved in the oxidation, it would have initially formed hydroxycamphor via hydroxy insertion of the distal oxygen atom of the ferric-hydroperoxo species. Hydroxycamphor would be required to displace the hydroxyl/water that was bound to heme, but this displacement reaction was implausible to occur at 200 K. Furthermore, ENDOR spectroscopy showed that the hydrogen attached to the hydroxyl oxygen in the hydroxycamphor product originated from the C-5 position of camphor, further supporting the ferryl mechanism. Involvement of the ferric-hydroperoxo species would have required this H atom to originate from the surrounding solvent.

Shaik and coworkers examined the mechanism of hydrocarbon hydroxylation using theoretical calculations and proposed a two-state reactivity instead of two-oxidant reactivity.[85-88] The researchers showed that the porphyrin radical cation ferryl species exists in two spin states, a quartet spin state and a doublet spin state that are close in energy. Both species initiate the reaction by nearly identical H atom abstraction transition states. The species in the doublet state can quickly collapse to the product in a barrierless reaction with no formation of an intermediate. This almost-concerted mechanism is aided by the increased interaction of the cysteine thiolate ligand with the heme iron, the push effect. On the other hand, the quartet state must overcome a significant energy barrier to form the product, thus allowing formation and rearrangements of radicals if any. The two-state reactivity model has provided a good explanation for the stereochemical scrambling and structural rearrangement resulting from the radical clock experiments. Direct observation and characterization of Cpd I has cemented the H atom abstraction/hydroxyl rebound mechanism of P450 enzymes.[89]

1.4.5 Fe^{III}–(H_2O_2) as an Oxidant in Sulfoxidation Reactions

As described earlier, Jones and coworkers, based on the oxidation of a substrate with both amine and thioether functional groups in P450BM3, proposed that two different oxidants can be responsible for their oxidation. The ferric-hydroperoxo species was proposed as the oxidant responsible for sulfur oxidation.[65] In the same vein, De Voss and coworkers analyzed the oxidation of thia fatty acids using P450BM3 (Scheme 1.13).[90]

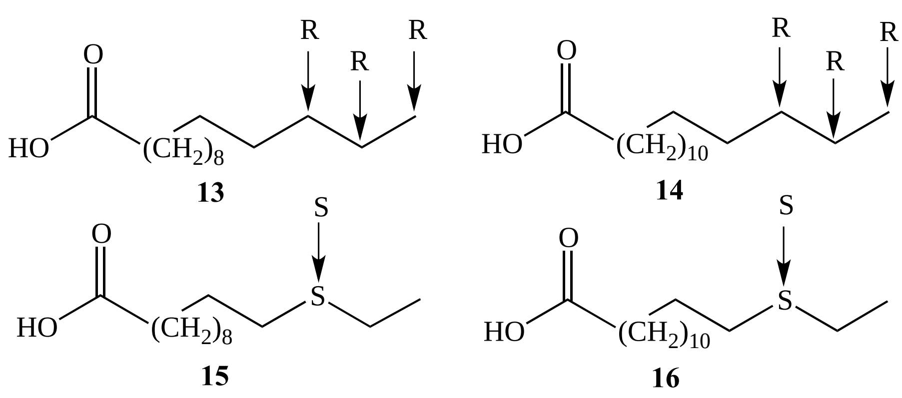

Scheme 1.13 Fatty acid oxidation by P450BM3, arrows indicate sites of oxidation and stereochemistry of products formed, see Ref. 90.

Analysis of the products indicated that presence of the thioether functionality dramatically shifted the regiochemistry of the reaction. With substrates **13** and **14**, the oxidation was distributed across the last three methylene groups. However, replacement of the second methylene group with sulfur resulted in the oxidation in **15** and **16** occurring exclusively at the sulfur. Interestingly, the sulfoxides were S enantiomers whereas the alcohols were R enantiomers. While it was speculated that thioethers undergo unusual binding to yield S sulfoxides, it has been shown in the past that modified fatty acids undergo R oxidation exclusively.[90-92] Substrates were also reacted with the P450BM3 Thr268Ala active-site mutant, based on previous studies showing that the mutant enzyme formed very little Cpd I and was able to accumulate the ferric-hydroperoxo species.[18, 29, 30] Despite the low turnover in the mutant for substrate **14**, product distribution and enantioselectivity remained unchanged between the wild-type and mutant enzyme. This demonstrated that there occurred reduced Cpd I formation in the mutant. For the thia fatty acid substrates, negligible change was observed in the turnover, product distribution and enantioselectivity of the products between the products of the wild-type and mutant enzyme. The authors proposed that sulfur oxidation must be easily catalyzed by the ferric-hydroperoxo species, thereby enabling the mutant enzyme to form comparable amounts of product compared to that of the wild-type enzyme.[90]

However, Shaik and coworkers have recently used theoretical calculations to show that the Fe^{III}–(H_2O_2) complex (Scheme 1.2, **9**) is a very efficient oxidant for sulfoxidation reactions in P450s and iron corrolazine compounds.[93] The Fe^{III}–(H_2O_2) complex was shown to undergo a nucleophilic attack from the distal oxygen atom of the peroxo complex resulting in heterolytic O–O bond scission that is coupled to proton transfer (Scheme 1.14). The Fe^{III}–(H_2O_2) complex could also catalyze the oxidation on sulfur much faster than could Cpd I. The ferric-hydroperoxo intermediate, in contrast, had a high barrier via the homolysis pathway of oxygen insertion.[93] This finding offers a new paradigm for sulfoxidation reactions in P450s and their synthetic monologues.

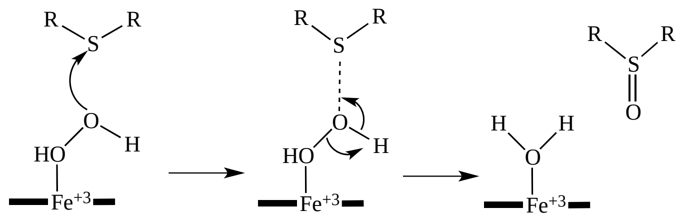

Scheme 1.14 Fatty acid oxidation by P450BM3, arrows indicate sites of oxidation and stereochemistry of products formed, see Ref. 93.

1.5 Conclusions

The mechanistic complexity of P450 enzymes has been intensely debated for the last few decades. The recent direct observation of P450 Cpd I and resulting studies of its reactivity have provided strong support for the validity of the hydrogen atom abstraction/radical rebound mechansim. The role of the ferric-peroxo intermediate as a nucleophilic oxidant is also well established. The proposed role of the ferric-hyroperoxo intermediate as an electrophilic oxidant remains to be established. Its role as an oxidant has been proposed mainly based on turnover studies in P450 mutants with impaired ability to form Cpd I. A recent addition to this oxidant puzzle is the Fe^{III}–(H_2O_2) intermediate which has been proposed to be more active than Cpd I in thio-ether oxidation reactions. The two-state reactivity theory involving Cpd I has also provided some explanations for the disparate experimental data. Additional experimental and theoretical data are still needed to provide further insights into the mechanisms of P450 catalysis.

1.6 References

1. Poulos, T. L., and Johnson, E. F. (2005) Structures of Cytochrome P450 Enzymes, In *Cytochrome P450: Structure, Mechanism, and Biochemistry* (DeMontellano, P. R. O., Ed.) 3rd ed., pp 87-114, Kluwer Academic/ Plenum, New York.

2. Sono, M., Roach, M. P., Coulter, E. D., and Dawson, J. H. (1996) Heme-Containing Oxygenases, *Chem. Rev. 96*, 2841-2888.

3. Omura, T., and Sato, R. (1964) The Carbon Monoxide-binding Pigment of Liver Microsomes: I. Evidence for its hemoprotein nature., *J. Biol. Chem. 239*, 2370-2378.

4. Filatov, M., Reckien, W., Peyerimhoff, S. D., and Shaik, S. (2000) What Are the Reasons for the Kinetic Stability of a Mixture of H2 and O2, *J. Phys. Chem. A 104*, 12014-12020.

5. Blanksby, S. J., and Ellison, G. B. (2003) Bond Dissociation Energies of Organic Molecules, *Acc. Chem. Res. 36*, 255-263.

6. Sligar, S. G., Makris, T. M., and Denisov, I. G. (2005) Thirty years of microbial P450 monooxygenase research: Peroxo-heme intermediates—The central bus station in heme oxygenase catalysis, *Biochem. Biophys. Res. Commun. 338*, 346-354.

7. Meunier, B. (1992) Metalloporphyrins as versatile catalysts for oxidation reactions and oxidative DNA cleavage, *Chem. Rev. 92*, 1411-1456.

8. Glieder, A., Farinas, E. T., and Arnold, F. H. (2002) Laboratory evolution of a soluble, self-sufficient, highly active alkane hydroxylase, *Nat Biotech 20*, 1135-1139.

9. Schlichting, I., Berendzen, J., Chu, K., Stock, A. M., Maves, S. A., Benson, D. E., Sweet, R. M., Ringe, D., Petsko, G. A., and Sligar, S. G. (2000) The Catalytic Pathway of Cytochrome P450cam at Atomic Resolution, *Science 287*, 1615-1622.

10. Nebert, D. W., and Gonzalez, F. J. (1987) P450 Genes: Structure, Evolution, and Regulation, *Annu. Rev. Biochem. 56*, 945-993.

11. Narhi, L. O., and Fulco, A. J. (1986) Characterization of a catalytically self-sufficient 119,000-dalton cytochrome P-450 monooxygenase induced by barbiturates in Bacillus megaterium, *J. Biol. Chem. 261*, 7160-7169.

12. Ruettinger, R. T., Wen, L. P., and Fulco, A. J. (1989) Coding nucleotide, 5' regulatory, and deduced amino acid sequences of P-450BM-3, a single peptide cytochrome P-450:NADPH-P-450 reductase from Bacillus megaterium, *J. Biol. Chem. 264*, 10987-10995.

13. Poulos, T. L., Finzel, B. C., Gunsalus, I. C., Wagner, G. C., and Kraut, J. (1985) The 2.6-A crystal structure of Pseudomonas putida cytochrome P-450, *J. Biol. Chem. 260*, 16122-16130.

14. Gunsalus, I. C., Pederson, T. C., and Sligar, S. G. (1975) Oxygenase-Catalyzed Biological Hydroxylations, *Annu. Rev. Biochem. 44*, 377-407.

15. Meunier, B., de Visser, S. P., and Shaik, S. (2004) Mechanism of Oxidation Reactions Catalyzed by Cytochrome P450 Enzymes, *Chem. Rev. 104*, 3947-3980.

16. Winfield, M. E. (1965) Mechanisms of oxygen uptake: The autoxidation of myoglobin and of reduced cyanocobaltates and their significance to oxidase reactions., In *Oxidases and Related Redox Systems* (T.E. King, H.S. Mason, and Morrison, M., Eds.), pp 115-130, Wiley, New York.

17. Dunford, H. B., and Stillman, J. S. (1976) On the function and mechanism of action of peroxidases, *Coord. Chem. Rev. 19*, 187-251.

18. Imai, M., Shimada, H., Watanabe, Y., Matsushima-Hibiya, Y., Makino, R., Koga, H., Horiuchi, T., and Ishimura, Y. (1989) Uncoupling of the cytochrome P-450cam monooxygenase reaction by a single mutation, threonine-252 to alanine or valine: possible role of the hydroxy amino acid in oxygen activation, *Proc Natl Acad Sci U S A 86*, 7823-7827.

19. Egawa, T., Shimada, H., and Ishimura, Y. (1994) Evidence for Compound I Formation in the Reaction of Cytochrome-P450cam with m-Chloroperbenzoic Acid, *Biochem. Biophys. Res. Commun. 201*, 1464-1469.

20. Schünemann, V., Lendzian, F., Jung, C., Contzen, J., Barra, A.-L., Sligar, S. G., and Trautwein, A. X. (2004) Tyrosine Radical Formation in the Reaction of Wild Type and Mutant Cytochrome P450cam with Peroxy Acids: A multifrequency EPR study of intermediates on the millisecond time scale, *J. Biol. Chem. 279*, 10919-10930.

21. Spolitak, T., Dawson, J. H., and Ballou, D. P. (2005) Reaction of Ferric Cytochrome P450cam with Peracids: Kinetic chracterization of intermediates on the reaction pathway, *J. Biol. Chem. 280*, 20300-20309.

22. Shimada, H., Y Watanabe, M. Imai, R. Makino, H. Koga, T Horiuchi et al. (1991) The role of threonine252 in the oxygen activation by cytochrome P-450cam: Mechanistic studies by site-directed mutagenesis., In *Dioxygen Activation and Homogeneous Catalytic Oxidation.* (Simandi, L. I., Ed.), pp 3136-3319, Elsevier Science Publishers, Amsterdam.

23. Auclair, K., Moënne-Loccoz, P., and Ortiz de Montellano, P. R. (2001) Roles of the Proximal Heme Thiolate Ligand in Cytochrome P450cam, *J. Am. Chem. Soc. 123*, 4877-4885.

24. Perera, R., Sono, M., Sigman, J. A., Pfister, T. D., Lu, Y., and Dawson, J. H. (2003) Neutral thiol as a proximal ligand to ferrous heme iron: Implications for heme proteins that lose cysteine thiolate ligation on reduction, *Proc Natl Acad Sci U S A 100*, 3641-3646.

25. Yoshioka, S., Takahashi, S., Ishimori, K., and Morishima, I. (2000) Roles of the axial push effect in cytochrome P450cam studied with the site-directed mutagenesis at the heme proximal site, *J. Inorg. Biochem. 81*, 141-151.

26. Yoshioka, S., Tosha, T., Takahashi, S., Ishimori, K., Hori, H., and Morishima, I. (2002) Roles of the Proximal Hydrogen Bonding Network in Cytochrome P450cam-Catalyzed Oxygenation, *J. Am. Chem. Soc. 124,* 14571-14579.

27. Dawson, J. H. (1988) Probing structure-function relations in heme-containing oxygenases and peroxidases, *Science 240*, 433-439.

28. Dawson, J. H., Holm, R. H., Trudell, J. R., Barth, G., Linder, R. E., Bunnenberg, E., Djerassi, C., and Tang, S. C. (1976) Oxidized cytochrome P-450. Magnetic circular dichroism evidence for thiolate ligation in the substrate-bound form. Implications for the catalytic mechanism, *J. Am. Chem. Soc. 98*, 3707-3709.

29. Martinis, S. A., Atkins, W. M., Stayton, P. S., and Sligar, S. G. (1989) A conserved residue of cytochrome P-450 is involved in heme-oxygen stability and activation, *J. Am. Chem. Soc. 111*, 9252-9253.

30. Yeom, H., Sligar, S. G., Li, H., Poulos, T. L., and Fulco, A. J. (1995) The role of Thr268 in oxygen activation of cytochrome P450BM-3, *Biochemistry 34*, 14733-14740.

31. Imai, Y., and Nakamura, M. (1988) The importance of threonine-301 from cytochromes P-450 (laurate (ω-1)-hydroxylase and testosterone 16α-hydroxylase) in substrate binding as demonstrated by site-directed mutagenesis, *FEBS Lett. 234*, 313-315.

32. Raag, R., Martinis, S. A., Sligar, S. G., and Poulos, T. L. (1991) Crystal structure of the cytochrome P-450CAM active site mutant Thr252Ala, *Biochemistry 30*, 11420-11429.

33. Schlichting, I., Berendzen, J., Chu, K., Stock, A. M., Maves, S. A., Benson, D. E., Sweet, B. M., Ringe, D., Petsko, G. A., and Sligar, S. G. (2000) The catalytic pathway of cytochrome P450cam at atomic resolution, *Science 287*, 1615-1622.

34. Harris, D. L., and Loew, G. H. (1996) Investigation of the Proton-Assisted Pathway to Formation of the Catalytically Active, Ferryl Species of P450s by Molecular Dynamics Studies of P450eryF, *J. Am. Chem. Soc. 118*, 6377-6387.

35. Truan, G., and Peterson, J. A. (1998) Thr268 in substrate binding and catalysis in P450BM-3, *Arch Biochem Biophys 349*, 53-64.

36. Vidakovic, M., Sligar, S. G., Li, H., and Poulos, T. L. (1998) Understanding the Role of the Essential Asp251 in Cytochrome P450cam Using Site-Directed Mutagenesis, Crystallography, and Kinetic Solvent Isotope Effect†, *Biochemistry 37*, 9211-9219.

37. Gerber, N. C., and Sligar, S. G. (1994) A role for Asp-251 in cytochrome P-450cam oxygen activation, *J. Biol. Chem. 269*, 4260-4266.

38. Rittle, J., and Green, M. T. (2010) Cytochrome P450 Compound I: Capture, Characterization, and C-H Bond Activation Kinetics, *Science 330*, 933-937.

39. Loida, P. J., and Sligar, S. G. (1993) Molecular recognition in cytochrome P-450: Mechanism for the control of uncoupling reactions, *Biochemistry 32*, 11530-11538.

40. Eisenstein, L., Debey, P., and Douzou, P. (1977) P450cam: Oxygenated complexes stabilized at low temperature, *Biochem. Biophys. Res. Commun. 77*, 1377-1383.

41. Antonini, E., and Brunori, M. (1971) In *Hemoglobin and Myoglobin in Their Reactions with Ligands* (Neuberger, A., and Tatum, T. L., Eds.), North-Holland Publishing Co., Amsterdam.

42. Couture, M., Stuehr, D. J., and Rousseau, D. L. (2000) The Ferrous Dioxygen Complex of the Oxygenase Domain of Neuronal Nitric-oxide Synthase, *J. Biol. Chem. 275*, 3201-3205.

43. Macdonald, I. D. G., Sligar, S. G., Christian, J. F., Unno, M., and Champion, P. M. (1998) Identification of the Fe−O−O Bending Mode in Oxycytochrome P450cam by Resonance Raman Spectroscopy, *J. Am. Chem. Soc. 121*, 376-380.

44. Sono, M., Eble, K. S., Dawson, J. H., and Hager, L. P. (1985) Preparation and properties of ferrous chloroperoxidase complexes with dioxygen, nitric oxide, and an alkyl isocyanide. Spectroscopic dissimilarities between the oxygenated forms of chloroperoxidase and cytochrome P-450, *J. Biol. Chem. 260*, 15530-15535.

45. Bangcharoenpaurpong, O., Rizos, A. K., Champion, P. M., Jollie, D., and Sligar, S. G. (1986) Resonance Raman detection of bound dioxygen in cytochrome P-450cam, *J. Biol. Chem. 261*, 8089-8092.

46. Fischer, R. T., Trzaskos, J. M., Magolda, R. L., Ko, S. S., Brosz, C. S., and Larsen, B. (1991) Lanosterol 14 alpha-methyl demethylase. Isolation and characterization of the third metabolically generated oxidative demethylation intermediate, *J. Biol. Chem. 266*, 6124-6132.

47. Akhtar, M., Corina, D., Miller, S., Shyadehi, A. Z., and Wright, J. N. (1994) Mechanism of the Acyl-Carbon Cleavage and Related Reactions Catalyzed by Multifunctional P-450s: Studies on Cytochrome P-45017.alpha, *Biochemistry 33*, 4410-4418.

48. Akhtar, M., Alexander, K., Boar, R. B., McGhie, J. F., and Barton, D. H. (1978) Chemical and enzymic studies on the characterization of intermediates during the removal of the 14alpha-methyl group in cholesterol biosynthesis. The use of 32-functionalized lanostane derivatives, *Biochem. J. 169*, 449-463.

49. Corina, D. L., Miller, S. L., Wright, J. N., and Akhtar, M. (1991) The mechanism of cytochrome P-450 dependent C-C bond cleavage: studies on 17[small alpha]-hydroxylase-17,20-lyase, *J. Chem. Soc., Chem. Commun.*, 782-783.

50. Roberts, E. S., Vaz, A. D., and Coon, M. J. (1991) Catalysis by cytochrome P-450 of an oxidative reaction in xenobiotic aldehyde metabolism: deformylation with olefin formation, *Proc Natl Acad Sci U S A 88*, 8963-8966.

51. Kuo, C.-L., Raner, G. M., Vaz, A. D. N., and Coon, M. J. (1999) Discrete Species of Activated Oxygen Yield Different Cytochrome P450 Heme Adducts from Aldehydes†, *Biochemistry 38*, 10511-10518.

52. Bestervelt, L. L., Vaz, A. D., and Coon, M. J. (1995) Inactivation of ethanol-inducible cytochrome P450 and other microsomal P450 isozymes by trans-4-hydroxy-2-nonenal, a major product of membrane lipid peroxidation, *Proc Natl Acad Sci U S A 92*, 3764-3768.

53. Korth, H. G., Sustmann, R., Thater, C., Butler, A. R., and Ingold, K. U. (1994) On the mechanism of the nitric oxide synthase-catalyzed conversion of N omega-hydroxyl-L-arginine to citrulline and nitric oxide, *J. Biol. Chem. 269*, 17776-17779.

54. Wertz, D. L., Sisemore, M. F., Selke, M., Driscoll, J., and Valentine, J. S. (1998) Mimicking Cytochrome P-450 2B4 and Aromatase: Aromatization of a Substrate Analogue by a Peroxo Fe(III) Porphyrin Complex, *J. Am. Chem. Soc. 120*, 5331-5332.

55. Sisemore, M. F., Burstyn, J. N., and Valentine, J. S. (1996) Epoxidation of Electron-Deficient Olefins by a Nucleophilic Iron(III) Peroxo Porphyrinato Complex, Peroxo(tetramesitylporphyrinato)ferrate(1−), *Angew. Chem. Int. Ed 35*, 206-208.

56. Davydov, R., Macdonald, I. D. G., Makris, T. M., Sligar, S. G., and Hoffman, B. M. (1999) EPR and ENDOR of Catalytic Intermediates in Cryoreduced Native and Mutant Oxy-Cytochromes P450cam: Mutation-Induced Changes in the Proton Delivery System, *J. Am. Chem. Soc. 121*, 10654-10655.

57. Davydov, R., Makris, T. M., Kofman, V., Werst, D. E., Sligar, S. G., and Hoffman, B. M. (2001) Hydroxylation of Camphor by Reduced Oxy-Cytochrome P450cam: Mechanistic Implications of EPR and ENDOR Studies of Catalytic Intermediates in Native and Mutant Enzymes, *J. Am. Chem. Soc. 123*, 1403-1415.

58. Vaz, A. D. N., McGinnity, D. F., and Coon, M. J. (1998) Epoxidation of olefins by cytochrome P450: Evidence from site-specific mutagenesis for hydroperoxo-iron as an electrophilic oxidant, *Proc Natl Acad Sci U S A 95*, 3555-3560.

59. Jin, S., Makris, T. M., Bryson, T. A., Sligar, S. G., and Dawson, J. H. (2003) Epoxidation of Olefins by Hydroperoxo−Ferric Cytochrome P450, *J. Am. Chem. Soc. 125*, 3406-3407.

60. de Visser, S. P., Ogliaro, F., Harris, N., and Shaik, S. (2001) Multi-State Epoxidation of Ethene by Cytochrome P450: A Quantum Chemical Study, *J. Am. Chem. Soc. 123*, 3037-3047.

61. de Visser, S. P., Ogliaro, F., Sharma, P. K., and Shaik, S. (2002) What Factors Affect the Regioselectivity of Oxidation by Cytochrome P450? A DFT Study of Allylic Hydroxylation and Double Bond Epoxidation in a Model Reaction, *J. Am. Chem. Soc. 124*, 11809-11826.

62. Ogliaro, F., Cohen, S., de Visser, S. P., and Shaik, S. (2000) Medium Polarization and Hydrogen Bonding Effects on Compound I of Cytochrome P450: What Kind of a Radical Is It Really?, *J. Am. Chem. Soc. 122*, 12892-12893.

63. Ogliaro, F., de Visser, S. P., Cohen, S., Sharma, P. K., and Shaik, S. (2002) Searching for the Second Oxidant in the Catalytic Cycle of Cytochrome P450: A Theoretical Investigation of the Iron(III)-Hydroperoxo Species and Its Epoxidation Pathways, *J. Am. Chem. Soc. 124*, 2806-2817.

64. de Visser, S. P., Ogliaro, F., Sharma, P. K., and Shaik, S. (2002) Hydrogen Bonding Modulates the Selectivity of Enzymatic Oxidation by P450: Chameleon Oxidant Behavior by Compound I, *Angew. Chem. Int. Ed. 41*, 1947-1951.

65. Volz, T. J., Rock, D. A., and Jones, J. P. (2002) Evidence for Two Different Active Oxygen Species in Cytochrome P450 BM3 Mediated Sulfoxidation and N-Dealkylation Reactions, *J. Am. Chem. Soc. 124*, 9724-9725.

66. Watanabe, Y. (2001) Alternatives to the oxoferryl porphyrin cation radical as the proposed reactive intermediate of cytochrome P450: two-electron oxidized Fe(III) porphyrin derivatives, *J. Biol. Inorg. Chem. 6*, 846-856.

67. Newcomb, M., Shen, R., Choi, S.-Y., Toy, P. H., Hollenberg, P. F., Vaz, A. D. N., and Coon, M. J. (2000) Cytochrome P450-Catalyzed Hydroxylation of Mechanistic Probes that Distinguish between Radicals and Cations. Evidence for Cationic but Not for Radical Intermediates, *J. Am. Chem. Soc. 122*, 2677-2686.

68. Toy, P. H., Newcomb, M., Coon, M. J., and Vaz, A. D. N. (1998) Two Distinct Electrophilic Oxidants Effect Hydroxyl- ation in Cytochrome P-450-Catalyzed Reactions, *J. Am. Chem. Soc. 120*, 9718-9719.

69. Newcomb, M., Le Tadic-Biadatti, M.-H., Chestney, D. L., Roberts, E. S., and Hollenberg, P. F. (1995) A nonsynchronous concerted mechanism for cytochrome P-450 catalyzed hydroxylation, *J. Am. Chem. Soc. 117*, 12085-12091.

70. Newcomb, M., Aebisher, D., Shen, R., Chandrasena, R. E. P., Hollenberg, P. F., and Coon, M. J. (2003) Kinetic Isotope Effects Implicate Two Electrophilic Oxidants in Cytochrome P450-Catalyzed Hydroxylations, *J. Am. Chem. Soc. 125*, 6064-6065.

71. Chandrasena, R. E. P., Vatsis, K. P., Coon, M. J., Hollenberg, P. F., and Newcomb, M. (2003) Hydroxylation by the Hydroperoxy-Iron Species in Cytochrome P450 Enzymes, *J. Am. Chem. Soc. 126*, 115-126.

72. Toy, P. H., Dhanabalasingam, B., Newcomb, M., Hanna, I. H., and Hollenberg, P. F. (1997) A Substituted Hypersensitive Radical Probe for Enzyme-Catalyzed Hydroxylations: Synthesis of Racemic and Enantiomerically Enriched Forms and Application in a Cytochrome P450-Catalyzed Oxidation, *J. Org. Chem. 62*, 9114-9122.

73. Montellano, P. R. O. d., and Wilks, A. (2000) Advances in Inorganic Chemistry, In *Iron Porphyrins* (Sykes, G., and Mauk, A. G., Eds.), pp 359-407, Academic Press, San Diego, California.

74. Tenhunen, R., Marver, H., Pinstone, N. R., Trager, W. F., Cooper, D. Y., and Schmid, R. (1972) Enzymic degradation of heme. Oxygenative cleavage requiring cytochrome P-450, *Biochemistry 11*, 1716-1720.

75. Wilks, A., Ortiz de Montellano, P. R. (1993) Rat liver heme oxygenase. High level expression of a truncated soluble form and nature of the meso-hydroxylating species, *J. Biol. Chem. 268*, 22357-22362.

76. Wilks, A., Torpey, J., Ortiz de Montellano, P. R. (1994) Heme oxygenase (HO-1). Evidence for electrophilic oxygen addition to the porphyrin ring in the formation of alpha-meso-hydroxyheme, *J. Biol. Chem. 269*, 29553-29556.

77. Sundaramoorthy, M., Terner, J., and Poulos, T. L. (1995) The crystal structure of chloroperoxidase: a heme peroxidase–cytochrome P450 functional hybrid, *Structure 3*, 1367-1378.

78. Groves, J. T., and Wang, C. C. Y. (2000) Nitric oxide synthase: models and mechanisms, *Curr. Opin. Chem. Biol. 4*, 687-695.

79. Makris Thomas M., I. D., Ilme Schlichting, and Sligar Stephen G. (2005) Activation of Molecular Oxygen by Cytochrome P450, In *Cytochrome P450: Structure, Mechanism, Biochemistry.* (Montellano, P. R. O. d., Ed.) 2nd ed., pp 149-182, Plenum, New York.

80. Groves, J. T. (2003) The bioinorganic chemistry of iron in oxygenases and supramolecular assemblies, *Proc Natl Acad Sci U S A 100*, 3569-3574.

81. Groves, J. T., Haushalter, R. C., Nakamura, M., Nemo, T. E., and Evans, B. J. (1981) High-valent iron-porphyrin complexes related to peroxidase and cytochrome P-450, *J. Am. Chem. Soc. 103*, 2884-2886.

82. Groves, J. T., and McClusky, G. A. (1976) Aliphatic hydroxylation via oxygen rebound. Oxygen transfer catalyzed by iron, *J. Am. Chem. Soc. 98*, 859-861.

83. Groves, J. T., and Watanabe, Y. (1988) Reactive iron porphyrin derivatives related to the catalytic cycles of cytochrome P-450 and peroxidase. Studies of the mechanism of oxygen activation, *J. Am. Chem. Soc. 110*, 8443-8452.

84. Shapiro, S., Piper, J. U., and Caspi, E. (1982) Steric course of hydroxylation at primary carbon atoms. Biosynthesis of 1-octanol from (1R)- and (1S)-[1-3H,2H,1H; 1-14C]octane by rat liver microsomes, *J. Am. Chem. Soc. 104*, 2301-2305.

85. Shaik, S., Filatov, M., Schröder, D., and Schwarz, H. (1998) Electronic Structure Makes a Difference: Cytochrome P-450 Mediated Hydroxylations of Hydrocarbons as a Two-State Reactivity Paradigm, *Chemistry – A European Journal 4*, 193-199.

86. Harris, N., Cohen, S., Filatov, M., Ogliaro, F., and Shaik, S. (2000) Two-State Reactivity in the Rebound Step of Alkane Hydroxylation by Cytochrome P-450: Origins of Free Radicals with Finite Lifetimes, *Angew. Chem. Int. Ed. 39*, 2003-2007.

87. Ogliaro, F., de Visser, S. P., Groves, J. T., and Shaik, S. (2001) Chameleon states: High-valent metal-oxo species of cytochrome P450 and its ruthenium analogue, *Angew Chem Int Edit 40*, 2874-2878.

88. Ogliaro, F., Harris, N., Cohen, S., Filatov, M., de Visser, S. P., and Shaik, S. (2000) A model "rebound" mechanism of hydroxylation by cytochrome P450: Stepwise and effectively concerted pathways, and their reactivity patterns, *J. Am. Chem. Soc. 122*, 8977-8989.

89. Krest, C. M., Onderko, E. L., Yosca, T. H., Calixto, J. C., Karp, R. F., Livada, J., Rittle, J., and Green, M. T. (2013) Reactive Intermediates in Cytochrome P450 Catalysis, *J. Biol. Chem. 288*, 17074-17081.

90. Cryle, M. J., and De Voss, J. J. (2006) Is the ferric hydroperoxy species responsible for sulfur oxidation in cytochrome p450s?, *Angew. Chem. Int. Ed. Engl. 45*, 8221-8223.

91. Truan, G., Komandla, M. R., Falck, J. R., and Peterson, J. A. (1999) P450BM-3: absolute configuration of the primary metabolites of palmitic acid, *Arch. Biochem. Biophys. 366*, 192-198.

92. Capdevila, J. H., Wei, S., Helvig, C., Falck, J. R., Belosludtsev, Y., Truan, G., Graham-Lorence, S. E., and Peterson, J. A. (1996) The Highly Stereoselective Oxidation of Polyunsaturated Fatty Acids by Cytochrome P450BM-3, *J. Biol. Chem. 271*, 22663-22671.

93. Wang, B., Li, C., Cho, K.-B., Nam, W., and Shaik, S. (2013) The FeIII(H2O2) Complex as a Highly Efficient Oxidant in Sulfoxidation Reactions: Revival of an Underrated Oxidant in Cytochrome P450, *J. Chem. Theo. and Comp. 9*, 2519-2525.

1.7 Copyright Permissions:

May 31st, 2014

To whom it may concern,

This is Dr. Eugene G. Hrycay, chief science editor of the Cytochrome P450 eBook titled "Monooxygenase, Peroxidase and Peroxygenase Properties and Mechanisms of Cytochrome P450" that will be published by Springer SMB NL in the "Advances in Experimental Medicine and Biology" book series that will appear at the beginning of 2015. Ms. Anuja Modi and Dr. John H. Dawson are authors of Chapter Four in this series and I have accepted their chapter for publication. The eBook should contain 15 chapters. Ms. Anuja Modi is a candidate for the Ph. D. degree in the Department of Chemistry and Biochemistry, University of South Carolina, Columbia, SC, 29208, USA, and Ms. Modi will be including this chapter in her thesis. Best regards, Dr. Eugene G. Hrycay.

Dr. Eugene G. Hrycay (retired)
Faculty of Pharmaceutical Sciences
The University of British Columbia
2405 Wesbrook Mall
Vancouver, BC, V6T1Z3, Canada
Email: eugenehrycay@netscape.net

Eugene G Hrycay

CHAPTER 2

PROBING HETEROATOM-CONTAINING SUBSTRATE OXIDATION IN P450-CAM FOR NON-FERRYL REACTIVE INTERMEDIATES.

Abstract:

The multiple oxidant hypothesis of P450 catalysis has been probed in this study using P450-CAM from *Pseudomonas putida*, a prototypical P450 enzyme. The oxidation of substrates is accomplished by a catalytic cycle via a series of intermediates generated sequentially at the active site. Of these intermediates, the iron(IV)-oxo porphyrin radical cation, also known as Compound I, is believed to be the ultimate oxidant. However according to several studies in different types of P450s, it has been shown that the peroxoferric and the hydroperoxoferric intermediates formed prior to the Compound I may also be responsible for substrate oxidations depending on the reactivity of the specific substrate. P450-CAM is a versatile catalyst that has been shown to catalyze many typical P450 reactions in camphor analog substrates. The active site threonine-252 to alanine (T252A) mutant of P450-CAM on reaction with camphor yields H_2O_2 and minimal 5-hydroxycamphor, presumably because it makes very little Compound I while still generating the peroxoferric and hydroperoxoferric species. This makes T252A P450-CAM an ideal catalyst to probe the multiple oxidant hypothesis. Using primarily electrophilic substrates, including camphor analog substrates modified at the fifth position, we have compared the quantitative product formation between wild type (WT) and T252A P450-CAM to gain an insight in the multiple oxidant hypothesis.

2.1 Cytochrome P450-CAM as Prototype

Much of the current information about P450s has been achieved through extensive studies of P450-CAM from the camphor degrading bacterium *Pseudomonas putida*. P450-CAM, the first soluble P450 was discovered by Gunsalus and co-workers.[1] Later, Poulos and co-workers published its crystal structure, which provided important insight into the mechanistic details of the reaction cycle.[2] Although P450-CAM shares less than 30% sequence identity with other P450s, the all-important aspects of active site are conserved in the enzyme.[3] The active site lies buried deep within the protein with the hydrophobic inner environment of the protein surrounding the heme macrocycle as well as the substrate camphor. The conserved proximal cysteine residue C357, which tethers the heme to the protein, and the conserved acid-alcohol pair, D251-T252 are seen in the active site (Fig. 2.1A and B). The acid-alcohol pair has an important role to play in formation of the catalytic cycle intermediates. In wild-type P450-CAM enzyme the T252 residue lies on the distal side of the heme and is implicated in the protonation of the outer oxygen atom in the ferric hydroperoxo species that leads to water being formed as a leaving group with concomitant formation of Compound I. In the mutant enzyme where the active site threonine 252 was changed to alanine (T252A), the catalytic cycle has been found to undergo a short circuit pathway (Scheme 2.1, A). In this case the second protonation happens incorrectly on the proximal oxygen on the hydroperoxo ferric intermediate leading to H_2O_2 formation. D251 is known to support the chain of water molecules that supply protons to the active site. Alteration of the D251 residue leads to change in the rate-determining step of the catalytic cycle.[4]

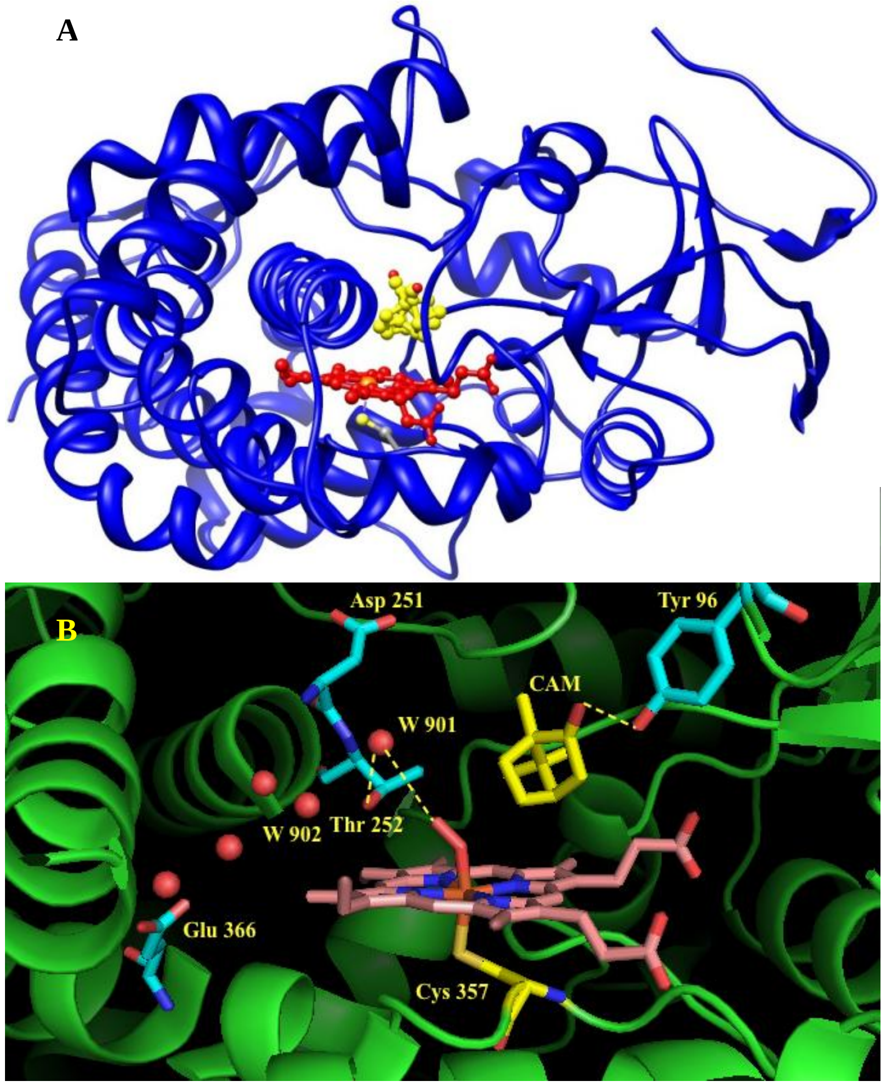

Figure 2.1 A) Crystal structure of P450CAM showing the heme macrocycle (red) and the substrate camphor (yellow) deep within the protein (blue) at the active site.[5] B) Active site of camphor-bound oxy-P450-CAM, showing conserved residues (Cys357, Glu366, Thr252, Asp251 and Tyr96) in the active site. Image constructed in PyMOL using PDB file 1DZ8. [6]

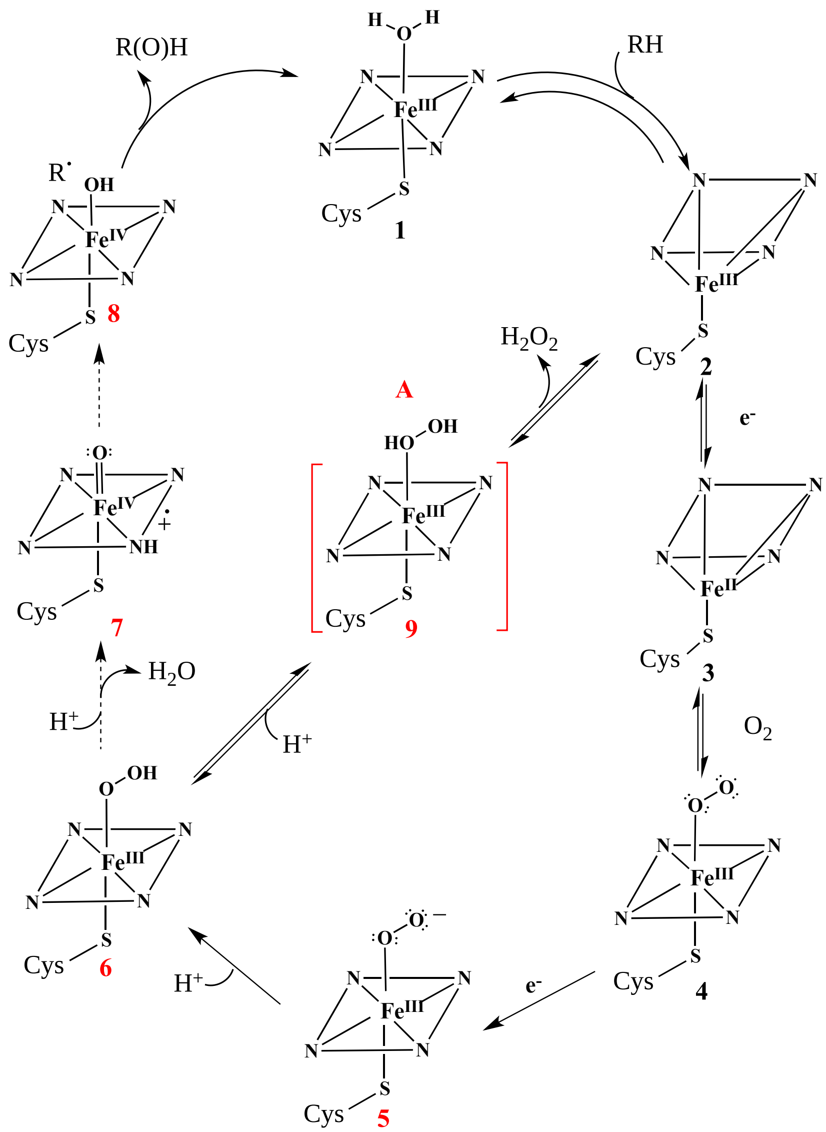

Scheme 2.1 P450 reaction cycle and intermediates. A non-productive uncoupling pathway that involves species 9 is shown in the inside of the outer cycle.

2.2 The Multiple Oxidant Hypothesis in P450 Catalysis

The exact intermediate responsible for adding oxygen to the hydrocarbon substrate has now been affirmatively shown to be Compound I; however the possibility of existence of multiple oxidants in the catalytic cycle also has been under consideration for past few years.[7] Scientists have used various techniques such as electron paramagnetic resonance, electron nuclear double resonance, electron absorption spectroscopy following cryoreduction of the oxyferrous enzyme, stopped flow rapid scan experiments and rapid freeze-quench methods by mixing ferric enzyme with oxygen atom donors, P450-like inorganic models and theoretical calculations to experimentally characterize the catalytic cycle intermediates.[8-11] In addition to Cpd I, scientists have looked at the reactivity of the peroxoferric intermediate (Scheme 2.1, **5**) in nucleophilic reactions and the hydro-peroxoferric intermediate (Scheme 2.1, **6**) in electrophilic reactions as shown in Scheme 2.2.

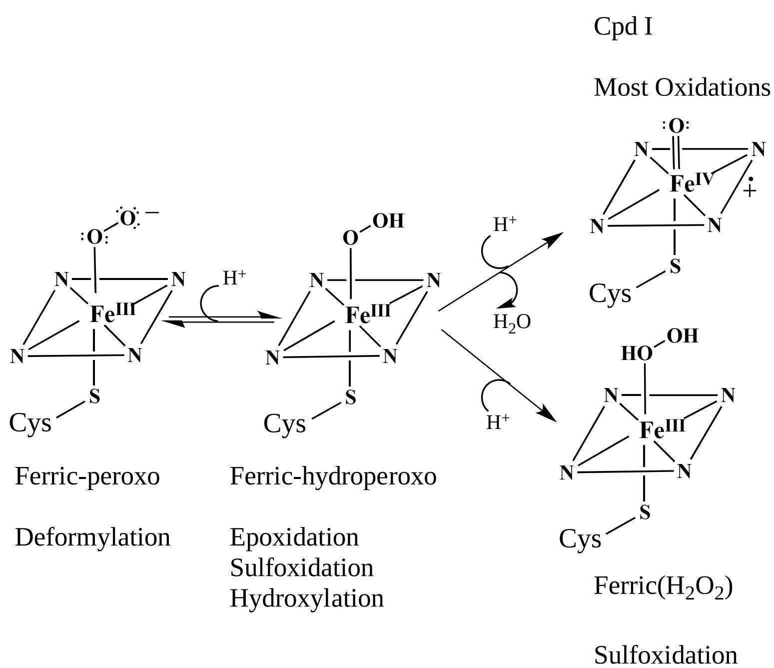

Scheme 2.2 Multiple oxidants in the P450 reaction cycle and types of reactions catalyzed by them.

Apart from reaction intermediates, Shaik and co-workers have proposed that the two states of Cpd I intermediate, i.e the high-spin and low-spin forms, are responsible for different reactions.[12] While the peroxoferric intermediate involves a nucleophilic role for P450 enzyme, most of the reactions catalyzed by P450s are electrophilic reactions in nature. Based on the turnover experiments of camphor, the T252A mutant of P450CAM has shown to be ineffective at catalyzing the hydroxylation of camphor, Table 2.1.

Table 2.1 Amounts of 5-*exo*-hydroxycamphor formed during turnover of WT and T252A P450-CAM with camphor, indicated as nmol product formed per nmol of P450 per min.

P450-CAM	WT	T252A	% of WT
1-R-camphor	1170.7 ± 2	21.2 ± 3.6	~ 1.8

In this study T252A P450CAM formed less than 2% of the oxidized product as compared to the WT. The T252A variant however, is capable of accepting electrons from NADH and reducing bound dioxygen to H_2O_2 (Scheme 2.1, pathway A).[13] This indicates that the T252A mutant is essentially incapable of forming Compound I and thus, is a good system to study the reactivity of the preceding alternate non-ferryl oxidants. The T252-A active site mutant of P450-CAM and analogous mutants of other P450s have been widely studied to understand the role played by active site residues in dioxygen activation and substrate oxidation mechanism.[14-17] The Dawson lab in collaboration with the Sligar lab first tested the reactivity of the T252A P450CAM mutant with camphor alkene analogues to look for the presence of alternate oxidants.[16] Reaction with alkene substrates gave the corresponding epoxide products, however the rate of epoxidation was only 15-20% of the rate at which the wild-type enzyme oxidized the substrate. The higher rate of epoxidation as compared to that of camphor hydroxylation indicated that the T252A mutant could utilize hydroperoxoferric intermediate for epoxidation, but that Compound I remained the oxidant of choice in the wild-type enzyme for epoxidation. It also indicated that the hydroperoxoferric intermediate is a rather sluggish oxidant.

In order to further investigate the multiple oxidant hypothesis of P450 catalysis, we have studied the reaction between other electrophilic substrates and T252A P450-CAM enzyme in this study. The substrates include camphor analogues containing reactive functional groups at C-5, which is the normal site of P450 catalyzed oxidation in camphor, and the corresponding functional groups in benzene substrates. Reactions of these substrates have been performed with both wild-type (WT) P450CAM as well as the T252A mutant using the fully reconstituted electron transfer system consisting of NADH, putidaredoxin (PdX) and putidaredoxin reductase (PdR). In this chapter, we report our findings from the quantitative comparison of the product formation between the WT and T252A to gain an insight into the multiple oxidant hypothesis.

2.3 Experimental Methods.

Expression and Purification of Proteins

a) WT and T252A P450-CAM: Both the WT and T252A P450-CAM enzymes were purified according to protocol described in Dr. Glascock's dissertation.[18] TB1 stock cells of *E. coli* bearing the pEMBL P450CAM containing plasmid were streaked on a LB-Ampicillin agar plate and incubated over night at 37^{o}C. A single colony from this plate was used to inoculate a 100 mL of LB-Broth supplemented with ampicillin and the cells are grown until the OD_{600} is about 0.8. 10 mL of this solution was then added to 6-L LB-broth supplemented with ampicillin and the cells are grown for 18 h. The cells are then harvested by centrifugation at 4^{o} C for 10 min at 5000 x g. The cells were finally washed with buffer containing 1 mM 1R-(+)-camphor, 50 mM potassium phosphate (KPi) at pH 7.4 (buffer A). To purify the protein, the cell pellet was dissolved in buffer A as described above in the washing step. The cell walls were broken by exposing them to 30

s. sonication intervals at 90% output with 2 min interval between sonication, while being stored on dry ice to prevent denaturation of the protein. The lysed cell debris was removed by centrifugation at 4^{o} C for 25 min at 10000 x g. The supernatant was loaded on a Whatman DE52 cellulose anion exchange column and washed with the 1 mM 1R-(+)-camphor, 50 mM KCl, 50 mM KPi at pH 7.4 (buffer B). The protein was eluted by a linear KCl gradient from 50-250 mM KCl in buffer B. The purity of each sample was analyzed by measuring the UV-visible (UV-vis) absorbance at 391 nm over that at 280 nm, the higher the ratio, better is the purity. To achieve higher purity, the protein was loaded onto a Biogel P-100 size exclusion column and eluted with 1 mM 1R-(+)-camphor, 50 mM KCl, 50 mM KPi at pH 7.4 (buffer C). Fractions with UV-vis absorbance ratio A(391)/A(280) values greater than 1.4 were used for experimental work. Proteins in buffer B containing excess camphor were concentrated to ~1 mM, flash-frozen in liquid nitrogen and stored at -80^{o} C.

<u>b) PdR and PdX</u>: Dr. Thomas Poulos (University of California, Berkeley, USA) kindly provided overexpression systems for PdR and PdX enzymes. Expression and purification of these proteins were achieved as per published protocols with minor modifications.[19, 20] For both PdR and PdX, the cell lysis was achieved by sonication as described above for P450-CAM. For PdX, the two-step column purification was achieved by first loading the lysate on to a Whatman DE52 cellulose anion exchange column, followed by a Biogel P-100 size exclusion column. Protein fractions with UV-vis absorbance ratio A(412)/A(280) values between 0.48-0.5 were used for experimental work. For PdR, the final step of column purification was achieved on a Biogel P-100 size exclusion column,

and the protein fractions with UV-vis absorbance ratio A(280)/A(454) values of 7.0 or less were used.

Turnover Experiments:

a) Camphor removal and buffer exchange: In order to perform turnover experiments, the P450-CAM enzymes had to be stripped of camphor. This was achieved using a Biogel P6DG desalting column equilibrated with 0.05 M MOPS buffer at pH 7.0, followed by buffer exchange on another Biogel P6DG desalting column equilibrated with camphor free buffer B. Successful removal of camphor was confirmed by a shift in the Soret absorbance from 391 nm to 417 nm.

b) Substrates: Benzene derivative substrates, styrene and thioanisole were purchased from Sigma-Aldrich. 5-methylenylcamphor was synthesized by Shengxi Jin.[21] (1R)-5-exo-thiomethoxycamphor was newly synthesized according to the methods described by Kemnitzer [22] and Jin [21] with minor modifications as described in Scheme 2.3. All the intermediates and the final products of the synthesis were monitored by ^{1}H-NMR and GC-MS and were confirmed by comparing with previously published data.

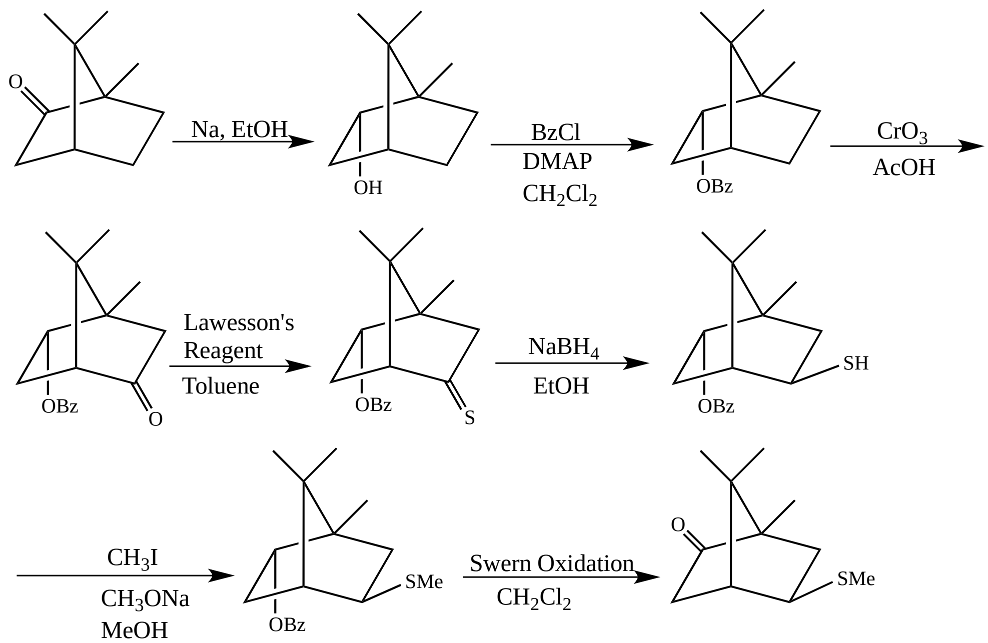

Scheme 2.3 Synthetic scheme for (<u>1R</u>)-5-*exo*-thimethoxycamphor.

<u>c) Catalytic turnover and NADH consumption experiments</u>: Reaction mixtures were set up in 50 mM KPi pH 7.4 buffer containing a mixture of the P450CAM-WT (0.5 µM), PdX (10 µM), substrate (0.5 mM for camphor analogues and 1 mM for benzene analogues), and NADH (1.0 mM). Catalase (5 µM, based on heme) was used for benzene substrates. The reactions were initiated by adding PdR (4.0 µM). Reactions were carried out for 15 min. for the camphor analog substrates and 30 min. for the benzene substrates and were quenched by adding 1 mL CH_2Cl_2. Suitable internal standards were added to the reaction mix before extracting the products. To measure the kinetic solvent isotope effect (KSIE), the reaction was carried out in D_2O KPi buffers (see above). Prior to the reaction, the P450-CAM enzymes were allowed to acclimatize in the buffer for at least 30 min. To monitor the NADH consumption during thioether substrate oxidation, the turnover reaction was conducted in a 0.5 cm quartz cuvette and the decrease in absorption at 340 nm was monitored on Agilent UV-vis instrument.

d) Calculation of product formed: Oxidized products were analyzed by GC-MS. The amount of products formed was quantitated using standard curves of the oxidized product and internal standard, 3-bromocamphor for camphor analog substrates and 4-*tert*-butylphenol for benzene substrates.

2.4 Results and Discussion

In the first set of turnover experiments (Scheme 2.4), we looked at the products of the turnover reaction of 5-methylenylcamphor (Scheme 2.4, **10**) and styrene (Scheme 2.4, **12**), followed by (1R)-5-exo-thiomethoxycamphor (Scheme 2.4, **14**) and thioanisole (Scheme 2.4, **15**) with the WT and T252A P450-CAM mutant enzymes. The two olefin-containing substrates formed epoxide products (Scheme 2.4, **11** and **13**) as has been demonstrated previously in WT P450-CAM.[16, 23] However, of the two sulfur-containing substrates, thioanisole formed a sulfoxide (Scheme 2.4, **17**) while the camphor analogue, [(1R)-5-exo-thiomethoxycamphor], underwent an oxidative dealkylation to form a ketone product (Scheme 2.4, **15**). The results of the turnover experiments are summarized in Table 2.2 below. With the olefinic substrates, the rate of epoxidation of styrene in T252A P450-CAM was observed to be about 25% of the rate seen in WT P450-CAM. This value is similar to the results previously reported for camphor olefin.[16] In similar reactions conducted in mammalian P450s, Coon and co-workers have reported similar findings and have proposed a mechanism involving the hydroperoxo intermediate in the epoxidation reaction.[15]

Oxidation of the two thiomethoxy substrates however, provided the most surprising results. Both in camphor analogue substrate (**14**) and benzene substrate (**16**), the rate of substrate oxidation observed in the T252A mutant was greater than 50% the rate seen with WT enzyme. We then looked at the NADH consumption and calculated the coupling and uncoupling data for the thiomethoxy substrates as shown in the Table 2.3 below.

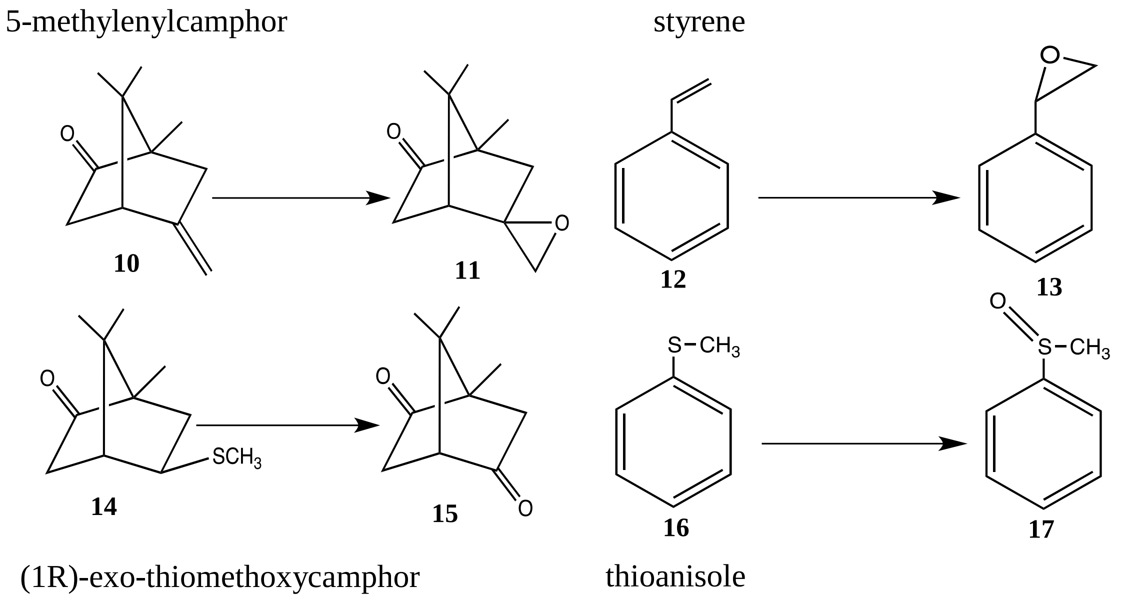

Scheme 2.4 Products of turnover reactions with olefins and thioethers catalyzed by P450-CAM.

Table 2.2 Amounts of products formed with WT and T252A camphor indicated as nmol product formed per nmol of P450 per min.

Substrate	P450CAM-WT	P450CAM-T252A	Rate of product formed by T252A compared to WT
5-Methylenyl-camphor (**10**)	107.5± 0.2[a]	22.9 ± 0.6[a]	21.4 %
Styrene (**12**)	0.9 ± 0.2[a]	0.2 ± 0.1	24.4 %
5-(1R)-exo-Thiomethoxy-camphor (**14**)	3.35 ± 0.6	1.79 ± 0.3	53.5 %
Thioanisole (**16**)	2.14 ± 0.2	1.65 ± 0.04	68.4 %

[a] Amounts of product formed is in agreement with values published previously

Table 2.3 Amounts of NADH consumed by turnover of P450 CAM with (A) 5-(1R)-exo-thiomethoxycamphor (**14**) and (B) thioanisole (**16**) indicated as nmol NADH consumed per nmol of P450 per min compared with the amount of oxidized product formed.

(A) 5-(1R)-exo-thiomethoxy-camphor (**14**)	P450-CAM WT	P450-CAM T252A
NADH consumed	61.4 ± 1.8	61.8 ± 2.7
Product formed	3.35 ± 0.6	1.79 ± 0.3
Coupling %	5.6 ± 1	2.9 ± 0.6
Uncoupling %	94.5 ± 1	97.1 ± 0.6

(B) Thioanisole (**16**)	P450-CAM WT	P450-CAM T252A
NADH consumed	44.8 ± 0.6	12.23 ± 2.8
Product formed	2.41 ± 0.2	1.65 ± 0.04
Coupling %	5.4 ± 0.5	13.9 ± 2.6
Uncoupling %	94.6 ± 0.5	86.0 ± 2.6

Sulfoxidation was exclusively observed for thioanisole (**16**). Consistent with previously reported results, thioanisole was never observed to undergo S-dealkylation of the methyl group attached to the sulfur group.[24] In the sulfoxidation reaction, the T252A mutant underwent oxidation at about 70% of the rate observed for that of the WT. It has been recently proposed by Shaik and co-workers that the Fe^{III}-(H_2O_2) (9 in Scheme 2.1) complex could be a highly efficient oxidant in sulfoxidation reactions.[25] The reaction has been proposed to occur by a nucleophilic attack from the distal oxygen atom of the Fe^{III}-(H_2O_2) complex resulting in heterolytic O–O bond scission that is coupled to proton transfer as shown in Scheme 2.5

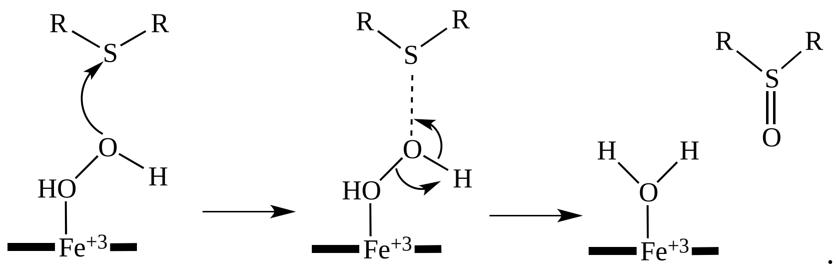

Scheme 2.5 Proposed mechanism of sulfoxidation by the Fe^{III}–(H_2O_2) intermediate.[25]

It is to be noted that the Fe^{III}-(H_2O_2) complex is formed in the uncoupling pathway thereby correlating with the observed high turnover despite low NADH coupling in thioanisole sulfoxidation. Although Shaik and co-workers have proposed that Fe^{III}-(H_2O_2) intermediate is more efficient than Cpd I in thioether oxidation, the higher rate of sulfoxidation by the WT enzyme suggests that Cpd I is still the strongest oxidant at play.

Oxidation at the sulfur atom was not observed in the thiomethoxy camphor substrate (**14**). The reaction with the camphor analog is presumed to occur in two steps, first C-hydroxylation followed by S-demethylation (Scheme 2.6). The hydroxylated intermediate is too unstable to be observed and has never been seen as a detectable product in our turnover reactions. The T252A mutant is able to oxidize the substrate at a rate that is 60% of that seen with WT. For the camphor analogue, a higher coupling is observed in the WT enzyme, although the coupling in the mutant enzyme is only reduced by half despite forming product at a rate equal to 60% seen with the wild type.

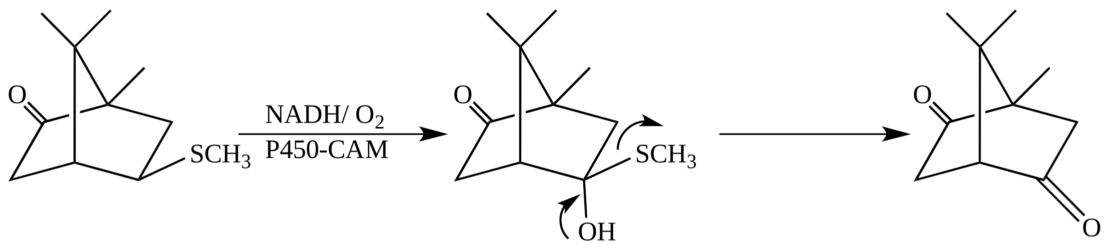

Scheme 2.6 P450 catalyzed oxidative demethylation reaction in 5-(1R)-thiomethoxycamphor.

Since the first step of this oxidation is C-hydroxylation, if Cpd I was the oxidant of choice, oxygen insertion would occur by the hydrogen atom abstraction-hydroxyl radical rebound mechanism. Davydov and co-workers have shown that little camphor hydroxylation in T252A proceeds via the ferryl intermediate,[26] thus the higher hydroxylation rate in the T252A mutant as seen in our data strongly indicates that alternative oxidant(s) may be involved in reactions catalyzed by the mutant. The theoretical examination of the bond energies of the 5-(1R)-thiomethoxycamphor structure show that the presence of sulfur atom significantly weakens the C-H bond thus making it susceptible to attack from weaker oxidants as well (Shengxi Jin, Feng Xu, Vitaly Rassolov, John Dawson unpublished data).

Given the electrophilic nature of these reactions, and the high rate of reaction with the T252A mutant which forms little Cpd I, either the ferric-hydroperoxo or Fe^{III}–(H_2O_2) species are likely to be involved in the oxidation. The Fe^{III}–(H_2O_2) species has been proposed to perform oxidation faster than it converts to Cpd I, thereby bypassing Cpd I in presence of thioether,[25] although the camphor thioether analog does not undergo sulfoxidation. If the Fe^{III}–(H_2O_2) species is involved in the oxidative dealkylation and were to proceed by O-O cleavage, we hypothesize the hydroxyl insertion mechanism shown in Scheme 2.7 below.

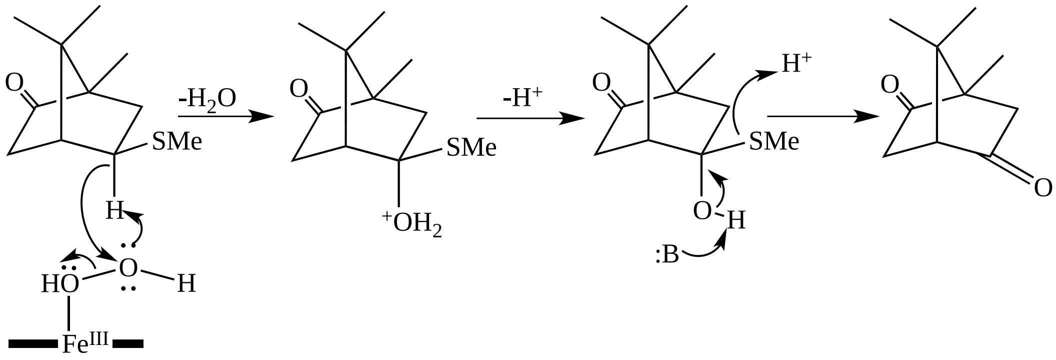
9

Scheme 2.7 Putative mechanism for oxidative demethylation of 5-(1R)-thiomethoxycamphor reaction involving Fe^{III}–(H_2O_2) intermediate.

Similarly, if the ferric-hydroperoxo was the involved in oxidation, the mechanism could occur by insertion of the distal oxygen to form protonated alcohol, followed by loss of proton to give a thio-hemiketal type intermediate. Loss of methanethiol results in formation of ketone product. This mechanism is summarized in Scheme 2.8 below.

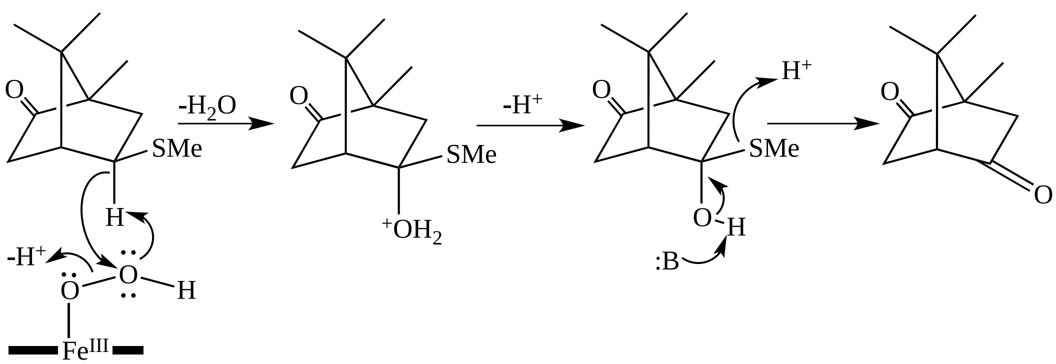
6

Scheme 2.8 Putative mechanism for oxidative demethylation of 5-(1R)-thiomethoxycamphor reaction involving ferric-hydroperoxo intermediate.

Involvement of ferric-hydroperoxo intermediate in hydrocarbon hydroxylation has been unconvincing due to lack of compelling evidence. So far in nature, the only evidence for direct involvement of ferric-hydroperoxo species in oxidation has been shown in the oxidation of heme to biliverdin by the heme oxygenase (HO) enzyme.[27] However the lack of well-defined catalytic residues in the HO active site have led to the proposal that such HO catalyzed oxidations may be an exception in cases where O-O bond scission to yield Cpd I is inefficient,[27, 28] like in threonine to alanine mutations of P450s active sites.

2.5 Conclusions

The involvement of multiple oxidants in P450 catalysis stems from the idea of 'induced reactivity' in which the substrate modulates the properties of a reactive intermediate.[29] In this work, we have demonstrated that compared with the WT enzyme, the T252A P450-CAM mutant exhibits considerable reactivity toward heteroatom containing substrates. It is especially notable that in the case of thioether substrates, the relative oxidation rates are close to 50% the rate seen with the wild-type enzyme. Since the T252A P450-CAM mutant has almost no hydroxylation activity toward camphor, it is presumed to form little if any Cpd I and therefore its ability to carry out substrate oxygenations must be attributed to alternate reactive intermediates. In oxidation of the benzene derivative substrate, thioanisole, theoretical calculations have shown that the Fe^{III}–(H_2O_2) species can be an effective oxidant, even better than Cpd I. The involvement of other oxidants, possibly ferric-hydroperoxo or Fe^{III}–(H_2O_2) is further affirmed in the case of the T252A-camphor thioether substrate turnover as it undergoes hydroxylation followed by demethylation. Once again, since this mutant does not form significant amounts of Cpd I, its ability to carry out the S-demethylation reaction must be due to involvement of another reactive intermediate, presumably the ferric-hydroperoxo species. While the ferric-hydroperoxo intermediate may not be the oxidant of choice in the most challenging oxidation reactions, the reactivity of this intermediate may be sufficient to oxygenate more reactive substrate such as the heteroatom-containing substrates examined herein.

2.6 References.

1. Gunsalus, I. C., and Sligar, S. G. (1978) Oxygen reduction by the P450 monoxygenase systems, *Adv. Enzymol. Relat. Areas Mol. Biol. 47*, 1-44.

2. Poulos, T. L., Finzel, B. C., Gunsalus, I. C., Wagner, G. C., and Kraut, J. (1985) The 2.6-A crystal structure of Pseudomonas putida cytochrome P-450, *J. Biol. Chem. 260*, 16122-16130.

3. Nelson, D. R. (2011) Progress in tracing the evolutionary paths of cytochrome P450, *Biochim. Biophys. Acta -Proteins and Proteomics 1814*, 14-18.

4. Gerber, N. C., and Sligar, S. G. (1994) A role for Asp-251 in cytochrome P-450cam oxygen activation, *J. Biol. Chem. 269*, 4260-4266.

5. Schlichting, I., Jung, C., and Schulze, H. (1997) Crystal structure of cytochrome P-450cam complexed with the (1S)-camphor enantiomer, *FEBS Lett. 415*, 253-257.

6. Schlichting, I., Berendzen, J., Chu, K., Stock, A. M., Maves, S. A., Benson, D. E., Sweet, R. M., Ringe, D., Petsko, G. A., and Sligar, S. G. (2000) The Catalytic Pathway of Cytochrome P450cam at Atomic Resolution, *Science 287*, 1615-1622.

7. de Montellano, P. R. O., and De Voss, J. J. (2002) Oxidizing species in the mechanism of cytochrome P450, *Nat. prod. rep. 19*, 477-493.

8. Sono, M., Eble, K. S., Dawson, J. H., and Hager, L. P. (1985) Preparation and properties of ferrous chloroperoxidase complexes with dioxygen, nitric oxide, and an alkyl isocyanide. Spectroscopic dissimilarities between the oxygenated forms of chloroperoxidase and cytochrome P-450, *J. Biol. Chem. 260*, 15530-15535.

9. Spolitak, T., Dawson, J. H., and Ballou, D. P. (2005) Reaction of Ferric Cytochrome P450cam with Peracids: Kinetic chracterization of intermediates on the reaction pathway, *J. Biol. Chem. 280*, 20300-20309.

10. Davydov, R., Macdonald, I. D. G., Makris, T. M., Sligar, S. G., and Hoffman, B. M. (1999) EPR and ENDOR of Catalytic Intermediates in Cryoreduced Native and Mutant Oxy-Cytochromes P450cam: Mutation-Induced Changes in the Proton Delivery System, *J. Am. Chem. Soc. 121*, 10654-10655.

11. Meunier, B., de Visser, S. P., and Shaik, S. (2004) Mechanism of Oxidation Reactions Catalyzed by Cytochrome P450 Enzymes, *Chem. Rev. 104*, 3947-3980.

12. Shaik, S., Filatov, M., Schröder, D., and Schwarz, H. (1998) Electronic Structure Makes a Difference: Cytochrome P-450 Mediated Hydroxylations of Hydrocarbons as a Two-State Reactivity Paradigm, *Chemistry – A European Journal 4*, 193-199.

13. Imai, M., Shimada, H., Watanabe, Y., Matsushima-Hibiya, Y., Makino, R., Koga, H., Horiuchi, T., and Ishimura, Y. (1989) Uncoupling of the cytochrome P-450cam monooxygenase reaction by a single mutation, threonine-252 to alanine or valine: possible role of the hydroxy amino acid in oxygen activation, *Proc. Natl. Acad. Sci. U S A 86*, 7823-7827.

14. Martinis, S. A., Atkins, W. M., Stayton, P. S., and Sligar, S. G. (1989) A conserved residue of cytochrome P-450 is involved in heme-oxygen stability and activation, *J. Am. Chem. Soc. 111*, 9252-9253.

15. Vaz, A. D. N., McGinnity, D. F., and Coon, M. J. (1998) Epoxidation of olefins by cytochrome P450: Evidence from site-specific mutagenesis for hydroperoxo-iron as an electrophilic oxidant, *Proc. Natl. Acad. Sci. U S A 95*, 3555-3560.

16. Jin, S., Makris, T. M., Bryson, T. A., Sligar, S. G., and Dawson, J. H. (2003) Epoxidation of Olefins by Hydroperoxo−Ferric Cytochrome P450, *J. Am. Chem. Soc. 125*, 3406-3407.

17. Cryle, M. J., and De Voss, J. J. (2006) Is the ferric hydroperoxy species responsible for sulfur oxidation in cytochrome p450s?, *Angew. Chem. Int. Ed. Engl. 45*, 8221-8223.

18. Glascock, M. C. (2003) PhD, In *Dissertation*, p 183, University of South Carolina, Columbia, SC, USA.

19. Sevrioukova, I. F., Garcia, C., Li, H., Bhaskar, B., and Poulos, T. L. (2003) Crystal Structure of Putidaredoxin, the [2Fe–2S] Component of the P450cam Monooxygenase System from< i> Pseudomonas putida</i>, *J. Mol. Biol. 333*, 377-392.

20. Sevrioukova, I. F., Hazzard, J. T., Tollin, G., and Poulos, T. L. (2001) Laser flash induced electron transfer in P450cam monooxygenase: putidaredoxin reductase-putidaredoxin interaction, *Biochemistry 40*, 10592-10600.

21. Jin, S. (2005) PhD, In *Dissertation*, p 55, University of South Carolina, Columbia, SC, USA.

22. Kemnitzer, W. E. (1998) PhD, In *Dissertation*, p 30, University of South Carolina, Columbia, SC, USA.

23. Fruetel, J. A., Collins, J. R., Camper, D. L., Loew, G. H., and Ortiz de Montellano, P. R. (1992) Calculated and experimental absolute stereochemistry of the styrene and. beta.-methylstyrene epoxides formed by cytochrome P 450cam, *J. Am. Chem. Soc. 114*, 6987-6993.

24. Fruetel, J., Chang, Y.-T., Collins, J., Loew, G., and Ortiz de Montellano, P. R. (1994) Thioanisole sulfoxidation by cytochrome P450cam (CYP101): experimental and calculated absolute stereochemistries, *J. Am. Chem. Soc. 116*, 11643-11648.

25. Wang, B., Li, C., Cho, K.-B., Nam, W., and Shaik, S. (2013) The FeIII(H2O2) Complex as a Highly Efficient Oxidant in Sulfoxidation Reactions: Revival of an Underrated Oxidant in Cytochrome P450, *J. Chem. Theor. Comp. 9*, 2519-2525.

26. Davydov, R., Makris, T. M., Kofman, V., Werst, D. E., Sligar, S. G., and Hoffman, B. M. (2001) Hydroxylation of Camphor by Reduced Oxy-Cytochrome P450cam: Mechanistic Implications of EPR and ENDOR Studies of Catalytic Intermediates in Native and Mutant Enzymes, *J. Am. Chem. Soc. 123*, 1403-1415.

27. Wilks, A., Torpey, J., Ortiz de Montellano, P. R. (1994) Heme oxygenase (HO-1). Evidence for electrophilic oxygen addition to the porphyrin ring in the formation of alpha-meso-hydroxyheme, *J. Biol. Chem. 269*, 29553-29556.

28. Schuller, D. J., Poulos, T. L., Wilks, A., and Montellano, P. O. D. (1998) Crystallization of recombinant human heme oxygenase- 1, *Protein Sci. 7*, 1836-1838.

29. Kim, S. H., Yang, T.-C., Perera, R., Jin, S., Bryson, T. A., Sono, M., Davydov, R., Dawson, J. H., and Hoffman, B. M. (2005) Cryoreduction EPR and 13C, 19F ENDOR study of substrate-bound substates and solvent kinetic isotope effects in the catalytic cycle of cytochrome P450cam and its T252A mutant, *Dalt. Trans.*, 3464-3469.

CHAPTER 3

HEME IRON COORDINATION STRUCTURAL ANALYSIS USING MAGNETIC CIRCULAR DICHROISM SPECTROSCOPY.[2]

[2] Section 3.2 of this chapter was published as a part of MCD analysis in Bastian Molitor, Samir El-Mashtoly, Anuja Modi, Marc Staßen, Christoph Laurich, Wolfgang Lubitz, John H. Dawson, Michael Rother and Nicole Frankenberg-Dinkel. 2013. *J. Biol. Chem.* 2013 288: 18458-18472.

Abstract:

Magnetic circular dichroism (MCD) spectroscopy also known as the Faraday effect is an excellent fingerprinting tool for various heme systems. It can be used for assigning axial ligand identity, coordination numbers as well as spin state determination of the heme iron, which can lead to important information about their structures and functions. Over the past 30 years, the Dawson laboratory has recorded and maintained a library of MCD spectra of numerous heme proteins from various collaborative projects and their own studies. Continuing the collaborative work, in this chapter we present results from the application of MCD spectroscopy in the axial ligand(s) identification analysis of three novel heme proteins, sGAF2, Z-ISO and Phu_R, and in characterization of the ferrous dioxygen complex of an engineered P450BM3 protein.

3.1 Magnetic Circular Dichroism Spectroscopy

Studies of the coordination structures of heme protein active sites provide important information about the mechanism of action of the native heme proteins. Particularly, the amino acids coordinating to the heme iron and those surrounding the active site along with the oxidation and spin states of the heme iron have been shown to play important roles in the structure and function of heme-proteins.[1-3] Magnetic circular dichroism (MCD) has long been used in the Dawson laboratory as a fingerprinting technique for various heme systems. The theory of MCD is based on the Faraday effect first discovered by Michael Faraday in 1845. Natural circular dichroism (CD) and MCD both measure the difference in absorption between left and right circularly polarized light. In MCD a magnetic field is applied parallel to the direction of propagation of light.[4-8] CD, however, is observable only in optically active species that exhibit dissymmetry within the structure of the chromophore (chirality) or environment. According to the Faraday effect, the application of a magnetic field parallel to the direction of light induces optical activity due to Zeeman splitting. Therefore all species can exhibit MCD spectra while only the optically active species can exhibit CD spectra.

Both CD and MCD signals can only be observed in the regions displaying electronic band absorption. An MCD spectrum is composed of several bands arising from different electronic transitions, and these bands are composed of three separate, ‘A’, ‘B’ and ‘C’ terms Fig. 3.1.[9] ‘A’ terms are temperature independent and have a typical derivative-shaped dispersion centered on the electronic absorption spectrum band. ‘A’ terms are seen only in those systems that demonstrate degeneracy in excited state that is lifted by the applied magnetic field, also known as Zeeman splitting and as such they are typically seen in spectra of systems exhibiting a three-fold or higher symmetry axis. ‘B’ terms arise from magnetic field-induced ground state and excited state mixing, typically seen in systems with less than three fold symmetry. They are Gaussian-shaped and are temperature independent similar to the ‘A’ terms. ‘C’ terms are temperature-dependent, arising from magnetic field-induced lifting of ground state degeneracies. This causes the ‘C’ terms to be Gaussian-shaped centered on the electronic absorption band.[10, 11]

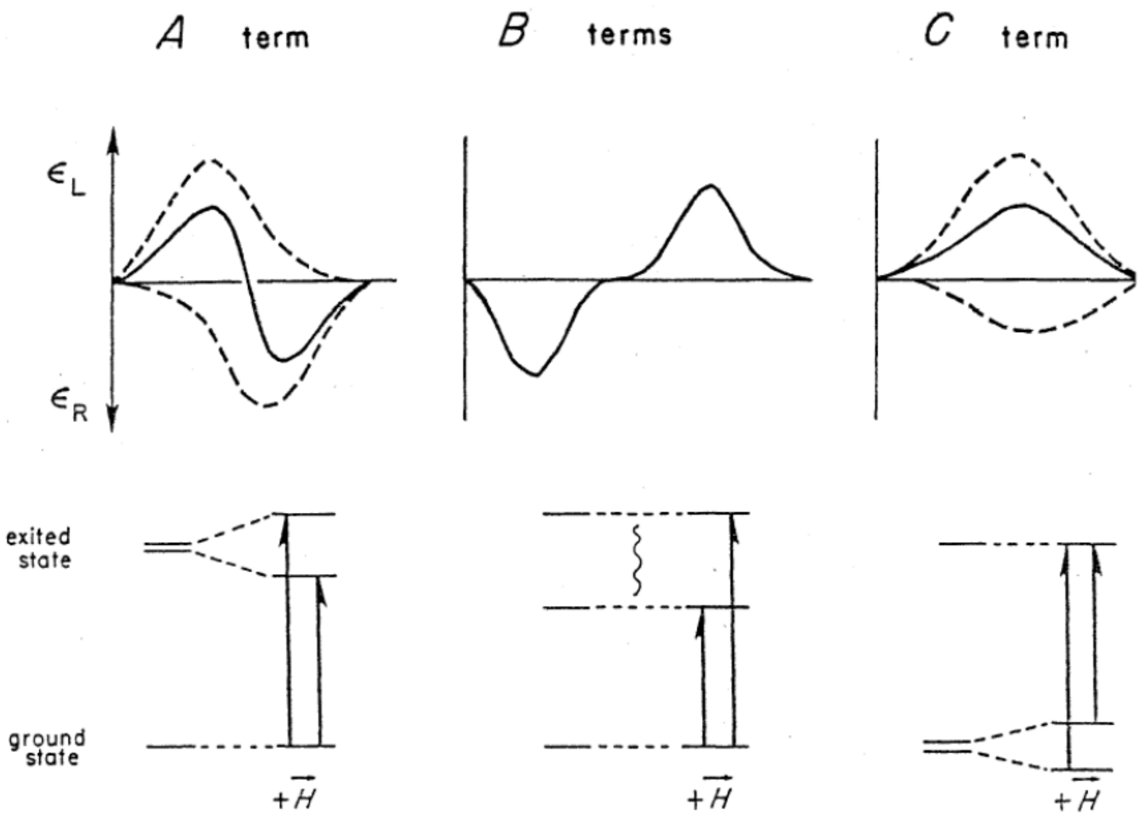

Figure 3.1 Diagram illustrating the origin of the A, B, and C terms of a MCD spectrum, reprinted with permission from Vickery, L. E. (1978) Spin states of heme proteins by magnetic circular dichroism, *Methods Enzymol. 54*, 284-303.

It has been shown that MCD is a powerful probe of the heme iron spin state, oxidation state, and the identity of the heme iron axial ligand(s) while being relatively insensitive to the surrounding factors other than the axial ligands.[12, 13] MCD spectra can be recorded over a range of temperatures, on dilute samples even in the micromolar range (10^{-6} M) and on both diamagnetic and paramagnetic species.[13, 14] Unlike the traditional UV-visible (UV-vis) absorption spectra, which only have positive sign features, MCD spectra have both positive and negative sign features, thereby presenting a finer electronic structural detail of the system being investigated. This 'fingerprinting' capacity combined with the intrinsic sensitivity to the electronic (and thus structural) aspects of the chromophore being examined and relative insensitivity of environmental factors makes MCD an extremely useful tool for coordination structural elucidation. MCD spectroscopy's potential applications include:

a) To determine ground state magnetic properties such as spin state, g-values, zero field splittings and magnetic coupling;

b) To assign electronic transitions pertaining to the electronic structure of a chromophore, including theoretical models;

c) To resolve individual components of electronic spectra of proteins containing several metal centers; and,

d) To compare novel proteins to model systems or vice-versa to determine the active site coordination structure with regards to ligands, spin state, oxidation state, geometry, etc. Comparisons of the proteins can be made regardless of the protein conformation effects.

Having introduced the theory and basic uses of MCD spectroscopy, in this chapter we will look at the application of MCD in the determination of axial ligand identity in novel heme proteins, sGAF2, Z-ISO and Phu_R, and in the characterization of the dioxygen complex of an engineered P450BM3 protein.

3.2 Part A: Axial Ligand Determination in sGAF2

The protein MA4561 from the methanogenic archaeon *Methanosarcina acetivorans* was predicted to be a phytochrome-like photoreceptor mainly because of the presence of a conserved cysteine residue in the first GAF domain.[15] However the recombinantly produced and purified protein was shown to not bind any known phytochrome chromophores, instead UV-vis absorption spectroscopy revealed the presence of a heme tetrapyrrole cofactor. The heme is covalently attached via one vinyl side chain to cysteine 656 in the second GAF domain. Majority of the heme-based sensors have a heme-b type non-covalently attached tetrapyrrole cofactor, but pyridine hemochromogen assay revealed that the α-band maximum in MA4561 is at 553 nm. This is typically seen in c-type cytochromes due to the saturation of only one heme vinyl group, whereas the other stays unsaturated.[16, 17] Functionally MA4561 has been proposed to be a heme-based sensor kinase that is able to autophosphorylate methyl sulfide methyltransferase depending on the heme redox state.[18] In order to get a better understanding of the heme co-ordination structure, Prof. Nicole Frankenberg-Dinkel (Ruhr-University, Bochum, Germany) collaborated with our laboratory for MCD studies of the heme domain containing MA4561 variant, sGAF2.

3.2.1 Methods:

Dr. Nicole Frankenberg-Dinkel provided us with the purified protein samples prepared as described in.[18] MCD spectra were measured on a Jasco J815 spectropolarimeter fitted with a Jasco MCD-1B magnet at a magnetic field strength of 1.41 T at 4° C using a 0.2 cm path length quartz cuvette. Jasco software was used for data acquisition and manipulation as reported previously.[19] Because the molar absorptivity of the pyridine hemochromogen of the heme in variant sGAF2-His6 (without imidazole (Im)) could not be determined, concentrations of the sGAF2 samples were tentatively determined based on an estimated value of ε = 115 mM^{-1} cm^{-1} (the value for ferric cytochrome b_5) for the Soret absorption peak (415 nm) of the Im complex of ferric sGAF2 at pH 7.0. UV-vis absorption spectra were recorded on Cary 400 spectrometer, before and after each MCD measurement to track sample integrity. sGAF2 protein samples were studied in 50 mM sodium phosphate buffer containing 100 mM NaCl (NaPi) at pH 7.0 and in 50 mM CAPS buffer at pH 10.0. The Im and tetrahydrothiophene (THT) adducts were prepared by adding 2 and 14 mM Im and THT to the ferric protein, respectively. The ferrous species of sGAF2 was prepared from ferric protein in the presence or absence of exogenous ligands (Im and THT) by flushing a rubber septum-sealed cuvette with nitrogen gas for about 10-15 min followed by the addition of a small amount of solid sodium dithionite.

3.2.2 Results and Discussion:

MCD spectra of ferric and ferrous states of sGAF2 are shown in Fig. 3.2, where the spectra of analogous states of horse heart myoglobin (Mb), horseradish peroxidase (HRP) and cytochrome *b5* (cyt *b5*) are overlaid for comparison. All of these three proteins contain His-ligated heme (iron-protoporphyrin IX) prosthetic group. At pH 7.0 ferric sGAF2 exhibits MCD spectrum (solid line in Fig. 3.2 A) in the visible region (450

– 700 nm) that is similar to that of ferric HRP (dashed line) and ferric Mb (dotted line), a five-coordinate and water-ligated six-coordinate heme respectively. However, a closer comparison of the trough intensities at ~640 nm indicates that the spectrum of ferric sGAF2 is more similar to that of HRP than Mb. In the Soret region (350 – 450 nm), an asymmetric MCD spectrum of ferric sGAF2 having a prominent peak at ~404 nm (intensity ~7.5 M^{-1} cm^{-1} T^{-1}) and two troughs at ~370 and ~430 nm (< 5 M^{-1} cm^{-1} T^{-1}) does not resemble either a weak negative feature (a trough at ~420 nm, ~4 M^{-1} cm^{-1} T^{-1}) of ferric HRP or a broadly symmetric derivative-shaped spectral feature (+/- ~15 M^{-1} cm^{-1} T^{-1}) of ferric Mb. These comparisons suggest the heme group in ferric sGAF2 at pH 7.0 is more likely to be five-coordinate rather than six-coordinate. The MCD spectrum of ferric sGAF2 at pH 10.0 (gray line) is clearly different from that at pH 7.0 in that one of the visible region trough (~550 nm) is shifted to ~575 nm and a Soret region feature becomes derivative-shaped with considerably enhanced intensity (+34/-40 M^{-1} cm^{-1} T^{-1}). The resultant spectral features are indicative of an increased low spin six-coordinate species.

Dithionite-reduced ferrous state sGAF2 (solid line in Fig. 3.2B) has MCD spectral features that are broadly similar to those of ferrous Mb (which contains a His-ligated five-coordinate heme, dotted line in Fig. 3.2B) including quite intense Soret peaks (~125 M^{-1} cm^{-1} T^{-1}) except for the more enhanced and derivative-like shape in the visible region around 555 nm for sGAF2 compared to Mb. At pH 10.0, this derivative-shaped spectral line becomes much more intense. Concomitantly, the Soret peak intensity diminishes by ~50% (gray line in Fig. 3.2B). These MCD spectral changes are indicative of an increase in the fraction of a ferrous six-coordinate low-spin heme such as bis-amine (or bis-His)-

ligated ferrous heme (see below). Fig. 3.3C compares ferric-Im (solid line) and ferric-THT (a cyclic thioether) adducts (dashed line) of sGAF2 with ferric cyt *b5* (dotted line). These three heme adducts display similar MCD spectral patterns, namely relatively intense derivative-shaped Soret spectra and mainly positive (450 – 560 nm) and negative (560 – 700 nm) features with a prominent trough at 570 – 580 nm. The MCD spectral similarity for the ferric-Im complex of sGAF2 and ferric cyt *b5*, (which contains a bis-His-ligated heme) suggests identical ligation modes for the two heme proteins. Since bis-amine- (or bis-His-) and bis-thioether-ligated ferric hemes have been shown to have similar MCD spectra [20], mono-Im (or His)/mono-thioether-bound ferric heme is expected also to share the similarity. In Fig. 3.3D, MCD spectra of ferrous-Im and ferrous-THT adduct are compared with the spectrum of ferrous cyt *b5*. As seen in their ferric state (Fig. 3.3C), the MCD spectral patterns of these three ferrous complexes show common patterns. In the visible region, extremely intense derivative-shaped features around ~555 nm are notable. In the Soret region, the MCD spectra of the THT-bound sGAF2 and cyt *b5* are similar to each other in pattern (except for some intensity difference) while the Im-complex of sGAF2 shows somewhat different pattern with a noticeably intense trough at ~425 nm. A possible cause of this difference could be incomplete formation of the Im-complex

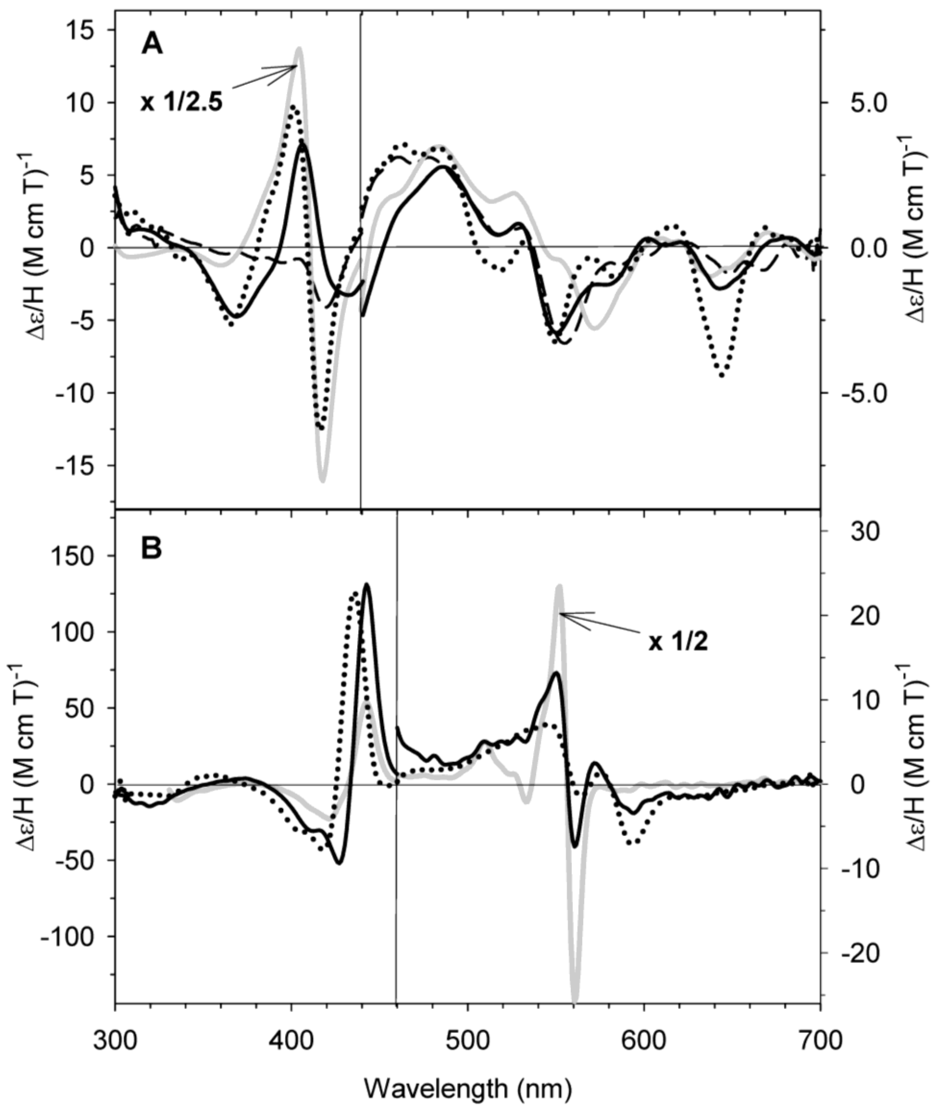

Figure 3.2 MCD spectra at 4 °C of ferric sGAF2 at pH 7.0 (solid line), ferric sGAF2 at pH 10.0 (gray line; reduced by 2.5 times in the 300-440 nm region), ferric horseradish peroxidase at pH 7.0 (dashed line), and ferric Mb at pH 7.0 (dotted line) (A) and ferrous sGAF2 at pH 7.0 (solid line), ferrous sGAF2 at pH 10.0 (gray line; reduced by 2 times in the 460-700 nm region), and ferrous Mb at pH 7.0 (dotted line) (B) are shown. The spectra of ferric HRP, ferric Mb, and ferrous Mb are replotted from Ref. 21. Figure reprinted with permission from Molitor, B., Stassen, M., Modi, A., El-Mashtoly, S. F., Laurich, C., Lubitz, W., Dawson, J. H., Rother, M., and Frankenberg-Dinkel, N. (2013) A heme-based redox sensor in the methanogenic archaeon Methanosarcina acetivorans, *J. Biol. Chem. 288*, 18458-18472.

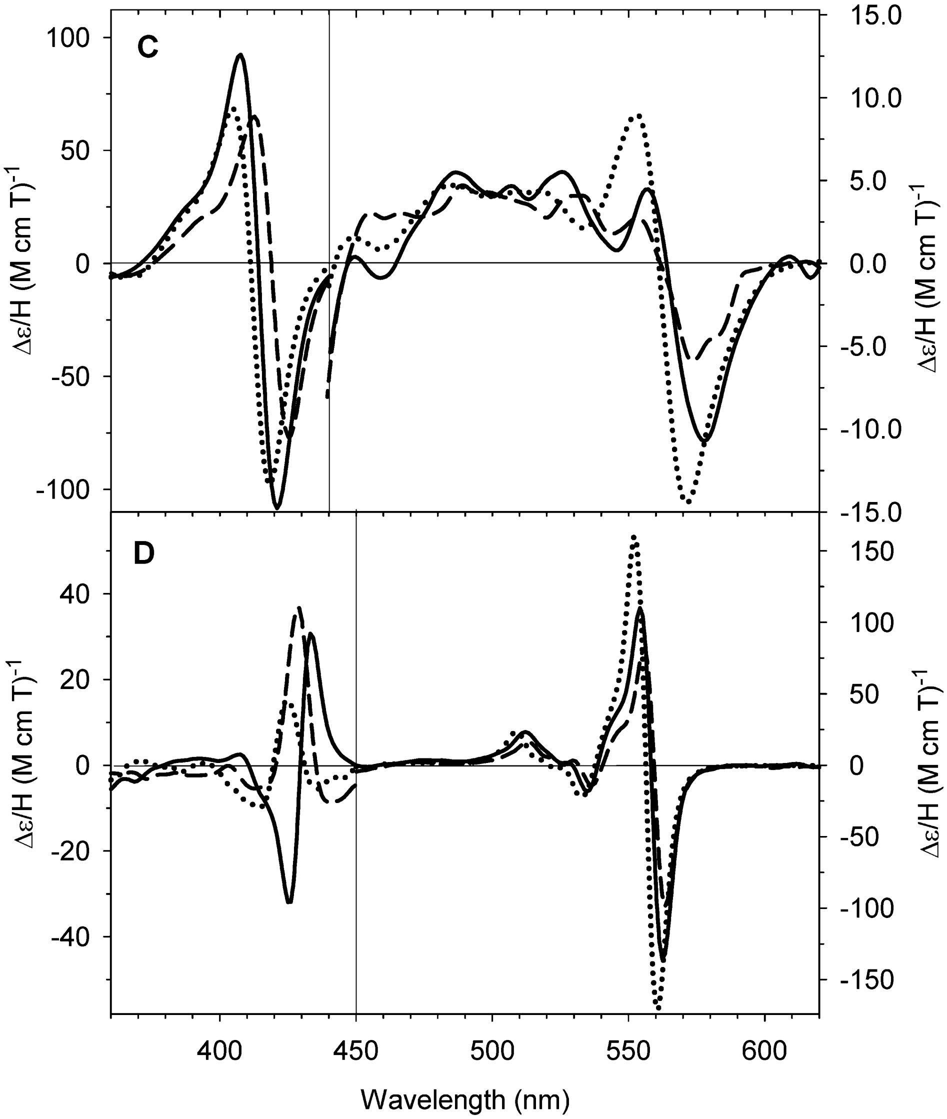

Figure 3.3 MCD spectra at 4°C of the ferric Im sGAF2 derivative at pH 7.0 (solid line; with 2mM Im), the ferric THT sGAF2 derivative at pH 7.0 (dashed line; with 14 mM THT), and 50 mM ferric cyt b_5 at pH 7.0 (dotted line) (C) and ferrous Im sGAF2 at pH 7.0 (solid line; with 2 mM Im), ferrous THT sGAF2 derivative in NaPi buffer at pH 7.0 (dashed line; with 14 mM THT), and ferrous cyt b5 at pH 7.0 (dotted line) (D). The spectra of ferric and ferrous cytochrome b5 are replotted from Ref. 22. See the text for the types of buffer used for sGAF2, see Ref. 21 for Mb and HRP, and see Ref. 22 for cyt b5. Figure reprinted with permission from Molitor, B., Stassen, M., Modi, A., El-Mashtoly, S. F., Laurich, C., Lubitz, W., Dawson, J. H., Rother, M., and Frankenberg-Dinkel, N. (2013) A heme-based redox sensor in the methanogenic archaeon Methanosarcina acetivorans, *J. Biol. Chem. 288*, 18458-18472..

In addition to MCD, the Dinkel group also used resonance Raman (RR) for heme-co-ordination determination. In the RR measurements, a six coordinate low spin heme was observed, whereas MCD data suggests a high-spin state and a five-coordinate structure rather than a six-coordinate structure. The conditions used in the RR experiments most likely would not allow detection of a five-coordinate high spin heme species. Therefore, a clear assignment of the coordination structure cannot be made, suggesting a mixture of different coordination states. When the pH of the buffer was changed to pH 10.0, a mixture of a high-spin and low-spin components were also detectable in MCD spectra, whereas the differences in UV-vis absorption spectra were minor. This low-spin component appears to be arising from a bis-His-type coordination structure as judged from the similarity to the Fe(III)-Im complex. Upon reduction of MA4561 with dithionite, an Fe(II) complex with a broad Soret band at about 432 nm and a visible band at about 557 nm with shoulders at about 528 and 574 nm is formed. An additional peak was observed at about 625 nm for the sGAF2 variants. These optical absorption properties cannot be clearly assigned to one coordination and spin state but again, rather appear like a mixture of different states. With RR data, a mixture of two different six coordinate low spin states was observed, and the existence of two species was confirmed in the MCD measurements. At pH 10.0, one of the two states becomes predominant as judged from the MCD data and is similar to the bis-His-ligated Fe(II) form of cyt b*5* . The addition of Im or THT for the MCD measurements led to typical six coordinate low spin hemes for the Fe(III)-(Im and THT) as well as the Fe(II)-(Im and THT) forms.[23, 24] The Im complexes were hardly distinguishable from the THT complexes with only minor differences in UV-visible as well as MCD spectra.

Similarities of the Im complexes to cyt *b5* led to the conclusion that a His/Im or a His/THT complex is formed that would resemble a bis-His (cyt *b5*) or His/Met (many **c** -type cytochromes) ligation structure.

The structural model of sGAF2 generated supports the spectral data with putative axial ligands in proximity of the heme cofactor. Specifically, two histidine residues (His702 and His704) are located at the proximal side of the heme pocket that might be involved in coordinating the heme iron (Fig. 3.4). Initial mutational analyses of these residues suggest His702 as the proximal ligand (Nicole Frankenberg-Dinkel, unpublished data). In the distal side of the heme two tyrosine (Tyr632 and Tyr665), one methionine (Met645), and one histidine (His646) are found. An alternating pair of these groups might become axial ligands involved in coordinating to the heme iron depending on the redox state. Because ligands like carbon monoxide (CO), THT, and Im are able to bind to the heme in MA4561, we envision the distal side of the heme pocket large enough to allow THT and Im molecules to enter and coordinate to the heme iron. The above mentioned amino acids might also be involved in stabilizing different ligation states of the heme without being a direct ligand to the heme iron. Alternatively, they might be exchanged as a direct ligand upon binding of external ligands as the above spectroscopic data suggest six-coordinate states also in the absence of external ligands. It is interesting to note that a cysteine residue (Cys-656) that is speculated to form a covalent bond with the heme is located near one of the heme vinyl groups, giving the modeled structure more confidence.

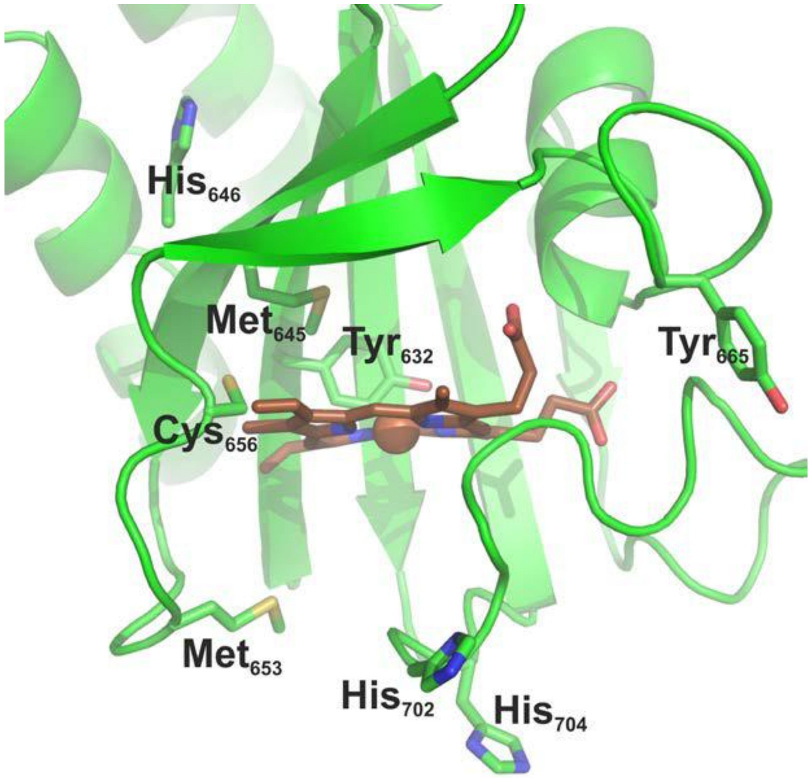

Figure 3.4 Structural model of the heme-binding pocket of MA4561, in the second GAF domain (aa 608–768) modeled using the PHYRE2 server [25], and the modeled structure is used to predict putative ligands binding to this structure using 3DLigandSite.[26] The heme cofactor is shown in middle in brown and the protein structure is shown as a green ribbon (important amino acids are shown as sticks). Figure reprinted with permission from Molitor, B., Stassen, M., Modi, A., El-Mashtoly, S. F., Laurich, C., Lubitz, W., Dawson, J. H., Rother, M., and Frankenberg-Dinkel, N. (2013) A heme-based redox sensor in the methanogenic archaeon Methanosarcina acetivorans, *J. Biol. Chem. 288*, 18458-18472.

3.3 Part B: Axial Ligand Determination in Z-ISO

Vitamin A deficiency is a global phenomenon especially in children, causing blindness, increased susceptibility to disease, and increased mortality.[27-29] A sustainable approach is to provide provitamin A carotenoids in plant food staples to maintain healthy serum levels of vitamin A, a process currently impeded by the lack of detailed understanding of the carotegenesis pathway. Dr. Eli Wurtzel's group (City University of New York, NY, USA) discovered the 15-*cis*-ζ-carotene isomerase (Z-ISO), a novel C=C double bond *cis*-to-*trans* isomerase.[30] Z-ISO is essential for provitamin A carotenoid biofortification and for plant adaptation to environmental variation, a significant stress which affects plant yield. Without Z-ISO, the biosynthetic pathway is blocked.[30] In-silico analysis of this membrane protein led to experimental proof that Z-ISO contains a nonheme iron and at least one heme-b. It is hypothesized that isomerization in Z-ISO is regulated by oxidation state of the heme b iron with redox-dependent ligand switching and a nonheme iron cofactor is indirectly involved. MCD spectroscopy was employed to test this working hypothesis.

3.3.1 Methods:

Dr. Eli Wurtzel's group provided us with purified protein samples. MCD spectra were measured on a Jasco J815 spectropolarimeter fitted with a Jasco MCD-1B magnet at a magnetic field strength of 1.41 T at 4 °C using a 0.5 cm pathlength quartz cuvette. Jasco software was used for data acquisition and manipulation as reported previously.[19] Concentrations of the heme in Z-ISO samples were determined based on the pyridine hemechromogen assay method using ε_{555} = 34.4 mM^{-1} cm^{-1}.[31] Using this method, a value of ε = 110 mM^{-1} cm^{-1} was calculated for the Soret absorption peak (415 nm) of ferric Z-

ISO at pH 7.4. UV-visible absorption spectra were recorded on a Cary 400 spectrometer, before and after each MCD measurement to track sample integrity. Z-ISO protein samples were studied in 20 mM Tris buffer containing 20 mM NaCl, 0.2% n-dodecyl-β-D-maltoside (DDM), 0.1 mM *tris*(2-carboxyethyl)phosphine (TCEP) and 5% glycerol at pH 7.4. The ferrous species of Z-ISO was prepared from ferric protein by flushing a rubber septum-sealed cuvette with nitrogen gas for about 10-15 min followed by the addition of a small amount of solid sodium dithionite. The CO adducts of the ferrous protein were prepared by bubbling the CO gas in to the reduced protein.

3.3.2 Results and Discussion:

MCD and UV-vis absorption spectra of ferric state of Z-ISO are shown in Fig. 3.5, overlaid for comparison with that of a simulated spectra consisting of 50% ferric cyt *b5* and 50% imidazole (Im)-bound P450-CAM. The spectra (MCD and UV-Vis) of the ferric Z-ISO (solid red line in Fig. 3.5) overlaps very well with the simulated spectra (dashed blue line in Fig. 3.5) of ferric cyt b5 (bis-His axial ligands) and Im-bound P450-CAM (His-Cys axial ligand pair). This indicates that the heme(s) in ferric Z-ISO appear to have two sets of ligand pairs (His-His and His-Cys) in a ~1:1 ratio, either as a single species (with a common His) or as two separate heme centers.

MCD and UV-vis absorption spectra of the ferrous state of Z-ISO are shown in Fig. 3.6, with analogous states of mono imidazole [H93G mono(Im)-Mb] and bis imidazole [H93G bis(Im)-Mb] bound H93G-myoglobin mutant are overlaid for comparison. The MCD spectral pattern of dithionite-reduced Z-ISO (red solid line in Fig. 3.6) is similar to that of ferrous H93G bis(Im)-Mb (blue dashed line in Fig. 3.6) which has a (His-His) coordination, indicating a ligand switch from a His-His or His-Cys coordination in oxidized state to a single His-His coordination in the reduced state. MCD and UV-vis absoprtion spectra of the CO-bound ferrous state of Z-ISO are shown in Fig. 3.7, (calculated for 100% CO saturation, red solid line in Fig 3.7) with those of cyclohexylamine-bound H93G myoglobin (H93G-(CHA) Mb) (blue dashed line in Fig 3.7) and wild type sperm whale myoglobin (Mb) (black dotted line in Fig 3.7) overlaid for comparison. The formation of the ferrous-CO complex did not appear to be complete even after extensive CO bubbling, judging from the double MCD troughs at ~555 and ~565 nm. Thus, we have tried to obtain spectra of the CO-saturated form by calculation assuming that the observed MCD spectrum was for incompletely CO-saturated ferrous Z-ISO. The best estimate for CO saturation was 70% CO-bound form in CO-bubbled Z-ISO. The MCD line shapes and spectral intensities (for main peaks and troughs) are roughly similar for the three proteins. MCD spectra of ferric Z-ISO show that the heme has two ligand pairs (His-His and His-Cys). This was determined by comparing the Z-ISO spectrum with that of a simulated mixture of Cyt *b5* (bis-His heme coordination) and imidazole (Im)-bound P450-CAM (His-Cys heme coordination) (Fig. 3.5). Thus, there appear to be two ligand coordination modes in low spin ferric Z-ISO in ~ 1:1 ratio. It appears that if there is only one heme center in the protein, His and Cys might occupy the distal side of the heme as alternative endogenous ligands while the proximal side is ligated by a common His. However if two heme centers exist, there should be two separate proximal histidines.

To help distinguish among the alternate hypotheses, we probed the MCD spectrum of the dithionite-reduced Z-ISO. We found that there is a single heme species in the reduced Z-ISO which shows only the bis-His species (Fig. 3.6). The data suggest that the heme may be undergoing ligand switching when the protein is reduced. A small fraction of high-spin heme b that is His-ligated and five coordinate was also detected, which may represent an intermediate. The MCD spectra of CO-bound Fe(II) Z-ISO also showed only about 70% CO saturation (Fig. 3.7), suggesting that while the distal His ligand is weak, it is not completely replaced by exogenous ligand.

Based on these data, a working hypothesis is proposed that an inactive Z-ISO carries an oxidized heme Fe(III), where cysteine blocks substrate access to the iron in the active site. Reduction of the heme switches coordination of the heme to bis-His, thus exposing the active site for substrate access to the heme Fe(II). A schematic representation of the heme ligand switching is summarized in below Scheme 3.1.

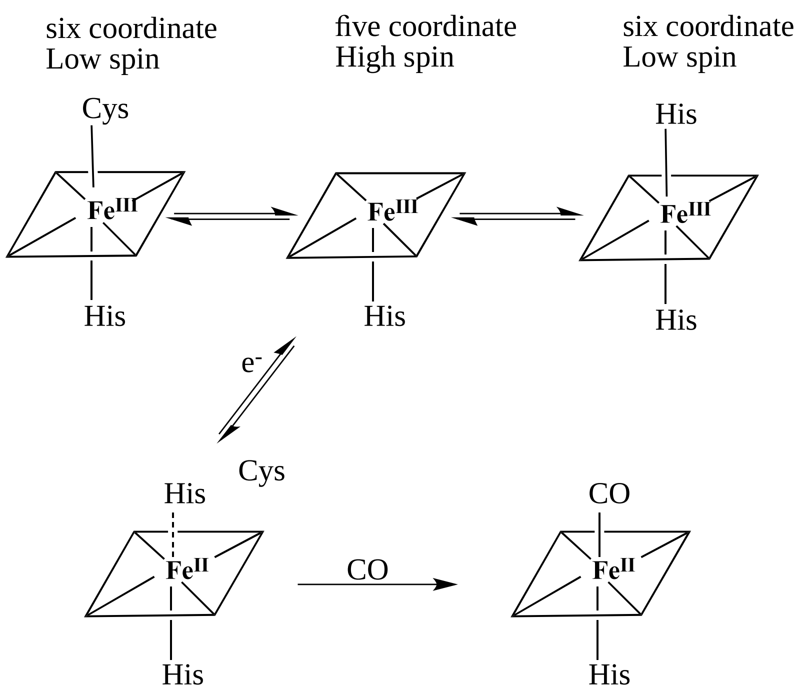

Scheme 3.1 Schematic representation of the heme ligand switching in Z-ISO.

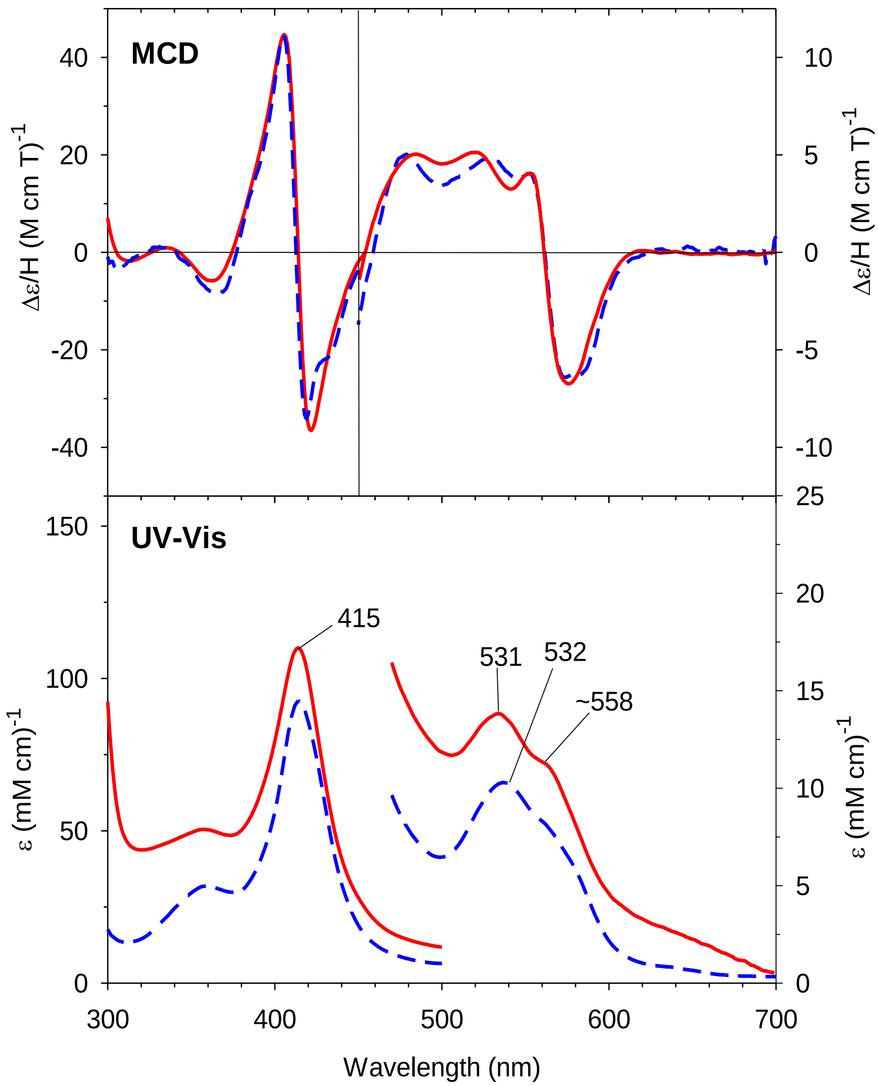

Figure 3.5 MCD and UV-vis absorption spectra at 4 °C of ferric Z-ISO at pH 7.0 (solid red line), overlaid with simulated spectra consisting of 50% ferric cyt *b5* and 50% ferric Im-bound P450-CAM (blue dashed line). The simulated spectra are replotted from individual spectra in Refs. 22 and 32 respectively

.

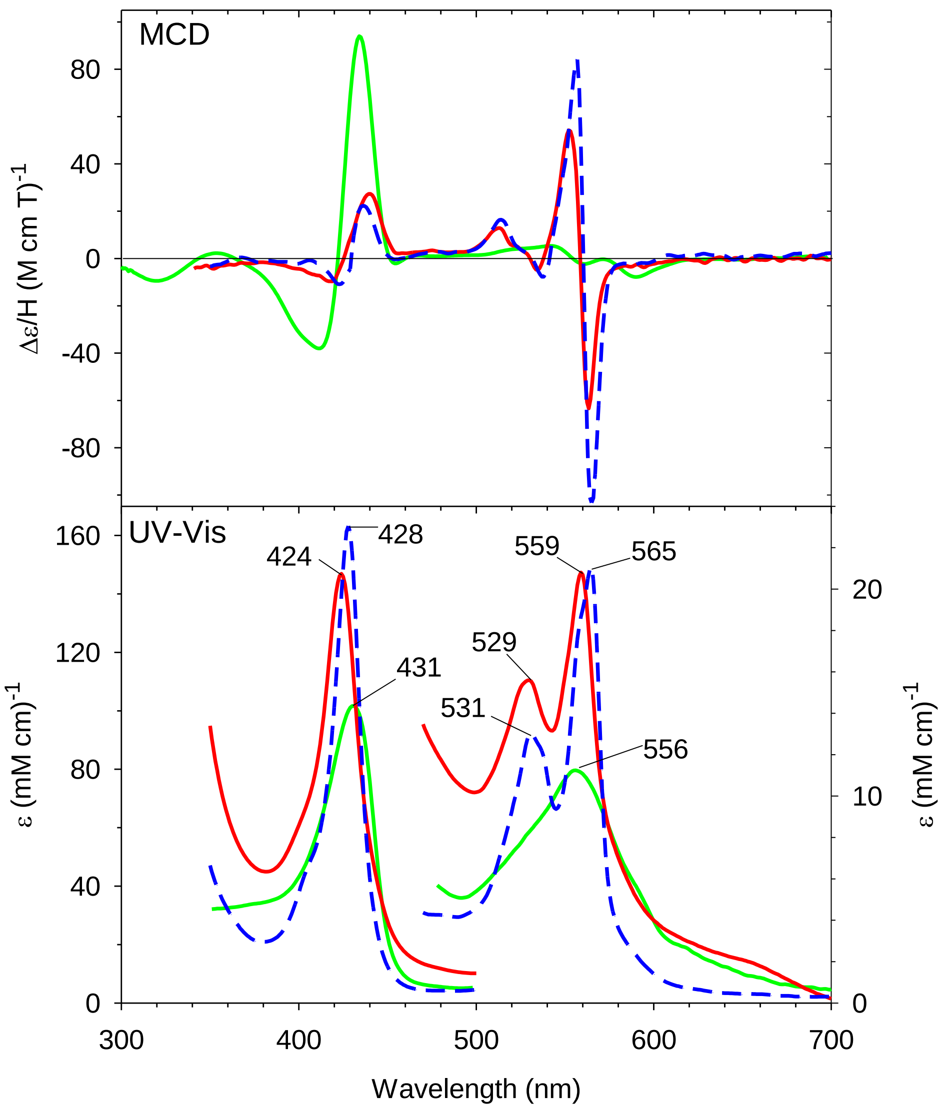

Figure 3.6 MCD and UV-vis absorption spectra at 4 °C of ferrous Z-ISO at pH 7.0 (solid red line), with H93G mono(Im)-Mb (green solid line) and H93G bis(Im)-Mb (blue dashed line). The spectra of ferrous mono- and bis- Im H93G-Mb are replotted from Ref. 33

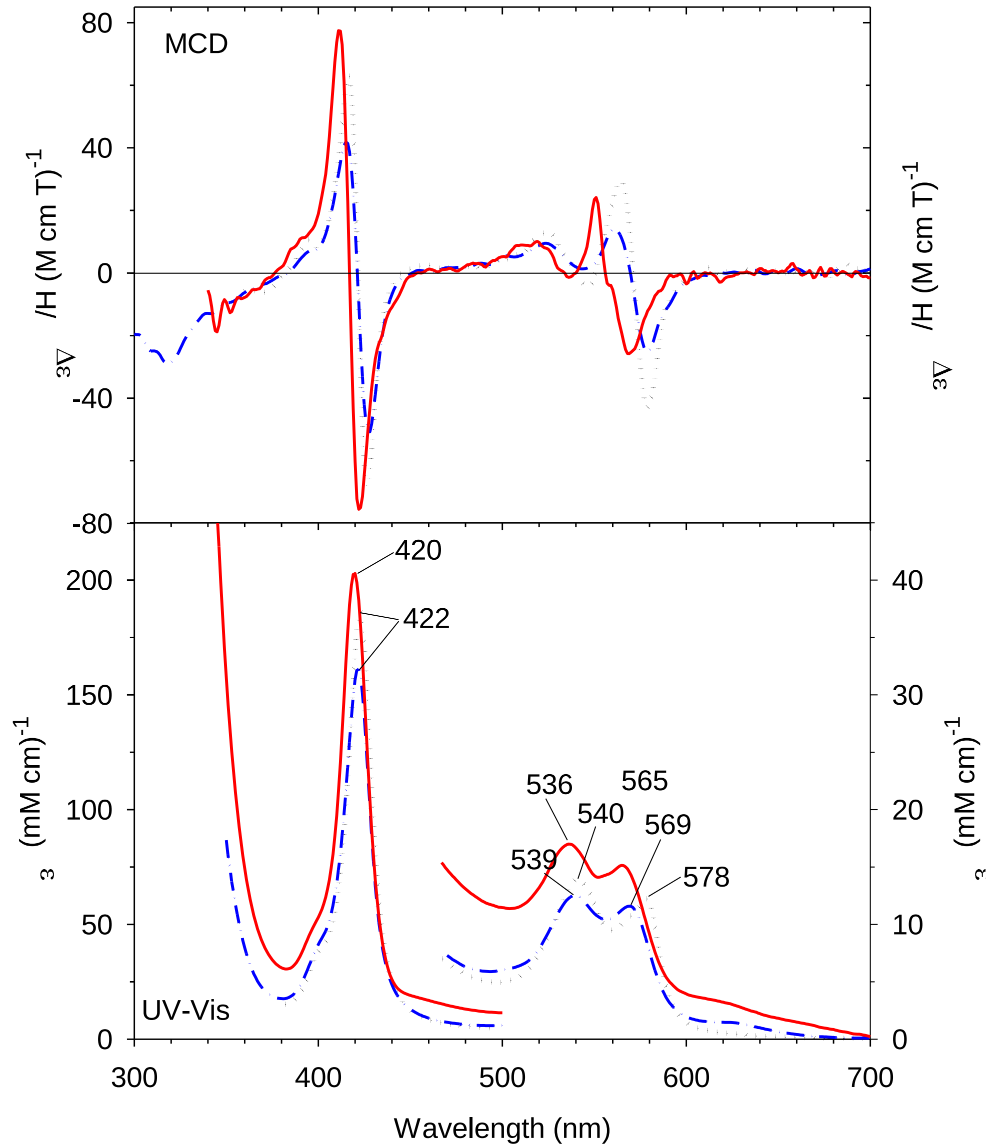

Figure 3.7 MCD and UV-vis absorption spectra at 4 °C of CO-bound ferrous Z-ISO calculated for 100% saturation at pH 7.0 (solid red line), with H93G-(cyclohexylamine) Mb (blue dashed line) and wild type (WT) Mb (black dotted line). The spectra of ferrous-CO H93G-(cyclohexylamine) Mb (UV-Vis data: Dawson, J. H., Kadkhodayan, S., Zhuang, C., Sono, M., unpublished data), and WT Mb spectra are replotted from Refs. 33 and 34 respectively

.

3.4 Part C: Demonstration of Oxy-ferrous Heme Adduct Formation in Ruthenium-diimine Photosensitizer Modified P450-BM3

Cytochrome P450 enzymes are capable of hydroxylating unactivated C-H bonds with the help of molecular dioxygen and reducing equivalents at ambient temperature and physiological pH with a high catalytic efficiency. This synthetic ability makes them particularly attractive for biotechnological applications; however complete dependence of the reactions on NAD(P)H and the reductase domain for electron transfer impedes their use as bio-catalysts. Amongst the numerous attempts to circumvent this issue, Dr. Lionel Cheruzel's lab (San Jose State University, San Jose, CA) has developed a series of hybrid enzymes using P450-BM3 (CYP102) and photosensitizer that could be activated using light. These hybrid enzymes consists of Ru(II)-diimine photosensitizer, covalently attached to non-native single cysteine residue close to the P450 BM3 heme domain.[35] Photoactivation converts the Ru(II) into a highly reductive Ru(I) species which provides the two necessary electrons to the heme domain in successive one-electron transfer steps.[36] Introduction of these mutations and/or covalent attachment of the Ru(II) photosensitizer does not significantly alter the binding of lauric or palmitic acid. Particularly the $Ru(bpy)_2phenA$ (bpy= bipyridine and phenA= 5-acetamido-1,10 phenanthroline) modified L407C mutant of P450-BM3 was found to have a high turnover number in the hydroxylation of lauric acid. In order to ascertain the ability of the hybrid enzyme to form the oxy-ferrous intermediate, Dr. Cheruzel's lab collaborated with our lab to use MCD spectroscopy to examine the integrity of the oxyferrous intermediate.

3.4.1 Methods:

Dr. Lionel Cheruzel provided us with purified protein samples of wild type (WT) and L407C-Ru-diimine hybrid sample prepared as described in [37]. MCD spectra were measured on a Jasco J815 spectropolarimeter fitted with a Jasco MCD-1B magnet at a magnetic field strength of 1.41 T at 4 °C and -50 °C in a mixed solvent (see below) using a 0.5-cm-path length quartz cuvette. Jasco software was used for data acquisition and manipulation as reported previously.[19] Concentrations of the P450-BM3 L407C-Ru-diimine hybrid sample were determined based on a value of ε = 104mM^{-1} cm^{-1} for the ferric protein. UV-vis absorption spectra were recorded on a Cary 400 spectrometer, before and after each MCD measurement to track sample integrity. Sample preparation and data collection was done as previously described in Ref. [38], and in complete detail in [39]. The L407C-Ru-diimine hybrid sample was analyzed in a buffer comprising of 0.3 M Tris at pH 8.0 and glycerol in a starting ratio of 30/70 (v/v), with the final concentration of glycerol in the protein sample being ~60% (after some dilution with dithionite aqueous solution). Before adding sodium dithionite, the sample was degassed over 3 h on ice with a slow stream of nitrogen gas in a rubber septum-sealed cuvette to ensure complete and highly anaerobic condition.

3.4.2 Results and Discussion:

We examined the oxy complex of P450-BM3 L407C-Ru-diimine hybrid sample in cryo-solvent in both the presence and absence of substrates. The oxy complex of the Ru-diimine labeled protein was made by bubbling O_2 in the reduced protein (dissolved in ~65% glycerol solution) at -50^{o} C. The P450-BM3 L407C-Ru-diimine hybrid (solid red line in Fig. 3.8) forms a stable oxy-complex at -50^{o} C whose MCD and UV-Vis absorption spectra are very similar to the O_2 adduct of wild-type P450 BM3 (blue dashed line in Fig. 3.8) as well as bacterial wild type P450-CAM (black dotted line in Fig. 3.8).

The O_2-bound Ru-diimine labeled as well as WT P450-BM3 may be stable even at slightly higher temperatures (such as -30^o C), but we have not examined the temperature dependence of its stability in this work. MCD and UV-vis absorption spectra of lauric acid (LA) and palmitic acid (PA)-bound P450-BM3 L407C-Ru-diimine hybrid (pink solid line and green solid line in Fig. 3.9) show that they form a stable oxy-complex just like the Ru-diimine labeled protein (red dotted line in Fig. 3.9) at -50^{o}C. Their MCD and UV-Vis absorption spectra are very similar to those of the O_2 adduct of the substrate-free enzyme, as seen in Fig. 3.9. With LA and PA substrates, we did not observe a marked conversion from low-spin species to high-spin species on substrate addition in the ferric protein in 60-70% glycerol buffer as is seen in aqueous buffer. We initially thought this was resulting from incomplete binding of the substrate although similar results have been reported earlier by Dawson and co-workers.[38] Thus we set out to test another substrate N-palmitoylglycine (NPG) that has been shown to bind P450-BM3 with a low K_d value.[40] We observed that conversion to a high-spin form spectrum upon substrate binding to ferric enzyme (low spin) is not pronounced in the 70:30 Glycerol/Tris buffer (pH 8). However, nearly complete conversion to a high-spin state can be clearly seen in the 50 mM Tris, pH 7.2 buffer (without glycerol) at room temperature (~22 ^{o}C) (blue dashed line in Fig. 3.10). Analogous P450-CAM spectra with and without the substrate camphor are overlaid for comparison in Fig. 3.10. Just like the other substrate containing samples, the oxy complex of the Ru-diimine labeled protein was made by bubbling O_2 in the reduced protein in ~65% glycerol solution (the initial 70/30 Glycerol/0.3M Tris buffer, pH 8.0 was slightly diluted by dithionite stock solution added to reduce the ferric protein),

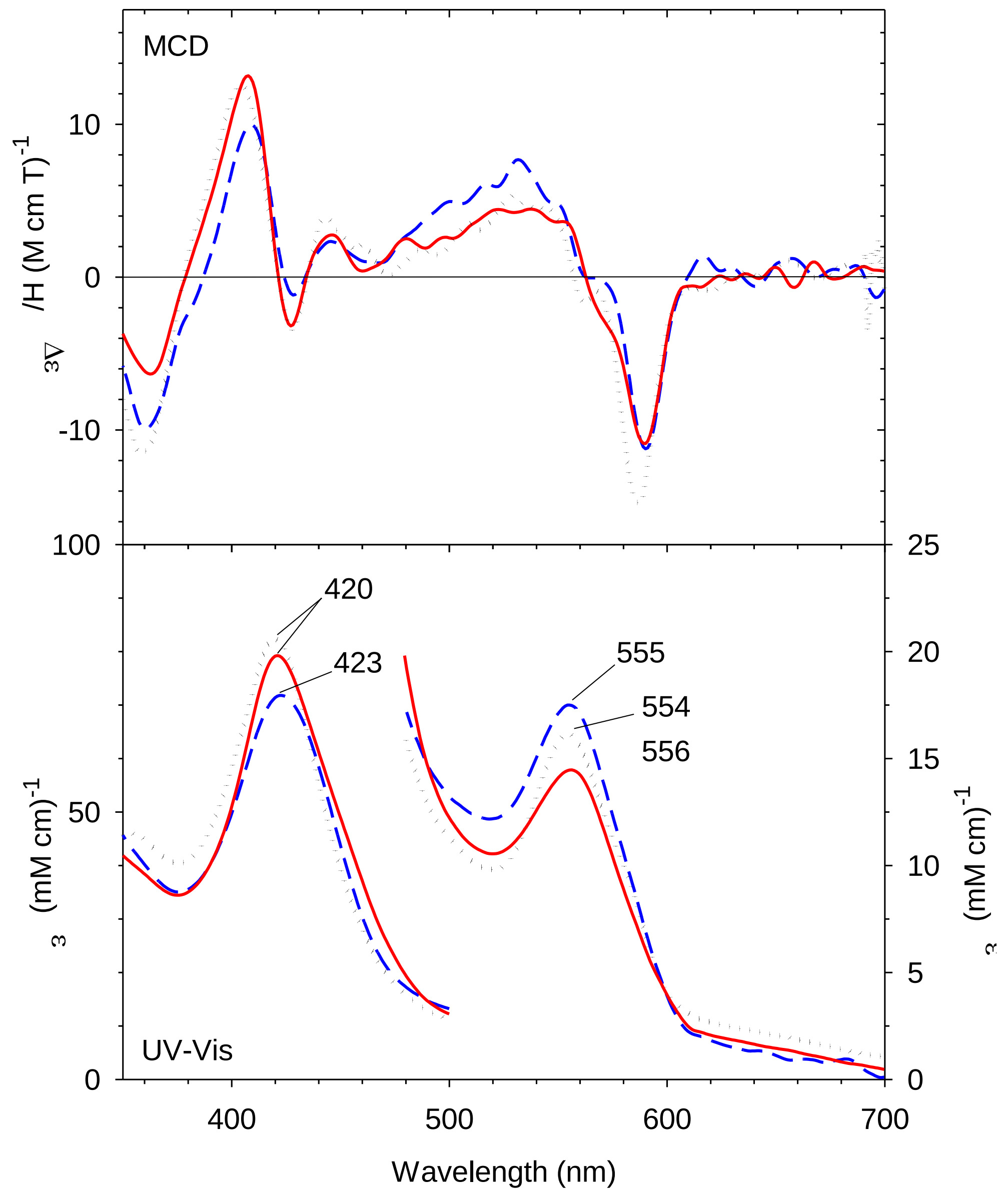

Figure 3.8 MCD and UV-Vis absorption spectra of the O_2 adduct of the P450-BM3 L407C-Ru hybrid (blue dashed line), wild-type P450 BM3 (blue dashed line) as well as bacterial wild-type P450CAM (black dotted line) recorded at -50°C in ~60% glycerol containing 0.3 M Tris buffer at pH 8.0. The spectra of ferrous di-oxy P450CAM are replotted from Ref. 41

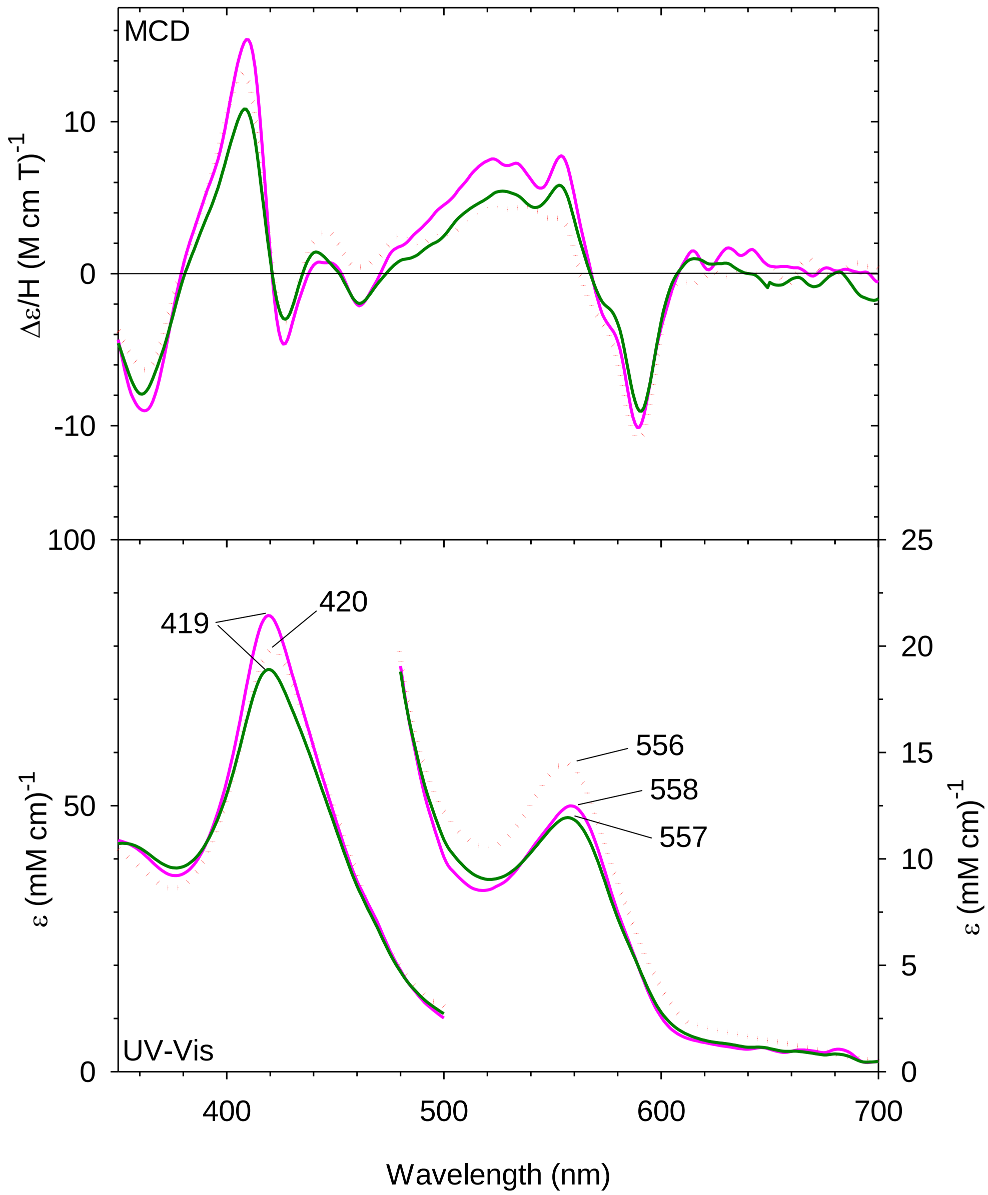

Figure 3.9 MCD and UV-Vis absorption spectra of the O_2 adduct of the substrate-free P450-BM3 L407C-Ru hybrid (red dotted line), LA-bound form (pink solid line) as well as PA-bound form (green solid line) recorded at -50°C in ~60% glycerol containing 0.3 M Tris buffer at pH 8.0

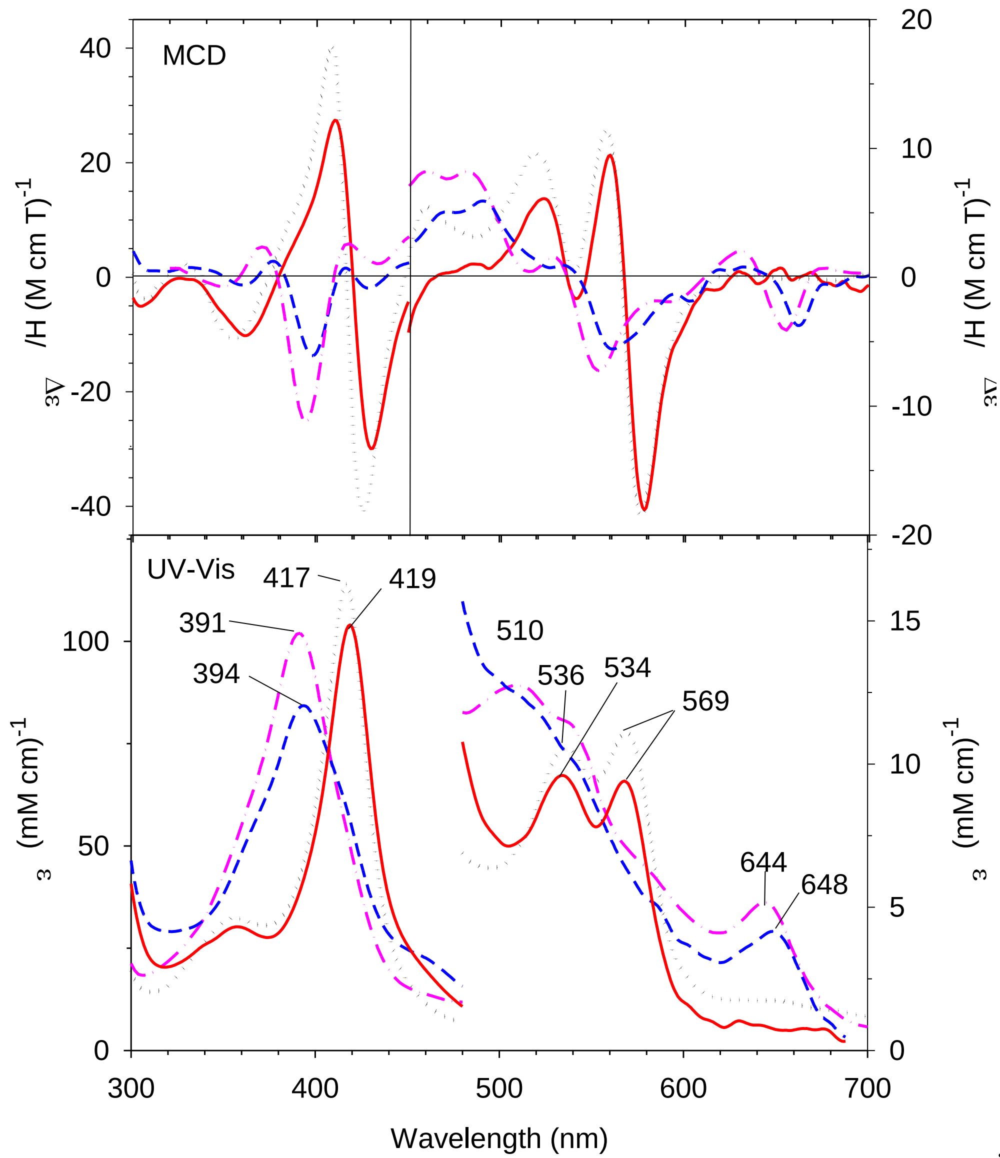

Figure 3.10 MCD and UV-Vis absorption spectra of the ferric substrate-free P450-BM3 L407C-Ru hybrid (red solid line), ferric NPG-bound form (blue dashed line) as well as ferric substrate-free P450-CAM form (black dotted line) and ferric camphor-bound P450-CAM (pink dashed line) recorded in aqueous buffer. The spectra of ferric substrate-free P450-CAM and ferric camphor-bound P450-CAM MCD are replotted from Ref. 42

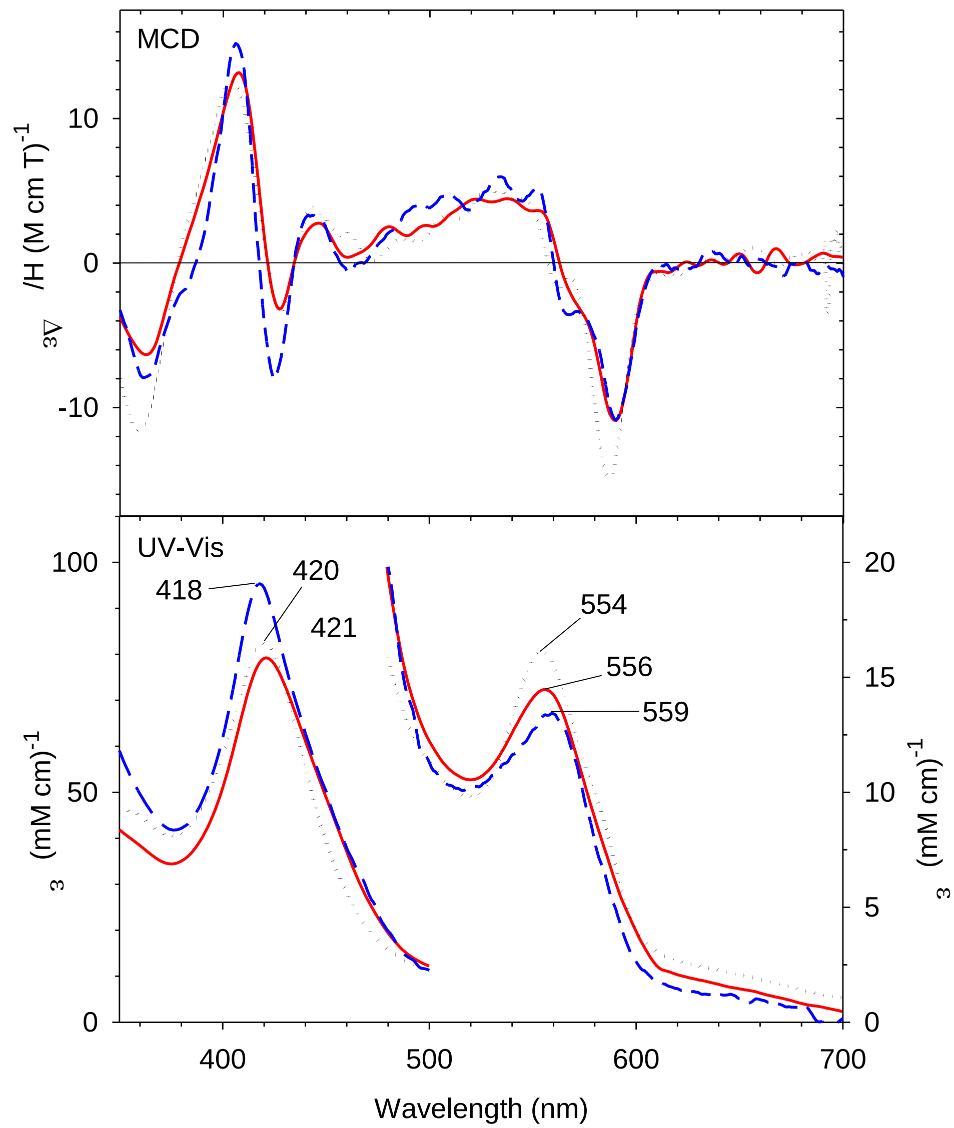

Figure 3.11 MCD and UV-Vis absorption spectra of the O_2 adduct of the substrate-free P450-BM3 L407C-Ru hybrid (red solid line), NPG-bound form (blue dashed line) as well as camphor-bound P450-CAM (black dotted line) recorded at -50°C in ~60% glycerol containing 0.3 M Tris buffer at pH 8.0. The spectra of oxy-ferrous camphor-bound P450CAM spectrum is replotted from Ref. 41.

solution at -50 ^oC. While the NPG-bound protein forms a comparable oxy-complex just like the substrate-free Ru-diimine-labeled protein at -50 ^oC, as seen in Fig. 3.11 the oxy-P450BM3-Ru + NPG complex appeared to be less stable than the oxy-complex without substrate or with LA or PA even at –50 ^oC. This was judged from the gradual MCD spectral changes (to the ferric state) upon O_2 bubbling into the deoxyferrous form at –50 ^oC compared with little spectral changes during the same treatments and time periods for substrate-free and LA- or PA-bound P450BM3-Ru-diimine proteins. In fact, the Soret MCD peak and trough intensities for the NPG-bound oxy-P450BM3-Ru are somewhat higher than the other samples, which is a sign of ferric form contamination.

3.5 Part D: Heme Axial Ligand Determination in Phu_R

The Phu_R is a TonB dependent outer membrane receptor that is part of the *Pseudomonas* heme uptake system from *Pseudomonas aeruginosa*.[43] Phu_R helps in the transport of heme to the periplasm from where a further cascade helps in retrieval of iron (an essential micronutrient for survival and virulence of bacterial pathogens) from the heme.[44, 45] Sequence alignments of TonB dependent outer membrane receptors have shown that heme is coordinated through two histidine residues, however, a conserved histidine observed on the extracellular FRAP loop of other receptors is missing in Phu_R. There are other potential ligands present in the vicinity, specifically His-102, Tyr-519, Tyr-529 and His-530. To confirm the correct identity of the heme coordinating ligands Dr. Angela Wilks (University of Maryland, Baltimore, MD) collaborated with our lab to conduct MCD experiments on the WT and mutant enzymes.

3.5.1 Methods:

Dr. Angela Wilks provided us with purified samples of WT and mutant Phu_R proteins Y529A, Y529H and H102A (data unpublished). MCD spectra were measured on a Jasco J815 spectropolarimeter fitted with a Jasco MCD-1B magnet at a magnetic field strength of 1.41 T at 4 °C using a 0.2 cm pathlength quartz cuvette. Jasco software was used for data acquisition and manipulation as reported previously.[19] Concentrations of the samples were tentatively determined (based on the pyridine hemochromogen method) for the Soret absorption peaks of ferric WT Phu_R (ε_{405} = 96.9 mM^{-1} cm^{-1}), Y529A Phu_R (ε_{404} = 114.0 mM^{-1} cm^{-1}) and Y529H Phu_R (temporary value of ε_{Soret} = 100 mM^{-1} cm^{-1}). UV-vis absorption spectra were recorded on a Cary 400 spectrometer, before and after each MCD measurement to track sample integrity. Phu_R protein samples were studied in 50 mM Tris pH 7.5, 50 mM NaCl, and 0.06% (w/v) lauryldimethylamine-oxide (*LDAO*) at pH 7.5. The imidazole (Im) and cyanide (CN^{-}) adducts were prepared by adding aliquots of Im and KCN stock solutions (1 M or diluted concentrations, pH adjusted to ~7) to the protein, respectively, until apparent saturation (no further spectral change) was reached. The ferrous species of Phu_R prepared from the ferric protein in the presence of exogenous ligands, by flushing a rubber septum-sealed cuvette with nitrogen gas for about 10-15 min followed by the addition of a small amount of solid sodium dithionite was found to denature the sample. Thus, for the purpose of this study we only looked at ferric forms of the protein.

3.5.2 Results and Discussion:

We have examined the Phu-R protein (enzyme) along with its mutants, with magnetic circular dichroism (MCD) and UV-visible (UV-Vis) absorption spectroscopy in its ferric [Fe(III)], ferric + cyanide [Fe(III)-CN] and ferric + imidazole [Fe(III)-Im] bound states. The spectra of PhuR are overlaid with those previously reported for the corresponding states of legehemeglobin-A + phenol, cytochrome b5 (bis-His-ligated heme protein), mono-4-methylimidazole (4-MeIm)-bound H93G Mb (proximal cavity Mb mutant), bis-His bound H93G Mb, and wild type myoglobin (WT-Mb), for comparison. The MCD spectral pattern of ferric WT PhuR as seen in Fig 3.12 (red solid line) is somewhat similar in both the Soret (350 - 450 nm) and visible regions (450 - 700 nm) to that of phenol-bound ferric leghemoglobin a (Lb-a) (black dashed line in Fig. 3.12) which has a proximal His and distal phenol (Tyr equivalent) heme ligation. This strongly suggests that ferric WT PhuR has His-Tyr type of heme ligation. Judging from the slightly larger MCD trough intensities at ~570 and ~420 nm, Fe(III) WT PhuR appears to contain more low-spin component than phenol-bound Lb-a. When the MCD and UV-vis absorption spectra of Fe(III) WT PhuR was titrated with cyanide as seen in Fig. 3.13, a spectral shift of 6 nm was observed on apparently saturation (Kd_{app} ~ 39.7 μM). However, the incomplete conversion of the ferric heme to low-spin (remaining absorption peak at ~620 nm and MCD trough at ~630 nm) indicates that the heme is not totally converted to a cyanide complex (100% low-spin species).

The MCD and UV-Vis absorption spectral patterns of ferric Y529A PhuR as seen in Fig. 3.14 shows the presence of charge-transfer UV-Vis spectral bands at ~610 and ~490 nm, an MCD trough at ~630 nm and relatively small MCD peak to trough intensity in the Soret region. This indicates that ferric Y529A PhuR protein (red solid line in Fig. 3.14) heme is high-spin; however, its MCD/UV-Vis absorption spectra do not resemble those of meta-aqua Mb (black dotted line in Fig. 3.14) or mono-4-methylimidazole-bound H93G Mb (blue dashed line in Fig. 3.14) well, although broad similarities may be found.

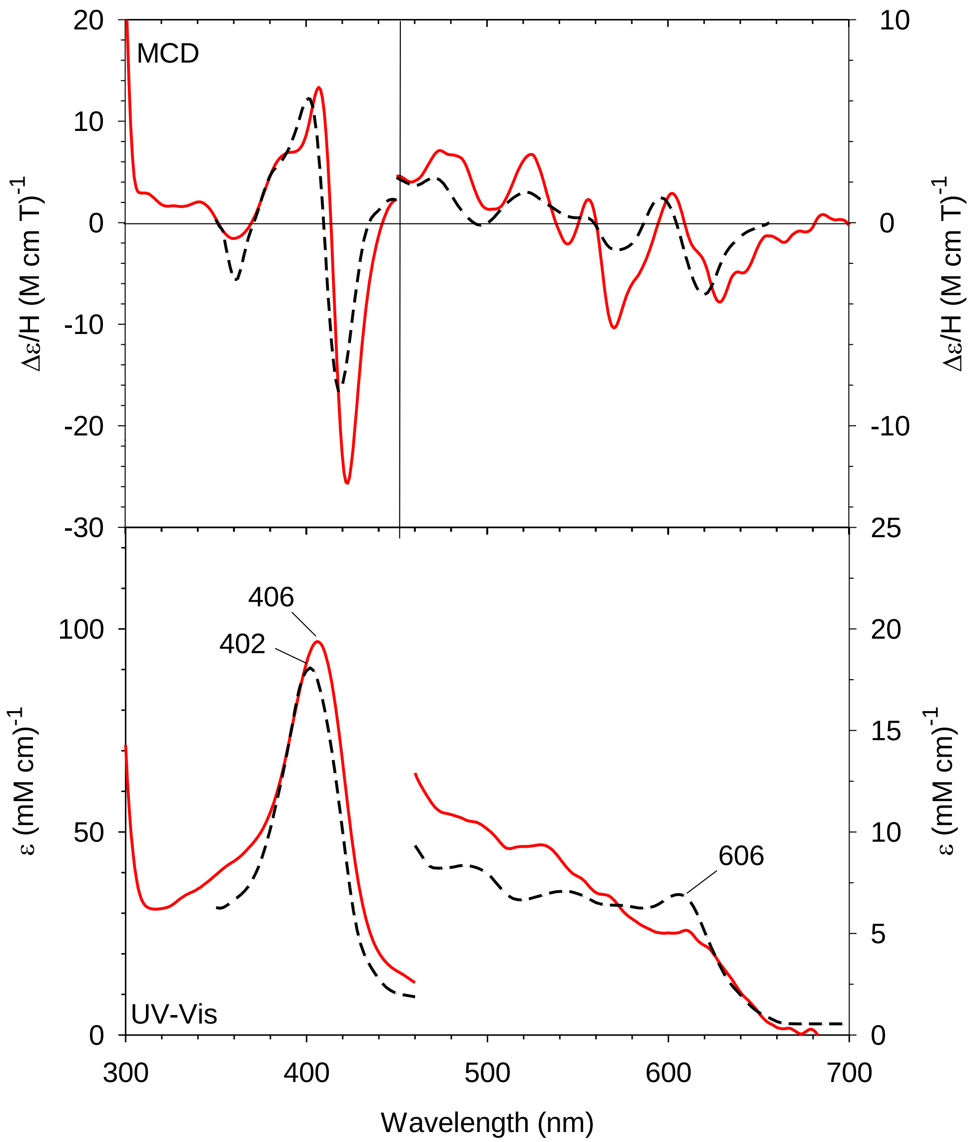

Figure 3.12 MCD and UV-vis absorption spectra of ferric WT PhuR (red solid line) overlaid for comparison with phenol-bound ferric Lb-A (black dashed line). The Lb-A spectra are replotted from Ref. 46

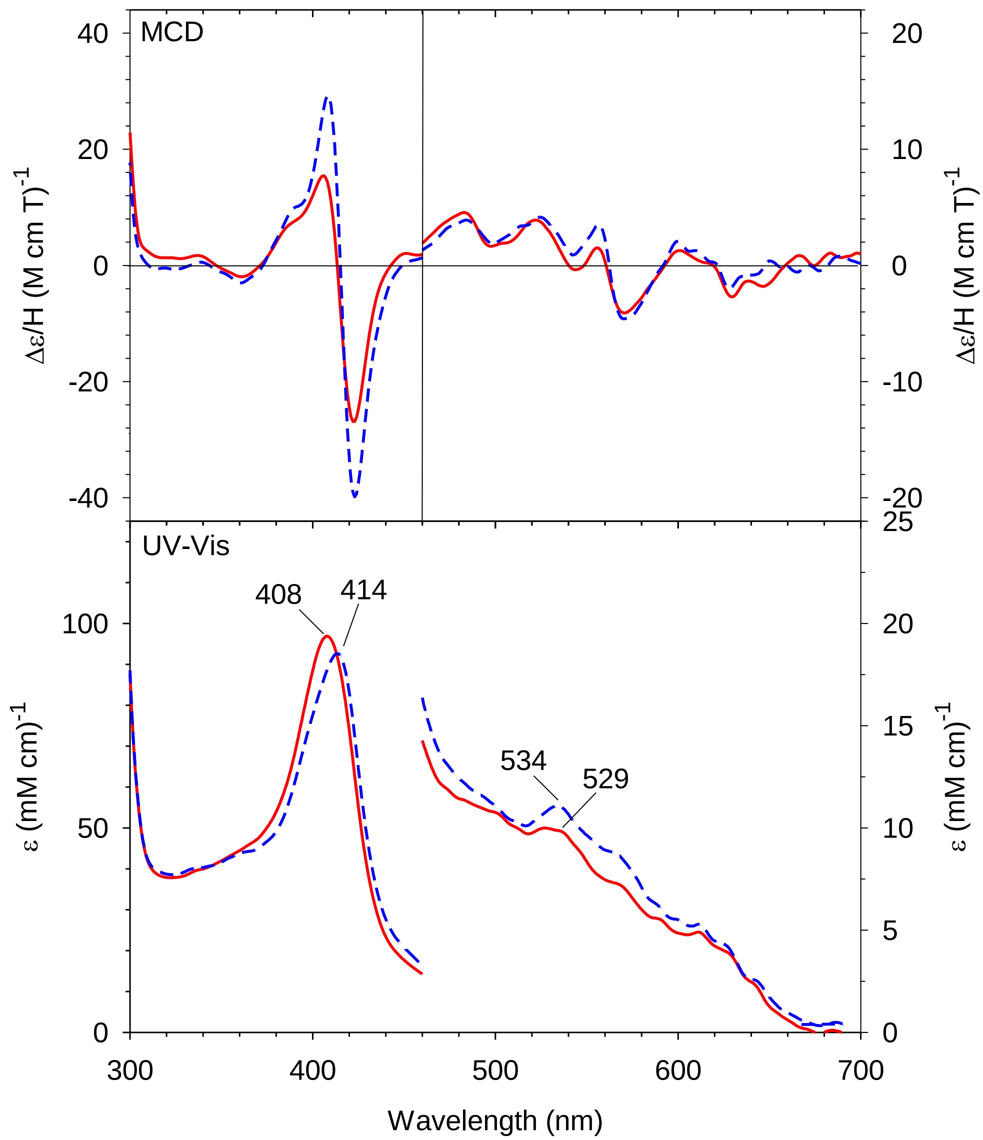

Figure 3.13 MCD and UV-vis absorption spectra of ferric WT PhuR (red solid line) overlaid for comparison with CN-bound ferric WT Phu_R (blue dashed line).

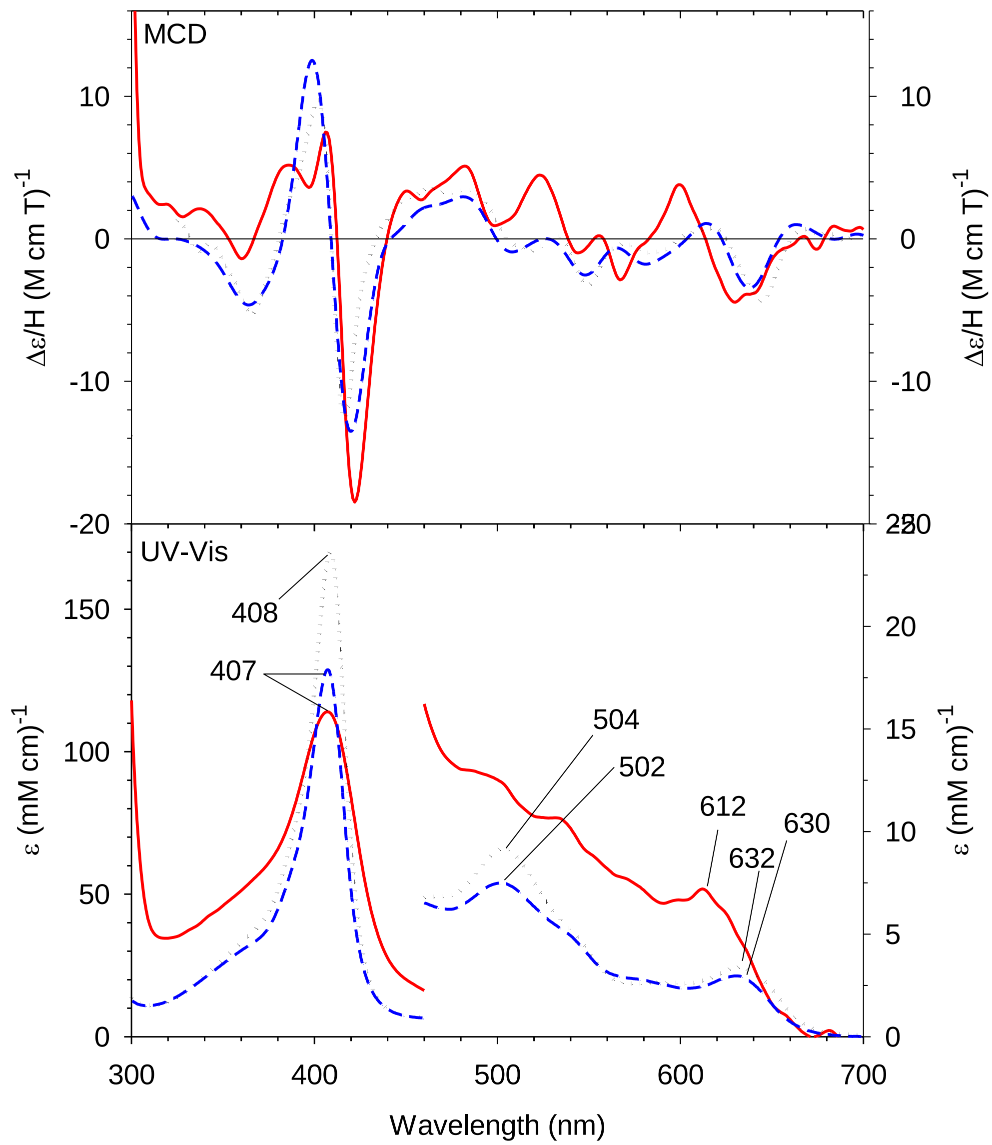

Figure 3.14 MCD and UV-vis absorption spectra of ferric Y529A PhuR protein (red solid line) overlaid for comparison with that of meta-aqua Mb (black dotted line) replotted from Ref. 21 (UV-Vis data: Dawson, J. H., Kadkhodayan, S., Zhuang, C., Sono, M., unpublished data) and mono-4-methylimidazole-bound H93G Mb (blue dashed line) replotted from Ref. 47.

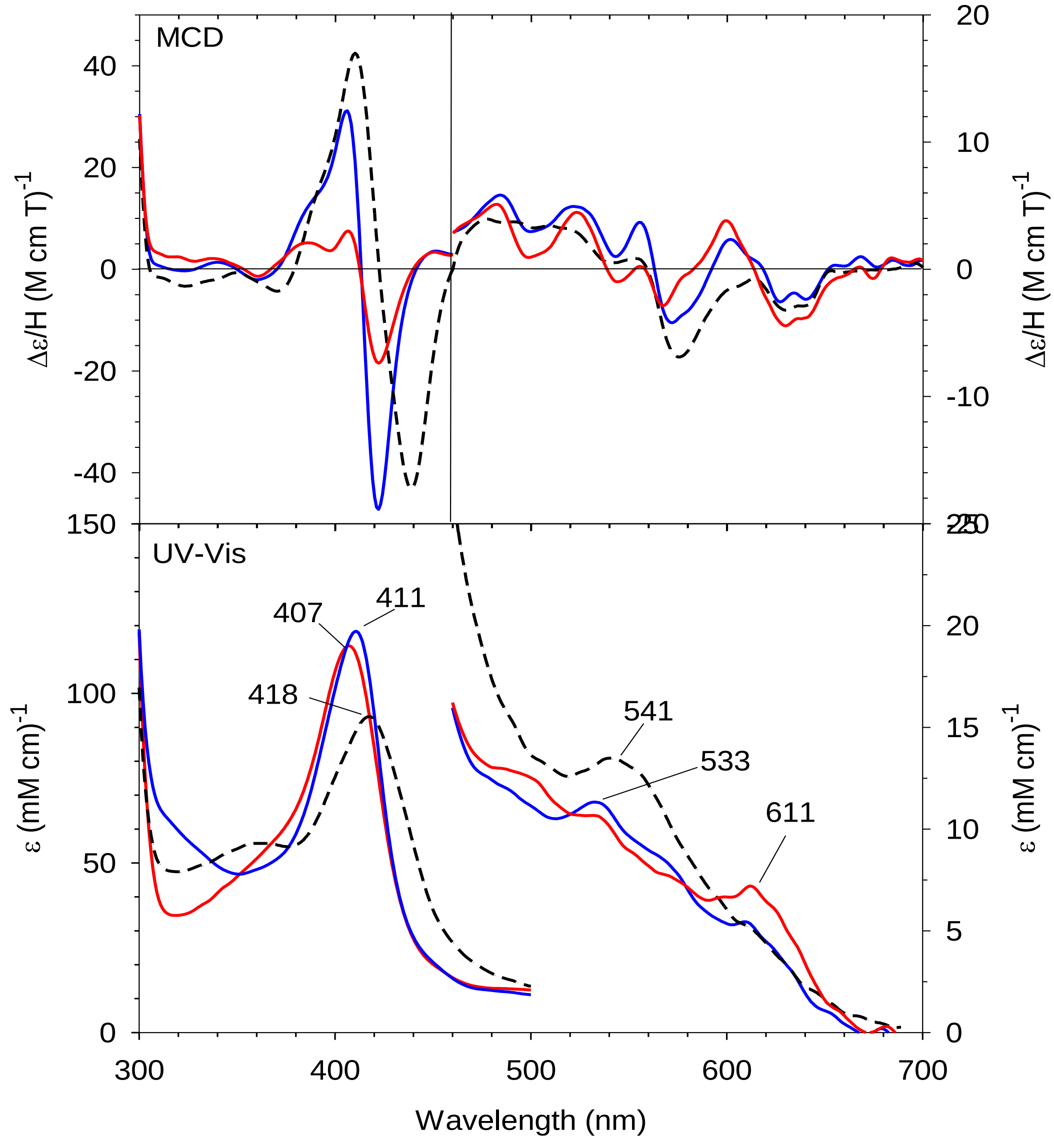

Figure 3.15 MCD and UV-vis absorption spectra of ferric Y529A Phu_R protein (red solid line) overlaid for comparison with and Im- adducts of ferric Y529A Phu_R (black dotted line) and (blue solid line), respectively.

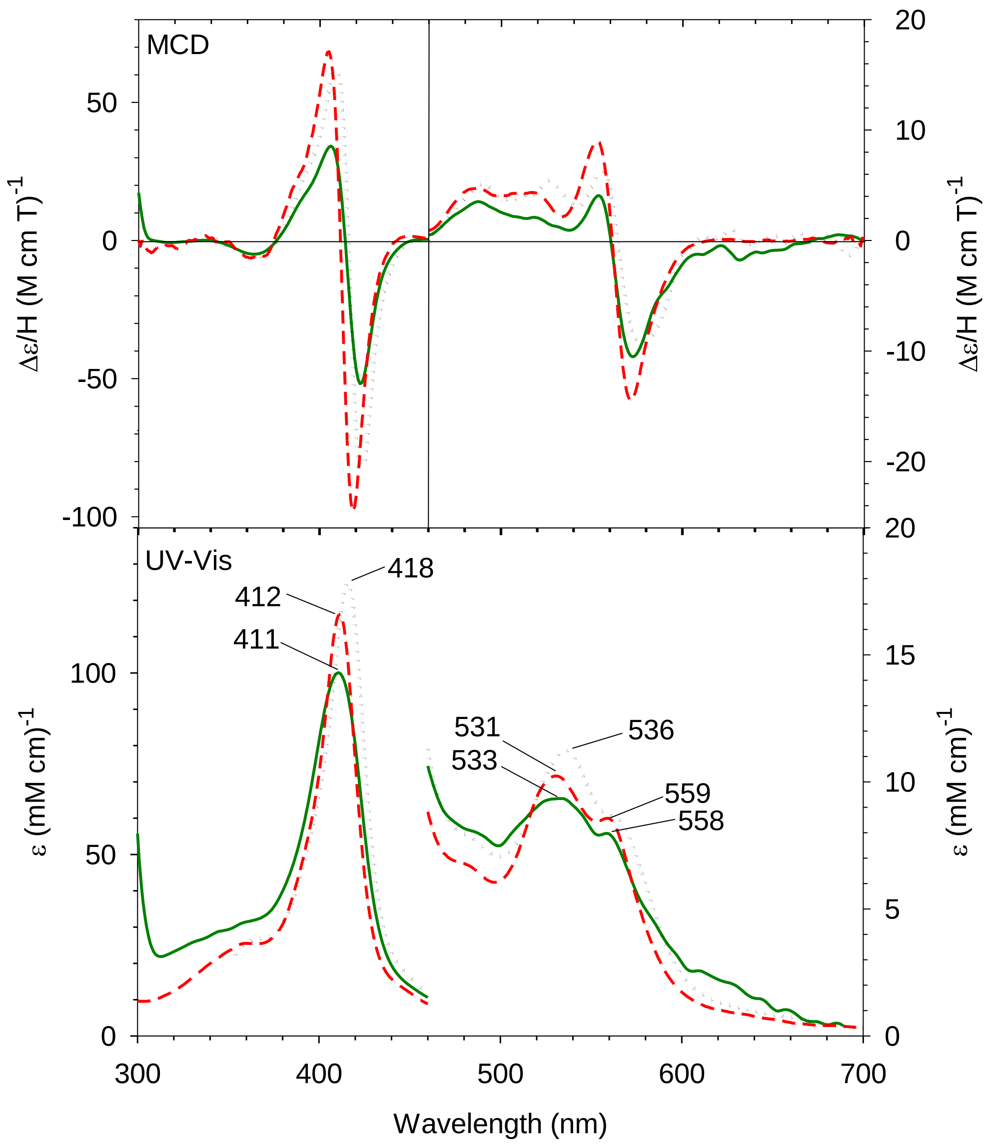

Figure 3.16 MCD and UV-vis absorption spectra of ferric Y529H PhuR protein (green solid line) overlaid for comparison with ferric cyt b5 (red dashed line) replotted from Ref 22 and bis-imidazole bound H93G Mb (black dotted line) replotted from Ref. 33

In addition, a noticeable MCD shoulder at ~380 nm is observed for the Fe(III) Y529A PhuR. KCN and Im titrations of ferric PhuR Y529A as seen in Fig. 3.15 resulted in formation of the respective ligand complexes of this mutant exhibiting Soret absorption peak shifts from 407 nm to 411 nm (Im) and 418 nm (CN-) and appearance of low-spin type visible region absorption peaks at ~533 nm (Im) and ~540 nm (CN-). Soret MCD peak-to-trough intensities also increase by more than two-fold for both ligands as a sign of formation of low-spin complexes. However, similar to the case of WT Fe(III) PhuR (Fig. 3.13), the high-spin charge-transfer band at ~610 nm does not disappear completely as well as the remaining MCD trough at ~630 nm for the both ligands. Thus, ligand complex formation seems to be incomplete, especially for the cyanide adduct that should be totally low-spin.

The MCD spectral pattern of ferric Y529H PhuR as seen in Fig 3.16 (green solid line) overlaps essentially perfectly in both the Soret (350 – 450 nm) and visible regions (450 – 700 nm) to that of ferric cyt b5 (red dashed line) and bis-imidazole bound H93G Mb (black dotted line), both of which have bis-His (Im) heme ligation, clearly suggesting that Y529 to H mutation imparts a bis-His ligation to the heme.

3.6 Conclusion:

We have analyzed the sGAF2, Z-ISO, P450-BM3 L407C-Ru hybrid sample and Phu_R heme proteins with MCD and compared their spectra against data from the heme protein spectral library recorded and maintained by our lab. In the case of sGAF2, Z-ISO and Phu_R proteins, MCD helped in identification of the heme coordinating ligands, whereas in the case of P450-BM3 L407C-Ru-diimine hybrid, MCD was used to characterize the ferrous dioxygen complex. Knowledge of the heme ligand identity has been used to hypothesize a working mechanism for the Z-ISO enzyme. For the P450-BM3 L407C-Ru-diimine hybrid, the MCD characterization of the ferrous dioxygen intermediate was used to ascertain that the engineered enzyme was following a normal P450 turnover pathway. The fingerprinting ability of MCD coupled with other spectroscopic techniques such as resonance Raman and EPR makes it a valuable tool in investigating the structure and function of novel heme enzymes.

3.7 References:

1. Dawson, J. H. (1988) Probing structure-function relations in heme-containing oxygenases and peroxidases, *Science 240*, 433-439.

2. Perutz, M. F., Muirhead, H., Cox, J. M., Goaman, L. C. G., Mathews, F. S., McGandy, E. L., and Webb, L. E. (1968) Three-dimensional Fourier synthesis of horse oxyhaemoglobin at 2.8 Å resolution:(I) X-ray analysis, *Nature 219*, 29-32.

3. Dunford, H. B. (1999) *Heme peroxidases*, John Wiley New York:.

4. Mason, W. R. (2007) *Magnetic Circular Dichroism Spectroscopy*, John Wiley & Sons.

5. Cheek, J., and Dawson, J. H. (2000) Magnetic circular dichroism spectroscopy of heme proteins and model systems, *The Porphyrin Handbook 7*, 339-369.

6. Buckingham, A. D., and Stephens, P. J. (1966) Magnetic optical activity, *Annu. Rev. Phys. Chem. 17*, 399-432.

7. Stephens, P. J. (1974) Magnetic circular dichroism, *Annu. Rev. Phys. Chem. 25*, 201-232.

8. Stephens, P. J. (1976) Magnetic circular dichroism, *Adv. Chem. Phys. 35*, 197-264.

9. Wright, J. R., Hendrickson, W. A., Osaki, S., and James, G. T. (1986) *Phys. methods inorg. biochem.*, Plenum Press.

10. Vickery, L. E. (1978) Spin states of heme proteins by magnetic circular dichroism, *Methods Enzymol. 54*, 284.

11. Vickery, L., Nozawa, T., and Sauer, K. (1976) Magnetic circular dichroism studies of low-spin cytochromes. Temperature dependence and effects of axial coordination on the spectra of cytochrome c and cytochrome b5, *J. Am. Chem. Soc. 98*, 351-357.

12. Holmquist, B. (1986) [12] Magnetic circular dichroism, In *Methods Enzymol.* (C. H. W. Hirs, S. N. T., Ed.), pp 270-290, Academic Press.

13. Suzuki, S., Yoshimura, T., Nakahara, A., Iwasaki, H., Shidara, S., and Matsubara, T. (1987) Electronic and magnetic circular dichroism spectra of pentacoordinate nitrosylhemes in cytochromes c'from nonphotosynthetic bacteria and their model complexes, *Inorg. Chem. 26*, 1006-1008.

14. Dawson, J. H., and Dooley, D. M. (1989) Magnetic circular dichroism spectroscopy of iron porphyrins and heme proteins, *Iron porphyrins, part 3*, 1-92.

15. Karniol, B., Wagner, J., Walker, J., and Vierstra, R. (2005) Phylogenetic analysis of the phytochrome superfamily reveals distinct microbial subfamilies of photoreceptors, *Biochem. J 392*, 103-116.

16. Daltrop, O., Smith, K. M., and Ferguson, S. J. (2003) Stereoselective in vitro formation of c-type cytochrome variants from Hydrogenobacter thermophilus containing only a single thioether bond, *J. Biol. Chem. 278*, 24308-24313.

17. Pipirou, Z., Bottrill, A. R., Metcalfe, C. M., Mistry, S. C., Badyal, S. K., Rawlings, B. J., and Raven, E. L. (2007) Autocatalytic formation of a covalent link between tryptophan 41 and the heme in ascorbate peroxidase, *Biochemistry 46*, 2174-2180.

18. Molitor, B., Stassen, M., Modi, A., El-Mashtoly, S. F., Laurich, C., Lubitz, W., Dawson, J. H., Rother, M., and Frankenberg-Dinkel, N. (2013) A heme-based redox sensor in the methanogenic archaeon Methanosarcina acetivorans, *J. Biol. Chem. 288*, 18458-18472.

19. Huff, A. M., Chang, C. K., Cooper, D. K., Smith, K. M., and Dawson, J. H. (1993) Imidazole-and alkylamine-ligated iron (II, III) chlorin complexes as models for histidine and lysine coordination to iron in dihydroporphyrin-containing proteins: characterization with magnetic circular dichroism spectroscopy, *Inorg. Chem. 32*, 1460-1466.

20. Du, J., Sono, M., and Dawson, J. H. (2011) Ferric His93Gly myoglobin cavity mutant and its complexes with thioether and selenolate as heme protein models, *J. Por. Phthalocyanines 15*, 29-38.

21. Dawson, J. H., Kadkhodayan, S., Zhuang, C., and Sono, M. (1992) On the use of iron octa-alkylporphyrins as models for protoporphyrin IX-containing heme systems in studies employing magnetic circular dichroism spectroscopy, *J. Inorg. Biochem. 45*, 179-192.

22. Cheek, J., Mandelman, D., Poulos, T. L., and Dawson, J. H. (1999) A study of the K+-site mutant of ascorbate peroxidase: mutations of protein residues on the proximal

side of the heme cause changes in iron ligation on the distal side, *JBIC J. Biol. Inorg. Chem. 4*, 64-72.

23. Tanaka, A., and Shimizu, T. (2008) Ligand Binding to the Fe(III)-Protoporphyrin IX Complex of Phosphodiesterase from Escherichia coli (Ec DOS) Markedly Enhances Catalysis of Cyclic di-GMP: Roles of Met95, Arg97, and Phe113 of the Putative Heme Distal Side in Catalytic Regulation and Ligand Binding†, *Biochemistry 47*, 13438-13446.

24. Tanaka, A., Takahashi, H., and Shimizu, T. (2007) Critical Role of the Heme Axial Ligand, Met95, in Locking Catalysis of the Phosphodiesterase from Escherichia coli (Ec DOS) toward Cyclic diGMP, *J. Biol. Chem. 282*, 21301-21307.

25. Kelley, L. A., and Sternberg, M. J. E. (2009) Protein structure prediction on the Web: a case study using the Phyre server, *Nat. prot. 4*, 363-371.

26. Wass, M. N., Kelley, L. A., and Sternberg, M. J. E. (2010) 3DLigandSite: predicting ligand-binding sites using similar structures, *Nucleic Acids Res. 38*, W469-W473.

27. WHO. (2009) Global prevalence of vitamin A deficiency in populations at risk 1995-2005: Who global data base on vitamina A deficiency, WHO Press Geneva.

28. West, K. P. (2002) Extent of vitamin A deficiency among preschool children and women of reproductive age, *J. Nutri. 132*, 2857S-2866S.

29. Underwood, B. A., and Arthur, P. (1996) The contribution of vitamin A to public health, *The FASEB journal 10*, 1040-1048.

30. Chen, Y., Li, F., and Wurtzel, E. T. (2010) Isolation and characterization of the Z-ISO gene encoding a missing component of carotenoid biosynthesis in plants, *Plant Physiol. 153*, 66-79.

31. Paul, K. G., Theorell, H., and Akeson, A. (1953) The molar light absorption of pyridine ferroprotoporphyrin (pyridine haemochromogen), *Acta chem. scand 7*.

32. Sono, M., Dawson, J. H., and Hager, L. P. (1986) Ligand and halide binding properties of chloroperoxidase: peroxidase-type active site heme environment with cytochrome P-450 type endogenous axial ligand and spectroscopic properties, *Biochemistry 25*, 347-356.

33. Du, J., Perera, R., and Dawson, J. H. (2011) Alkylamine-Ligated H93G Myoglobin Cavity Mutant: A Model System for Endogenous Lysine and Terminal Amine Ligation in Heme Proteins such as Nitrite Reductase and Cytochrome f, *Inorg. Chem. 50*, 1242-1249.

34. Bracete, A. M., Sono, M., and Dawson, J. H. (1991) Effects of cyanogen bromide modification of the distal histidine on the spectroscopic and ligand binding properties of myoglobin: magnetic circular dichroism spectroscopy as a probe of distal water ligation in ferric high-spin histidine-bound heme proteins, *Biochimica et Biophysica Acta (BBA)-Protein Structure and Molecular Enzymology 1080*, 264-270.

35. Whitehouse, C. J. C., Bell, S. G., and Wong, L.-L. (2012) P450BM3 (CYP102A1): connecting the dots, *Chem. Soc. Rev. 41*, 1218-1260.

36. Gray, H. B., and Winkler, J. R. (2005) Long-range electron transfer, *Proc. Natl. Acad. Sci. U. S. A. 102*, 3534-3539.

37. Tran, N.-H., Huynh, N., Chavez, G., Nguyen, A., Dwaraknath, S., Nguyen, T.-A., Nguyen, M., and Cheruzel, L. (2012) A series of hybrid P450 BM3 enzymes with different catalytic activity in the light-initiated hydroxylation of lauric acid, *J. Inorg. Biochem. 115*, 50-56.

38. Perera, R., Sono, M., Raner, G. M., and Dawson, J. H. (2005) Subzero-temperature stabilization and spectroscopic characterization of homogeneous oxyferrous complexes of the cytochrome P450 BM3 (CYP102) oxygenase domain and holoenzyme, *Biochem. Biophys. Res. Commun. 338*, 365-371.

39. Perera, R. (2005) PhD, In *Dissertation*, p 254, University of South Carolina, Columbia, SC, USA.

40. Brenner, S., Hay, S., Girvan, H. M., Munro, A. W., and Scrutton, N. S. (2007) Conformational dynamics of the cytochrome P450 BM3/N-palmitoylglycine complex: the proposed “proximal-distal” transition probed by temperature-jump spectroscopy, *The J. Phys. Chem. B 111*, 7879-7886.

41. Sono, M., Stuehr, D. J., Ikeda-Saito, M., and Dawson, J. H. (1995) Identification of nitric oxide synthase as a thiolate-ligated heme protein using magnetic circular dichroism spectroscopy Comparison with cytochrome P-450-CAM and chloroperoxidase, *J. Biol. Chem. 270*, 19943-19948.

42. Roach, M. P., Pond, A. E., Thomas, M. R., Boxer, S. G., and Dawson, J. H. (1999) The role of the distal and proximal protein environments in controlling the ferric spin state and in stabilizing thiolate ligation in heme systems: Thiolate adducts of the myoglobin H93G cavity mutant, *J. Am. Chem. Soc. 121*, 12088-12093.

43. Ochsner, U. A., Johnson, Z., and Vasil, M. L. (2000) Genetics and regulation of two distinct haem-uptake systems, phu and has, in *Pseudomonas aeruginosa*, *Microbiology 146*, 185-198.

44. Wilks, A., and Burkhard, K. A. (2007) Heme and virulence: how bacterial pathogens regulate, transport and utilize heme, *Natural prod. rep. 24*, 511-522.

45. Ochsner, U. A., and Vasil, M. L. (1996) Gene repression by the ferric uptake regulator in Pseudomonas aeruginosa: cycle selection of iron-regulated genes, *Proc. Natl. Acad. Sci. 93*, 4409-4414.

46. Sievers, G., Gadsby, P., Peterson, J., and Thomson, A. J. (1983) Magnetic circular dichroism spectra of soybean leghaemoglocin< i> a</i> at room temperature and 4.2 K, *Biochimica et Biophysica Acta (BBA)-Protein Structure and Molecular Enzymology 742*, 637-647.

47. Perera, R., and Dawson, J. H. (2004) Modeling heme protein active sites with the his93gly cavity mutant of sperm whale myoglobin: complexes with nitrogen-, oxygen- and sulfur-donor proximal ligands, *J. Porphyrins Phthalocyanines 8*, 246-254.

3.8 Copyright Permission:

Figure 3.1

This is a License Agreement between Anuja Modi ("You") and Elsevier ("Elsevier"). The license consists of your order details, the terms and conditions provided by Elsevier, and the payment terms and conditions.

Get the printable license.

License Number	3398920105787
License date	May 30, 2014
Licensed content publisher	Elsevier
Licensed content publication	Elsevier Books
Licensed content title	Methods in Enzymology, Volume 54
Licensed content author	Larry E. Vickery
Licensed content date	1978
Number of pages	19
Type of Use	reuse in a thesis/dissertation
Portion	figures/tables/illustrations
Number of figures/tables/illustrations	1
Format	both print and electronic
Are you the author of this Elsevier chapter?	No
Will you be translating?	No
Title of your thesis/dissertation	PROBING HETEROATOM-CONTAINING SUBSTRATE OXIDATION IN P450-CAM FOR NON-FERRYL REACTIVE INTERMEDIATES AND HEME IRON COORDINATION STRUCTURAL ANALYSIS USING MAGNETIC CIRCULAR DICHROISM SPECTROSCOPY
Expected completion date	Jun 2014
Estimated size (number of pages)	150
Elsevier VAT number	GB 494 6272 12
Permissions price	0.00 USD
VAT/Local Sales Tax	0.00 USD / 0.00 GBP
Total	0.00 USD

Figures 3.2, 3.3, and 3.4.

ASBMB

American Society for Biochemistry and Molecular Biology

11200 Rockville Pike
Suite 302
Rockville, Maryland 20852

August 19, 2011

To whom it may concern,

It is the policy of the American Society for Biochemistry and Molecular Biology to allow reuse of any material published in its journals (the Journal of Biological Chemistry, Molecular & Cellular Proteomics and the Journal of Lipid Research) in a thesis or dissertation at no cost and with no explicit permission needed. Please see our copyright permissions page on the journal site for more information.

Best wishes,

Sarah Crespi

American Society for Biochemistry and Molecular Biology
11200 Rockville Pike, Rockville, MD
Suite 302
240-283-6616
JBC | MCP | JLR

Tel: 240-283-6600 • Fax: 240-881-2080 • E-mail: asbmb@asbmb.org